e-ISSN:1307-3540

ADO Klinik Bilimler Dergisi
Journal Of Clinical Sciences

▶ Cilt/Volume:15 • Sayı/Issue:2 • 2026

▶ Cilt/Volume:15 • Sayı/Issue:2 •2026

ADO Klinik Bilimler Dergisi • Journal Of Clinical Sciences

15

ADO Klinik Bilimler Dergisi
Journal of Clinical Sciences
Ankara Dişhekimleri Odası'nın bilimsel yayın organıdır.
Scientific publication of the Ankara Chamber of Dentists
Yılda üç kez yayınlanır./Published three times a year.

YAYINA VERİLİŞ TARİHİ/Date of publication
20.05.2026
Cilt:15 - Sayı:2 e-ISSN:1307-3540

Ankara Dişhekimleri Odası Klinik Bilimler Dergisi "ULAKBİM tarafından taranan ulusal hakemli dergilerden olup, "TR Dizin Dergi Listesi"nde yer alan dergilerden biridir./ADO Journal of Clinical Sciences is a nationally peer-reviewed journal indexed by ULAKBİM and is included in the "TR Dizin Journal List."

Ankara Dişhekimleri Odası Klinik Bilimler Dergisi Türkiye Atıf Dizini üyesidir.

ADO Journal of Clinical Sciences is indexed in the Türkiye Atıf Dizini.

YAZIM KURALLARI

Derginin yayın dili Ocak 2024 tarihinden itibaren İngilizcedir.

Yazarlardan, göndermiş oldukları makalenin daha önce yayınlanmamış, yayına kabul edilmemiş veya herhangi bir dergide değerlendirme aşamasında olmadığını beyan etmeleri istenmektedir. Herhangi bir bilimsel toplantıda sunulan özetlerin gönderim sırasında belirtilmesi zorunludur. Yazarlar, gönderim ve hakem değerlendirmesi sürecinde makalenin tüm sorumluluğunu üstlenirler. Etik beyanı gerektiren ancak ETİK KURUL Kurum adı, karar tarihi ve kimlik numarası belirtilmeyen ORİJİNAL ARAŞTIRMA MAKALELERİ değerlendirmeye alınmayacaktır. Yazarlar, tüm olgu sunumları ve gerekli tüm çalışmalar için imzalı bilgilendirilmiş onam aldıklarını belirtmelidir. Bilgilendirilmiş onamlar sisteme ayrı bir pdf dosyası olarak yüklenmelidir. Etik Beyannameler, Gereç ve Yöntem bölümünde Etik Kurul adı, karar tarihi ve kimlik numarası ile birlikte verilmeli ve sisteme ayrı bir pdf dosyası olarak yüklenmelidir. **Her makalenin benzerlik raporunun sisteme pdf dosyası olarak yüklenmesi gerekmektedir.**

Değerlendirme Süreci

ADO Klinik Bilimler Dergisi, değerlendirme süreci boyunca hem hakemin hem de yazarın kimliklerinin birbirinden gizlendiği anlamına gelen çift-kör değerlendirme sürecini kullanır. Bu nedenle yazarların makale dosyalarının kimliklerini açığa çıkarmayacak şekilde hazırlamaları gerekmektedir. Editörler hakemleri derginin online sistemi üzerinden davet edecek, hakemlerin kabulü sonrasında değerlendirme süreci başlayacaktır. Hakemler dergi sistemine giriş yaparak ilgili dosyaların indirilmesi ve öneri süreci davetini kabul ederler. İncelemeler için izin verilen süre: 4 hafta olup, editöryal süreç gerektiği takdirde değiştirilebilir.

KABUL EDİLEN MAKALE TÜRLERİ

Orijinal araştırma makalesi: Başlıklar, Özet (İngilizce ve Türkçe), Giriş, Gereç ve Yöntemler, Bulgular, Tartışma, Sonuç, Teşekkür, Kaynaklar, Tablolar, Şekiller ve Şekil açıklamaları.

Olgu sunumu: Başlık (Uzun ve kısa), Özet (İngilizce ve Türkçe), Giriş, Olgu Sunumu, Tartışma, Sonuç,

Teşekkür, Kaynakça, Tablolar, Şekiller ve Şekil Açıklamaları

Teknik not: Başlık, Özet, Giriş, Sonuçlar, Kaynaklar, Tablolar, Şekiller ve Şekil açıklamaları (gerekli ise)

Editöre Mektup: Başlık, Özet, Giriş, Sonuçlar, Kaynaklar, Tablolar, Şekiller ve Şekil açıklamaları (gerekli ise)

MAKALE HAZIRLAMA

a- Her yazı normal ve düz yazı tipinde (12 punto Times New Roman), 1,5 satır aralıkla iki yana dayalı olarak yazılmalı ve tüm sayfalar orta alttan art arda numaralandırılmalıdır.

b- Her paragrafta satır girintisi kullanılmalıdır.

c- Latince terimler veya tür adlarında italik karakterler kullanılmalıdır. (örn. in vitro, Staphylococcus aureus).

d- Birimler ve kısaltmalarda, uygun olduğu durumlarda Uluslararası Birimler Sistemi (SI: http://www.bipm.org/en/si/) kullanılmalıdır. Yaygın olarak kullanılan birimler için kısaltma örnekleri şunlardır: yıl-y, hafta-hf, saat-sa., dakika-dk., saniye-sn., gram-g, litre-L, mikrolitre-µL, metre-m, Celsius derece-°C vb. Türkçe kısaltmalar dizini için Türk Dil Kurumu'nun internet sitesine bakmalıdır. (TDK; http://www.tdk.gov.tr).

e- Ondalık sayılarda ayırıcı olarak nokta (.) kullanılmalıdır ve rakam ile birim arasında boşluk bırakılmalıdır. (örn. 12.3 mm, 37 °C) Yüzde değeri verirken değer ile yüzde işareti arasına boşluk bırakılmamalıdır (örn. %0.2).

f- Kısaltma standart bir ölçü birimi olmadığı sürece, metinde ilk geçtiği yerde parantez içindeki kısaltmanın ardından açık bir şekilde belirtilmeli ve metin boyunca aynı kısaltma kullanılmalıdır.

g-Çalışmada kullanılan malzeme/ekipmanın kaynağı ilk bahsedildiğinde belirtilmelidir (isim, üretici, şehir, eyalet (varsa), parantez içinde ülke). Aynı ürüne ilişkin daha sonraki alıntılarda menşei belirtmeye gerek yoktur. Daha önce belirttiğiniz firmanın ürettiği başka bir üründen bahsederken sadece firmayı belirtmeniz yeterlidir.

BAŞLIK SAYFASI

Başlık sayfası aşağıdakilerden oluşmalıdır:

a- Makalenin başlığı (İngilizce ve Türkçe)

b- 5 kelimeyi geçmeyen kısa bir başlık. (İngilizce ve Türkçe)

c- Yazarların akademik dereceleri dahil tam adları. Yazarların bağlı oldukları kurum (şehir ve ülke dahil), soyadlarından sonra üst simge numarası verilerek adlar satırının altında belirtilmelidir.

d- Tüm yazarların ORCID tanımlayıcıları. Bir tane almalı veya https://orcid.org/ adresinden kendinizinkini kontrol etmelisiniz.

e- Sorumlu yazarın iletişim bilgileri (posta adresi, iş telefonu, cep telefonu numaraları ve e-posta adresi)

f- Makalenin türü (orijinal araştırma makalesi, editöre mektup, olgu sunumu…)

g- Özet ve ana metinde ayrı ayrı yer alan kelime sayısı (şekil açıklamaları, tablo başlıkları ve kaynaklar hariç), kaynak, şekil ve tablo sayıları.

h- Finansman kaynağı (hibe numarası, protokol numarası vb. belirtiniz)

i- Teşekkür (makalenin herhangi bir bilimsel etkinlikte daha önce sunulmuş olması)

j- Etik inceleme kurulu bilgilerini (tam ad, tarih ve numara) burada ve metinde belirtin. Onay belgesinin dijital kopyası, gönderim sırasında ayrı bir belge olarak sisteme yüklenmelidir.

k-Kayıt sitesi (örn., clinicaltrials.gov), kayıt numarası, kayıt tarihi ve internet bağlantısı (önerilen) dahil olmak üzere klinik araştırma kayıt bilgileri.

ÖZET ve ANAHTAR KELİMELER:

Özet, makalede yer alan bilgileri yansıtmalı ve makalenin ana metninde yer almayan bilgileri içermemelidir. Özet, şu başlıklar kullanılarak yapılandırılmalıdır: Araştırma makalesi için Amaç, Gereç ve Yöntemler, Bulgular ve Sonuç; olgu sunumları için Giriş, Vaka raporu ve Sonuç. Teknik notlar ve editörlere mektupta herhangi bir başlık bulunmamalıdır.

Özet ve anahtar kelimeler hem İngilizce hem de Türkçe olarak sunulmalıdır. Anahtar kelimeler Medical Subject Headings (MESH: www.nlm.nih.gov/mesh/MBrowser.html) ve Türkiye Bilim Terimleri (TBT; http://www.bilimterimleri.com) arasından seçilmelidir. MESH indeksi Türkçe olup alfabetik sıraya göre listelenmeli ve noktalı virgülle (;) ayrılmalıdır. Anahtar kelimeler başlık ve özetten seçilmemelidir çünkü bunlar otomatik olarak indekslenir; bunun yerine ana metinden seçilmelidir.

GİRİŞ

Ana fikir ve önemi anlatılmalıdır. Hiçbir sonuca, tartışmaya ve veriye yer verilmemelidir. Bölümün son paragrafında çalışmanın **amacı** açıkça belirtilmeli ve varsa araştırma hipotezi verilmelidir.

GEREÇ ve YÖNTEMLER

Tüm ticari ürün ve cihazların menşei açıklanmalı ve ticari isimleri ve kaynakları belirtilmelidir (isim, üretici, şehir ve ülke).

Bu bölümde etik onay belirtilmelidir (onay alınan Etik Kurul'un tam adı, onay tarihi, onay numarası yazılmalıdır). Varsa, bilgilendirilmiş onam alındığı belirtilmelidir.

Gözlemsel veya deneysel çalışmalarda katılımcıların (hastalar, kontrol grupları dahil laboratuvar hayvanları) seçimine ilişkin dahil etme ve hariç tutma kriterleri açıklanmalıdır.

Bu bölümün son paragrafında, istatistiksel analiz ayrıntılı olarak açıklanmalıdır. İstatistik terimleri ve sembolleri tanımlanmalıdır. Kullanılan bilgisayar yazılımı belirtilmelidir.

BULGULAR

İstatistiksel bulgular rapor edilmelidir, ancak bunların tartışılmasından veya yorumlanmasından kaçınılmalıdır. Gerekiyorsa tablo, grafik veya illüstrasyonlardan yararlanılmalıdır. Bu bölümde gerekli ise alt başlıklar kullanılabilir.

TARTIŞMA

Araştırmanın bulgularını tartışılmalı ve diğer çalışmalarla uyumu veya uyumsuzluğu belirtilmeli ve çalışmanın sınırlılıklarına yer verilmelidir. Giriş ve sonuç bölümlerinde verilen bilgilerin tekrarından kaçınılmalıdır.

SONUÇ

Bu bölümde yazarlar çalışmanın sonuçlarını kısaca ve net bir şekilde sıralamalı ve çalışmanın temel mesajlarını belirtmelidir. İstatistiksel ayrıntılara yer verilmemelidir.

TEŞEKKÜR

Çalışma bir hibe ya da başka bir fonla desteklenmişse bu bölümde destekleyen kuruluşun adı ya da hibe numarası verilmelidir.

ÇIKAR ÇATIŞMASI

Herhangi bir çıkar çatışması olmadığı belirtilmelidir.

KAYNAKLAR

ADO Klinik Bilimler Dergisi'nde alıntıların etiketlenmesi Vancouver sistemine göre yapılır. Kaynaklar ana metinde üst simge Arap rakamlarıyla ardışık olarak belirtilmelidir. Tam referans listesi numara sırasına göre verilmelidir.

Dergilerin başlıkları MEDLINE için İndekslenen Dergiler listesinde kullanılan stile göre kısaltılmalıdır. (http://www.ncbi.nlm.nih.gov/nlmcatalog/journals)

Yayınlanmamış veriler veya kişisel iletişimler referans olarak kabul edilmez.

Metinde alıntı yapma örnekleri:

…önceki bir çalışmada belirtildi.[1]

…önceki çalışmalarda belirtildi.[2,4-6,8]

Yılmaz[9] tarafından yakın zamanda yapılan bir araştırmada şöyle bildirildi:

Yılmaz ve Akın tarafından yakın zamanda yapılan bir çalışmada[10] şu rapor edildi:

Yılmaz ve ark.[11] tarafından yakın zamanda yapılan bir çalışmada şu rapor edilmiştir:

Standart dergi makalesi

1. Erkmen E, Şimşek B, Yücel E, Kurt A. Comparison of different fixation methods following sagittal split ramus osteotomies using three dimensional finite element analysis: Part 1: Advancement surgery-posterior loading. Int J Oral Maxillofac Surg 2005;34:551-8.

Altıdan fazla yazarlı standart dergi makalesi

2. Tüter G, Kurtiş B, Serdar M, Aykan T, Okyay K, Yücel A, et al. Effects of scaling and root planing and sub-antimicrobial dose doxycycline on oral and systemic biomarkers of disease in patients with both chronic periodontitis and coronary artery disease. J Clin Periodontol 2007;34:673-81.

Tez

3. Kayaoğlu G. Endodontik hastalık açısından Enterococcus faecalis'in Kahve ve direnç çıkışının incelenmesi [tez]. Ankara: Gazi Üniversitesi; 2007.

Kitap ve kitapta bölüm

4.Okeson JP. Management of Temporomandibular Disorders and Occlusion. 7th ed. St. Louis, Missouri: Elsevier Mosby; 2013. p. 171- 174.

5. Alaçam A. Pedodontik Endodonti. Alaçam T, Editör. Endodonti. 1.baskı. Ankara: GÜ Yayınları; 1990. s.809-859.

TABLOLAR ve ŞEKİLLER

Tüm tablo ve şekiller ana metinde yer alma sırasına göre Latin rakamlarıyla ardışık olarak numaralandırılmalı ve ayrıntılı olarak tartışılmalıdır. Yazılarda tablo ve şekiller ana metnin sonunda Kaynaklar kısmından sonra verilmelidir.

Tüm şekiller yüksek kalitede JPG, PNG, PDF veya TIFF formatında olmalı ve gönderim sırasında ayrı bir belge ile yüklenmelidir. Histopatolojik görüntülerde kullanılan renklendirici ve büyütme miktarı belirtilmelidir.

Kişi görüntülerinin yer aldığı yazılarda, bunların kullanılması için yazılı izin alınmalı ve yazıyla birlikte sunulmalıdır.

Tablo hazırlanırken ADO Klinik Bilimler Dergisi'nde daha önce yayınlanmış makaleler örnek olarak alınabilir. Tüm tabloların tablonun üst kısmında bir başlığı bulunmalı ve birlikte yüklenmelidir. Kısaltmalar, istatistiksel bilgiler (p değerleri veya istatistiksel analiz yöntemi vb.) tablonun altına dipnot olarak verilmelidir. Gerektiğinde yıldız işareti veya üst simge kullanılmalıdır.

Bir yazıdaki tablo ve şekillerin toplam sayısı 8'i geçmemelidir.

ÇIKAR ÇATIŞMASI FORMU (ICMJE FORMU)

Dosyanın tamamını indirmek için lütfen tıklayın.

TELİF HAKKI FORMU VE YAZAR SÖZLEŞMESİ

Makale dosyalarının yükleme aşamasında telif hakkı formu ve yazar sözleşmesini indirebilirsiniz.

ÖN DÜZELTME VE MAKALE İADE SÜRECİ

Sisteme yüklenen makaleler Editör Kurulu'muzun değerlendirmesi sonucu ilk olarak ön kontrole alınır. DergiPark sisteminde yazılı dergimiz yazım kuralları doğrultusunda makaleler incelenir. Ön kontrolde 2 kez düzeltme isteği alması ve gerekli düzeltmelerin verilen süre içerisinde yapılmaması halinde, makale sorumlu yazara iade edilir ve hakem değerlendirme sürecine alınmaz.

INSTRUCTIONS FOR AUTHORS

The publication language of the journal has been English since January 2024. Authors are required to declare that the submitted manuscript has not been previously published, accepted for publication, or submitted for evaluation in any other journal. Abstracts presented at any scientific meeting or congress must be clearly stated at the time of submission. Authors assume full responsibility for the manuscript throughout the submission and peer-review process. ORIGINAL RESEARCH ARTICLES requiring an ethical statement but lacking the name of the Ethics Committee/Institution, approval date, and approval number will not be considered for evaluation. Authors must state that signed informed consent was obtained for all case reports and all studies requiring informed consent. Informed consent forms must be uploaded to the system separately as PDF files. Ethical declarations should be provided in the Materials and Methods section together with the name of the Ethics Committee, approval date, and approval number, and must also be uploaded to the system separately

as PDF files. **For each submitted manuscript, the similarity report, must be uploaded to the system as a PDF file.**

Review Process

ADO Journal of Clinical Sciences employs a double-blind peer-review process, in which both the reviewers' and authors' identities are concealed throughout the evaluation process. Therefore, authors are required to prepare their manuscripts in a manner that does not reveal their identities. Editors invite reviewers through the journal's online submission system, and the review process begins upon acceptance of the invitation by the reviewers. Reviewers access the journal system to download the relevant files and accept the invitation to participate in the review process. The standard review period is 4 weeks; however, this duration may be modified by the editorial office when necessary.

ACCEPTED MANUSCRIPT TYPES

Original Research Article: Sections should include: Title, Abstract (English and Turkish), Introduction, Materials and Methods, Results, Discussion, Conclusion, Acknowledgements, References, Tables, Figures, and Figure Legends.

Case Report: Sections should include: Title (full and short title), Abstract (English and Turkish), Introduction, Case Report, Discussion, Conclusion, Acknowledgements, References, Tables, Figures, and Figure Legends.

Technical Note: Sections should include: Title, Abstract, Introduction, Results, References, Tables, Figures, and Figure Legends (if required).

Letter to the Editor: Sections should include: Title, Abstract, Introduction, Results, References, Tables, Figures, and Figure Legends (if required).

MANUSCRIPT PREPARATION

a) All manuscripts should be prepared in plain text format using 12-point Times New Roman font, with 1.5 line spacing and justified alignment. All pages should be numbered consecutively at the bottom center.

b) A first-line indentation should be used for each paragraph.

c) Italic characters should be used for Latin terms and species names (e.g., *in vitro, Staphylococcus aureus*).

d) The International System of Units (SI: http://www.bipm.org/en/si/) should be used for units and abbreviations where appropriate. Examples of commonly used abbreviations include: year (y), week (wk), hour (h), minute (min), second (s), gram (g), liter (L), microliter (µL), meter (m), and degree Celsius (°C). For Turkish abbreviations, authors should refer to the website of the Turkish Language Association (TDK; http://www.tdk.gov.tr).

e) A period (.) should be used as the decimal separator, and a space should be left between the numerical value and the unit (e.g., 12.3 mm, 37 °C). No space should be left between the numerical value and the percent symbol when expressing percentages (e.g., 0.2%).

f) Unless the abbreviation represents a standard unit of measurement, it should be clearly defined in parentheses at its first occurrence in the text, and the same abbreviation should be used consistently throughout the manuscript.

g) The source of all materials/equipment used in the study should be specified at first mention, including the product name, manufacturer, city, state (if applicable), and country in parentheses. It is not necessary to provide the origin information in subsequent mentions of the same product. When referring to another product manufactured by a previously mentioned company, stating only the company name is sufficient.

TITLE PAGE

The title page should include the following:

a) The title of the manuscript (in English and Turkish).

b) A short running title not exceeding 5 words (in English and Turkish).

c) Full names of all authors, including academic degrees. The institutional affiliations of the authors (including city and country) should be indicated below the author line using superscript numbers following the surnames.

d) ORCID identifiers of all authors. Authors should obtain or verify their ORCID identifiers via https://orcid.org/

e) Contact information of the corresponding author, including postal address, office telephone number, mobile phone number, and e-mail address.

f) The type of manuscript (e.g., original research article, letter to the editor, case report, etc.).

g) The word counts of the abstract and main text separately (excluding figure legends, table titles, and references), together with the numbers of references, figures, and tables.

h) Funding information (please specify grant number, protocol number, etc., if applicable).

i) Acknowledgements (including whether the manuscript has previously been presented at any scientific meeting or congress).

j) Ethics committee approval information (full name of the committee, approval date, and approval number) should be stated both here and within the manuscript text. A digital copy of the approval document must be uploaded to the system as a separate file during submission.

k) Clinical trial registration information, including the registry name (e.g., clinicaltrials.gov), registration number, registration date, and internet link (recommended).

ABSTRACT AND KEYWORDS

The abstract should accurately reflect the content of the manuscript and should not include information that is not presented in the main text. The abstract must be structured using the following headings: Aim, Materials and Methods, Results, and Conclusion for original research articles; and Introduction, Case Report, and Conclusion for case reports. No subheadings should be used in technical notes or letters to the editor.

Abstracts and keywords should be provided in both English and Turkish. Keywords should be selected from the Medical Subject Headings (MESH:www.nlm.nih.gov/mesh/MBrowser.html) and Türkiye Bilim Terimleri (TBT; http://www.bilimterimleri.com) databases. Keywords should be listed alphabetically and separated by semicolons (;). Keywords should not be selected from the title or abstract, as these are indexed automatically; instead, they should be selected from the main text.

INTRODUCTION

The main concept and significance of the study should be clearly explained. This section should not include any results, discussion, or data. In the final paragraph of the section, the aim of the study should be clearly stated, and the research hypothesis, if any, should be provided.

MATERIALS AND METHODS

The sources of all commercial products and devices used in the study should be specified, including their trade names and manufacturers (name, manufacturer, city, and country).

This section should include information regarding ethical approval (full name of the Ethics Committee granting approval, approval date, and approval number). If applicable, it should also be stated that informed consent was obtained.

In observational or experimental studies, the inclusion and exclusion criteria for participant selection (including patients, control groups, and laboratory animals) should be clearly described.

In the final paragraph of this section, the statistical analysis should be described in detail. Statistical terms and symbols should be defined, and the computer software used for statistical analysis should be specified.

RESULTS

Statistical findings should be reported without discussion or interpretation. Tables, graphs, or illustrations should be used when necessary. Subheadings may be used in this section if required.

DISCUSSION

The findings of the study should be discussed and compared with those of previous studies, indicating areas of agreement or disagreement. The limitations of the study should also be addressed. Repetition of information already presented in the Introduction and Conclusion sections should be avoided.

CONCLUSION

In this section, the authors should briefly and clearly summarize the conclusions of the study and emphasize its main messages. Statistical details should not be included.

ACKNOWLEDGEMENTS

If the study was supported by a grant or any other funding source, the name of the supporting organization and/or the grant number should be stated in this section.

CONFLICT OF INTEREST

The authors should declare that there is no conflict of interest.

REFERENCES

Citation and referencing in ADO Journal of Clinical Sciences should follow the Vancouver style. References should be cited consecutively in the text using superscript Arabic numerals. The complete reference list should be provided in numerical order according to the order of citation in the text.

Journal titles should be abbreviated according to the style used in the MEDLINE List of Journals Indexed for MEDLINE. [NLM Catalog Journals Indexed for MEDLINE (http://www.ncbi.nlm.nih.gov/nlmcatalog/journals).

Unpublished data or personal communications should not be included in the reference list.

Examples of in-text citations:
"…as reported in a previous study."[1]
"…as reported in previous studies."[2,4-6,8]
"A recent study by Yılmaz[9] reported that:"
"A recent study by Yılmaz and Akın[10] reported that:"
"A recent study by Yılmaz et al.[11] reported that:"

Standard journal article

1. Erkmen E, Şimşek B, Yücel E, Kurt A. Comparison of different fixation methods following sagittal split ramus osteotomies using three-dimensional finite element analysis: Part 1: Advancement surgery-posterior loading. Int J Oral Maxillofac Surg 2005;34:551-8.

Standard journal article with more than six authors

2. Tüter G, Kurtiş B, Serdar M, Aykan T, Okyay K, Yücel A, et al. Effects of scaling and root planing and sub-antimicrobial dose doxycycline on oral and systemic biomarkers of disease in patients with both chronic periodontitis and coronary artery disease. J Clin Periodontol 2007;34:673-81.

Thesis

3. Kayaoğlu G. Endodontik hastalık açısından Enterococcus faecalis'in Kahve ve direnç çıkışının incelenmesi [tez]. Ankara: Gazi Üniversitesi; 2007.

Book and book chapter

4.Okeson JP. Management of Temporomandibular Disorders and Occlusion. 7th ed. St. Louis, Missouri: Elsevier Mosby; 2013. p. 171-174.

5. Alaçam A. Pedodontik Endodonti. Alaçam T, Editör. Endodonti. 1.baskı. Ankara: GÜ Yayınları; 1990. s.809-859.

TABLES AND FIGURES

All tables and figures should be numbered consecutively using Arabic numerals according to the order in which they are cited in the text and should be discussed in detail within the manuscript. Tables and figures should be presented at the end of the main text, following the References section.

All figures must be of high quality and submitted in JPG, PNG, PDF, or TIFF format as separate files during submission. For histopathological images, the staining method and magnification level used should be specified.

For manuscripts containing identifiable images of individuals, written permission for their use must be obtained and submitted together with the manuscript.

Previously published articles in the ADO Journal of Clinical Sciences may be used as examples for table preparation. All tables should include a title placed above the table and should be uploaded together. Abbreviations and statistical information (e.g., p values or statistical analysis methods) should be provided as footnotes below the table. Asterisks or superscript symbols should be used when necessary.

The total number of tables and figures in a manuscript should not exceed 8.

Conflict of Interest Form (ICMJE Form)

Please click to download the complete file.

COPYRIGHT FORM AND AUTHOR AGREEMENT

The copyright form and author agreement can be downloaded during the manuscript submission process.

PRELIMINARY REVIEW AND MANUSCRIPT RETURN PROCESS

Manuscripts uploaded to the system are initially subjected to a preliminary review by our Editorial Board. Submissions are evaluated in accordance with the journal's author guidelines available on the DergiPark system. If a manuscript receives requests for revision twice during the preliminary review process and the required corrections are not completed within the specified time, the manuscript will be returned to the corresponding author and will not proceed to the peer-review stage.

İçindekiler/Contents

Cilt/Volume: 15 • Sayı/Issue: 2 • 2026

Özgün Araştırma Makaleleri / Original Research Articles

Olgu Sunumu/Case Report

HAKEMLERE TEŞEKKÜR

15. Cilt 2. Sayı için değerlendirilen taslak makaleleri bilimsel ve tarafsız gözle inceleyen ve aşağıda isimleri belirtilmiş olan hakemlerimize ve bütün danışma kurulu üyelerimize teşekkür ederiz.

Cemile Kedici Alp

Deniz Yılmaz

Ebru Küçükkaraca

Emine Dilara Çolpak

Fatma Yılmaz

Gülin Acar

Hacer Eberliköse

Hanife Altınışık

Kübra Öztürk

Kübra Gülnur Topsakal

Merve Nezir Güngör

Nazmiye Şen

Sara Samur Ergüven

Serdar Polat

DOI: https://doi.org/10.54617/adoklinikbilimler.1722215

Original Research Article

Effect of Preload on Different Implant Abutments in Terms of Screw Loosening

Mehmet Ali Kılıçarslan[1*], Bora Akat[1], Yezdan Dilan Erkcan[1], Burak Bilecenoğlu[2], Kaan Orhan[3]

[1]Department of Prosthodontics, Faculty of Dentistry, Ankara University, Ankara, Türkiye
[2]Department of Anatomy, Faculty of Medicine, Ankara Medipol University, Ankara, Türkiye
[3]Department of Dentomaxillofacial Radiology, Faculty of Dentistry, Ankara University, Ankara, Türkiye

ABSTRACT

Aim: This study aimed to compare the mechanical behavior of the implant-abutment connection in cases where appropriate preloading is performed or not.

Materials and Methods: A total of 54 bone-level implants with a diameter of 3.5 mm were employed in this study. Each group was further divided into subgroups, each of which was tightened manually and with a torque wrench, and a total of six groups were tested, three of them being control groups. Manual tightening was performed by the same researcher with maximum manual force and tightening with a torque wrench was performed with a value of 30 Ncm by the same researcher. Sample measurement values in which connection compliance is evaluated using micro-CT.

Results: The total space volume between the screw and the implant body (single torque minimum 0.32 mm^3) decreased significantly in the samples tightened for the second time (minimum 0.20 mm^3). Still, no difference was observed between tightening manually or with a torque wrench a second time, except for the angled abutment group.

C**onclusion:** Tightening a second time after preload significantly reduced the gap values, especially when using a torque wrench. Therefore, tightening the implants repeatedly using a torque wrench after preloading (retightening) plays a significant role in clinically preventing screw loosening and consequently major clinical problems such as screw fractures.

Keywords: Dental Implants; Preload; Screw Loosening

Citation: Kılıçarslan MA, Akat B, Erkcan YD, Bilecenoğlu B, Orhan K. Effect of Preload on Different Implant Abutments in Terms of Screw Loosening. ADO Klinik Bilimler Dergisi 2026;15(2):77-85

Editor: Yeliz Kılınç, Gazi University, Ankara, Türkiye

INTRODUCTION

Implant-abutment connection is crucial for the long-term success and stability of the prosthesis.[1] Incompatibility between these components is an issue that should be taken into consideration because, in addition to mechanical problems such as screw loosening and damage to the internal screw threads, it causes biological complications due to microorganism colonization in the interior section of the implant.[2]

According to data obtained from *in vitro* studies, an increase in stability was observed with the use of internal connection.[3-9] In the design with internal connection, a lower incidence of abutment screw loosening was observed compared to external connection. It was stated that this situation provided a biomechanical advantage.[7,10] Since the loading force is not completely applied on the screw in the internal conical connection, it is possible for the abutment screw to reach a larger preload value in this connection type. The solid design of the friction-lock mechanism and friction-fit connection provides greater resistance to fracture and deformation under oblique compression loading compared to passive-fit designs.[11]

Received: 06.19.2025; Accepted: 02.21.2026
**Corresponding author: Dr. Mehmet Ali Kılıçarslan*
Ankara University, Faculty of Dentistry, Department of Prosthodontics
Emniyet Mahallesi, Mevlana Bulvarı, 06500 Ankara, Türkiye
E-mail: mmkilicarslan@yahoo.com

An inevitable gap occurs between the implant and abutment, since cold fusion does not occur when the abutments are compressed in the passive-fit connection.[12-18] The gap may cause micromobility during clinical loading. Micromobility may create stress on the screw, causing loss of compression achieved by preload and loosening of the abutment. The harmful micromobility level has been determined by many researchers to be between 50 and 150 µm. It is possible for micromobility values measured beyond this level to result in bone loss in the part of the placed dental implants corresponding to the crestal bone region.[16]

Currently, many studies indicate that the inadequate tightening or loosening of the screw, the screw design, non-passive prosthetic structures or prosthetic extensions, inclined prosthetic components, incompatible parts, destruction of the support bone, lateral forces, and bruxism cause screw loosening.[19,20] The situation is disturbing for the physician and patient alike. Screw loosening can lead to fractured implant components and biological complications. One of the main causes of screw loosening is occlusal and lateral loads that are transferred from the implant to the bone.[21] Screw complications are more common with single-tooth implant restorations compared to multi-unit restorations.[22] Other factors that may cause screw loosening include the screw being tightened with inadequate force, insufficient prosthetic superstructure, the presence of incompatible superstructure and prosthetic components, overload, and bone elasticity.[12,23,24]

The preload applied to the screw increases the fatigue resistance and ensures the locking of the implant and abutment connection.[25] Preload enables the tightened abutment screw to transmit linear force to the abutment-implant body and hold these components together. Considering the elongation that occurs when torque is applied, the screw can be considered to have elastic properties similar to a stretched spring.[26] Preload is determined by three factors. These factors are the amount of torque, the shape of the screw head, and the type of material of which the screw and the abutment are made.[12] By applying sufficient preload to the screw, less mobility and fewer screw-loosening problems are observed at the abutment and screw interface.[27-29] Applying preload to the screw increases the resistance of the abutment to fatigue and ensures the locking of the implant and abutment connection. Occlusal forces applied to implant-supported prostheses cause changes in the preload applied to the abutment screws. This situation may result in loosening the abutment screw.[30,31] The head of the abutment screw is generally flat. The screw head produced in a conical shape reduces the compression and tensile forces occurring in the screw threads. A flat-head screw design distributes forces more evenly in the head and thread parts of the screw than a conical-shaped screw head design.[25,32]

All *in vitro* studies in this field, including the micro-CT analysis method employed in this study, are efforts to collect data to increase the survival time of implant-supported prostheses in the mouth and present ideas to manufacturers and users. The aim of this study was to examine the mechanical behavior of uniquely designed and manufactured dental implants and their different superstructure abutments while functioning. The aim was to compare the mechanical behavior (compatibility values) of the implant-abutment connection in cases where appropriate preloading was performed or not, on the grounds that they can distribute the loads that will fall on them in different directions in the use of straight and angled prefabricated abutments and custom abutments produced in CAD/CAM technique in a “deep internal hexagonal” connection when two different thickness implants were employed. The null hypothesis of this study was that in groups manually tightened, there will be no difference in the gap between the first compression and the second compression, but in the samples torqued with 30 Ncm as preload, relaxation will be observed after the first compression.

MATERIALS AND METHODS

A total of 54 NucleOSSTM T6 (Şanlılar Tıbbi Cihazlar Medikal Kimya San. Tic. Ltd. Şti., Türkiye) bone-level implants with a diameter of 3.5 mm were used in this study. The T6 implant is manufactured from pure titanium (Grade 4) that complies with international standards. Since this study was conducted *in vitro*, an ethics committee approval was not required. The internal structure of the T6 implant has a conical internal hex structure with a 140-degree connection. As the superstructure, Ti Grade 5

Table 1. Test Groups.

Group	Abutment and Connected Implant Body Diameter (mm)	Tightening Type
E1	T6 SD047 Straight - Ti Grade 5 prefabricated abutment (diameter: 3.5)	Manual
E3	T6 SD134 25° Angled Ti - Grade 5 prefabricated abutment (diameter: 3.5)	Manual
E5	T6 32804 CAD/CAM abutment (diameter: 3.5)	Manual
T9	T6 SD047 Straight - Ti Grade 5 prefabricated abutment (diameter: 3.5)	30 Ncm
T11	T6 SD134 25° Angled Ti - Grade 5 prefabricated abutment (diameter: 3.5)	30 Ncm
T13	T6 32804 CAD/CAM abutment (diameter: 3.5)	30 Ncm

straight abutment T6 SD047 straight, 5 mm platform diameter abutment, 25° Angled Ti Grade 5 fabricated abutment (T6 SD134 angled, 5 mm platform diameter) and CAD/CAM abutments were used, with n = 9. Each group was further divided into subgroups, each of which was tightened manually and with a torque wrench, and a total of six groups were tested, three of which were control groups (Table 1). Manual tightening was performed by the same researcher with maximum manual force and tightening with a torque wrench was performed at a value of 30 Ncm by the same researcher. Scans of the sample, which was compressed both manually and using a torque wrench, were completed 24 hours after both the first compression (before) and the second compression (after) to see the preload loss. The samples, whose first scans were completed, were immediately subjected to second compression.

For micro-CT scanning of the samples, a Bruker SkyScan 1275 (Bruker Skyscan, Kontich, Belgium) device with high-resolution scanning capacity was employed in the micro-CT-Laboratory of Ankara University Faculty of Dentistry. For scanning parameters, the rotation step was determined to be 0.5 for 100 kVp, 100 mA, and 10 µm pixel size. A 1 mm thick copper filter was employed to prevent radiological artifacts that may occur during shooting. These corrections were ring artifact correction, beam hardening, post-alignment, and smoothing at the optimum level for each sample. NRecon software and CtAn (Version 1.17.7.2, SkyScan) were used to visualize and quantitatively measure samples using the modified algorithm described by Feldkamp *et al*., and to obtain axial, two-dimensional, 1000 × 1000 pixel images. For reconstruction parameters, ring artifact correction and smoothing were fixed at 10, and beam artifact correction was set to 60%. Contrast limits were applied following SkyScan's instructions. Using NRecon software (Skyscan, Kontich, Belgium, 2020), images obtained by the scanner were reconstructed to show two-dimensional cross-sections of the samples. A total of 1014 cross-sectional images were reconstructed from the entire volume.

After the scans were completed, each scanned sample was individually reconstructed using NRecon (NRecon, Version 1.6.7.2, Skyscan, Kontich, Belgium, 2020) software. Dataviewer software was employed to obtain study images from the center of the dental implants, where measurements were made in coronal and sagittal directions. This software made it possible to select the region of interest (ROI) and the desired number of sections for the selected region. As a result, the number of sections could be standardized for all samples, and the same section corresponding to the center of the implants in all directions could be analyzed for each implant. The software was then employed to perform the measurements. All measurements were made by the same researcher. Since the presence of minor radiographic artifact precluded the use of any automated instrumentation, all measurements were taken manually, and measurement points were standardized to minimize errors. After the cross-sections of the projections of the samples were obtained through reconstruction, these cross-sections were transferred to the CTAn (CTAn, Version 1.17.7.2, Skyscan, Kontich, Belgium, 2020) software for mathematical analysis. For volumetric measurements, the upper and lower borders of the gap were marked with the software, and the gap boundaries to be calculated were determined in each of the remaining sections separately using the function called regions of interest (ROI). These sections were processed using the software's histogram, employing a grayscale of 0-255 to represent only the space to be calculated as a white object, while the rest of the area was blackened to

exclude it from calculation. Subsequently, three-dimensional volumetric calculations were performed (Figure 1). All measurements were performed by a single examiner blinded to the group allocation.

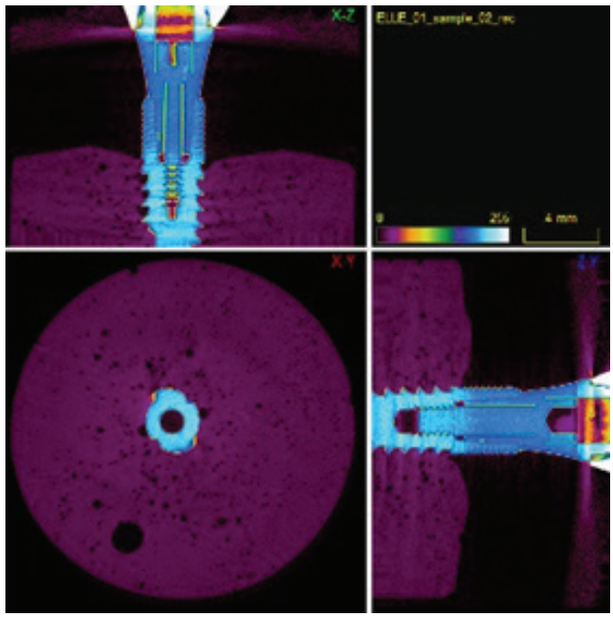

Figure 1. Micro-CT Images of implant body - abutment assemble.

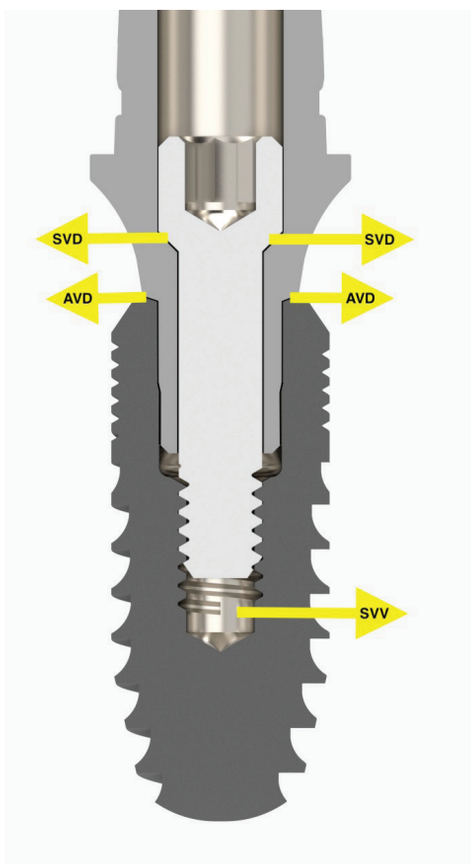

Figure 2. Measuring Points.

Sample measurement values in which connection compliance was evaluated using micro-CT were primarily divided into two groups: linear and volumetric. Linear measuring points were divided into subgroups to evaluate the gap between the connection screw and the abutment (Screw Vertical - SVD) and between the connection screw and abutment and the implant body (Abutment Vertical - AVD). In volumetric measurements, measurement areas were the main space (Screw Vertical Volume (SVV) between the screw and the screw slot in the implant body was evaluated (Figure 2).

Shapiro–Wilk test was used to assess the normality of data distribution. Data were evaluated using analysis of variance (ANOVA), with the size of the microgap expressed as mean ± standard deviation. The TUKEY HSD multiple comparison test was applied for post-hoc pairwise comparions. Statistical significance level, P, was determined as < 0.05. Homogeneity of variances was tested with the Levene test. Comparisons were made according to the factorial variance analysis technique, and primarily the “Tightening Type - Abutment” binary interaction, that is, the mutual interaction of the factors, was evaluated statistically.

RESULTS

A before and after comparison of sagittal SVD preload compression according to the “Tightening Type - Abutment” factors were made according to the factorial variance analysis technique. While all abutment groups differed significantly from each other in screw fit, whether manually tightened or torqued, it was determined that second tightening reduced the gap between the screw and the abutment in all groups and all placement techniques (Table 2). It was observed that the abutment-implant body compatibility relationship also reduced the gap with second tightening (Table 3). The total space volume between the screw and the implant body significantly decreased in samples that were tightened for the second time. On the other hand, no difference was observed between tightening manually or with a torque wrench a second time, except for the angled abutment group (Table 4).

Table 2. Descriptive Statistics of Screw Vertical Distal (SVD) Values According to Tightening Type.

Characteristic	Tightening Type	Abutment	CORONAL Right (µm)	CORONAL Left (µm)
			Mean ± SD	Mean ± SD
SVD- Before	Manual	T6 NR042 Straight	20.42^{A}±0.14	20.38^{A}±0.14
		T6 SD134 25° Angled	23.47^{B}±0.28	23.03^{B}±0.27
		T6 32804 CAD-CAM	18.76^{C}±0.25	18.52^{C}±0.25
	Torque wrench	T6 NR042 Straight	24.92^{A}±0.49	25.43^{A}±0.31
		T6 SD134 25° Angled	18.91^{B}±0.20	19.53^{B}±0.30
		T6 32804 CAD-CAM	17.41^{C}±0.24	17.83^{C}±0.17
SVD- After	Manual	T6 NR042 Straight	17.03^{A}±0.14	17.39^{A}±0.14
		T6 SD134 25° Angled	20.07^{B}±0.28	20.03^{B}±0.27
		T6 32804 CAD-CAM	15.38^{C}±0.26	15.53^{C}±0.25
	Torque wrench	T6 NR042 Straight	12.49^{A}±0.25	12.70^{A}±0.16
		T6 SD134 25° Angled	15.69^{B}±0.18	16.23^{B}±0.30
		T6 32804 CAD-CAM	14.19^{C}±0.26	14.53^{C}±0.17

*P<0.05 indicates the level at which statistical difference was determined.
**The superscripts (A, B, C) indicate whether there was a statistical difference between the groups based on letter similarity or difference.

Table 3. Descriptive Statistics of Abutment Vertical Distal (AVD) Values According to Tightening Type.

Characteristic	Tightening Type	Abutment	CORONAL Right (µm)	CORONAL Left (µm)
			Mean ± SD	Mean ± SD
AVD- Before	Manual	T6 NR042 Straight	20.49^{A}±0.21	21.00^{A}±0.13
		T6 SD134 25° Angled	23.60^{B}±0.38	23.52^{B}±0.19
		T6 32804 CAD-CAM	24.31^{C}±0.24	24.44^{C}±0.23
	Torque wrench	T6 NR042 Straight	34.52^{A}±0.77	34.57^{A}±0.49
		T6 SD134 25° Angled	22.08^{B}±0.14	22.28^{B}±0.14
		T6 32804 CAD-CAM	21.67^{B}±0.17	22.14^{B}±0.27
AVD- After	Manual	T6 NR042 Straight	17.11^{A}±0.23	17.51^{A}±0.14
		T6 SD134 25° Angled	20.26^{B}±0.40	20.02^{B}±0.19
		T6 32804 CAD-CAM	20.92^{C}±0.24	20.94^{C}±0.23
	Torque wrench	T6 NR042 Straight	17.24^{A}±0.37	17.30^{A}±0.25
		T6 SD134 25° Angled	18.40^{B}±0.13	18.42^{B}±0.14
		T6 32804 CAD-CAM	17.98^{C}±0.19	18.30^{B}±0.27

*P<0.05 indicates the level at which statistical difference was determined.
**The superscripts (A, B, C) indicate whether there was a statistical difference between the groups based on letter similarity or difference.

Table 4. Descriptive Statistics of Volume SVV Values According to Tightening Type.

Tightening Type	Abutment	Volume (mm3) SVV_Before	Volume (mm3) SVV_After
		Mean ± SD	Mean ± SD
Manual	T6 NR042 Straight	0.52^{A}±0.1	0.22^{A}±0.15
	T6 SD134 25° Angled	0.60^{A}±0.23	0.30^{A}±0.23
	T6 32804 CAD-CAM	0.53^{A}±0.05	0.23^{A}±0.05
Torque wrench	T6 NR042 Straight	0.32^{A}±0.04	0.20^{A}±0.00
	T6 SD134 25° Angled	0.76^{B}±0.05	0.23^{A}±0.05
	T6 32804 CAD-CAM	0.78^{B}±0.04	0.24^{A}±0.05

*P<0.05 indicates the level at which statistical difference is determined.
**The superscripts (A and B) indicate whether there is a statistical difference between the groups based on letter similarity or difference.

DISCUSSION

When the results of this study were critically evaluated, it was observed that, although the parts placed on the implant body were of the same geometry, the abutment superstructure design affected the connection compatibility, especially with the preload application. In addition, the null hypothesis of this *in vitro* study was partially accepted, as the second compression reduced preload relaxation in both the torque wrench and manually tightening groups.

The support or abutment can be attached to the implant externally or internally. In the first implant and superstructure design model proposed by Brånemark, the implant and abutment were connected using a 0.7 mm external hexagonal connection type.[36] Over the years, complications such as loosening of the implant abutment screw and the formation of microvoids and microbial penetration at the implant-abutment interface have been observed because of using this connection type. The partial success rate highlighted the need for some modifications.[37] According to data obtained from in-vitro studies, an increase in stability has been observed with the use of internal connections. In designs with internal connections, a lower incidence of support screw loosening was observed compared to external connections, and this has been stated to provide a biomechanical advantage.[7-9] Marginal bone loss was found to be greater in implants with external connections compared to those with internal connections. The implant support structure connected with an internal hexagon connection provides a wider force distribution area compared to an external hexagon structure, thus exhibiting higher stability.[15]

Screw loosening between the implant and the abutment is a widely reported problem in the literature.[19,20] When torque is applied, the contact between the screw threads and the inner surface of the implant causes embedment relaxation, also known as the settling effect. This means that the preload value decreases on these surfaces after a few minutes, as if the watch winder is discharging. It is considered normal for the initial torque value to decrease between 2% and 10%.[20,30] It has been observed that the removal torque value decreases in cases where tightening and loosening are applied at successive intervals.[11] It was observed that there was a significant decrease in the torque values of the abutments after mechanical cycling in the hexagonal connection compared to the Morse taper connection.

Loosening and fracture are potential problems for abutments and fixation screws. The frequency of screw loosening reached 12.7% in single crowns and 6.7% in fixed partial dentures. Loosening the abutment screw brings various complications. Various complications may occur, such as soft tissue advancing into the space between the loosened implant abutment and the implant, leading to fistula formation and infection of the soft tissue. Additionally, loose screws are more prone to breakage under load, which can lead to long-term prosthetic complications.[33] While abutment screw loosening was observed at a rate of 1.5% in abutments with internal connection, due to the biomechanical advantage, it was observed as 7.5% in abutments with external connection. Some researchers reported the loosening between different connection types, some suggested different screw designs, and some suggested different screws. They compared their materials, and some compared their surface coatings. In addition to the effect of the torque applied and the re-torquing of the screw after it was initially torqued, the number of times a screw can be torqued and whether this reduces screw loosening has been investigated by researchers.[10]

El-Sheikh *et al*.[33] aimed to investigate the effect of abutments on screw loosening by measuring their torque value at different angles and neck lengths before and after dynamic cyclic loading using a digital torque device. A total of 90 bone-level implants with a conical hybrid connection, 4.5 mm in diameter and 10 mm in length, were used. According to the abutment angle, they were divided into three groups: GI 0°, GII 15°, and GIII 25° abutments. Each group was divided into two subgroups, subgroup A (2 mm) and subgroup B (4 mm), each consisting of 15 samples. Each implant and abutment were placed vertically in acrylic resin using a stainless-steel cylindrical mold. Initial analysis was performed with the abutment screw tightened to a torque of 30 Ncm twice at 10-minute intervals using a digital torque indicator. RTV before and after cyclic loading of the abutment screws was measured in Newton centimeters using a digital torque gauge. One hundred thousand cycles

of eccentric dynamic cyclic loading were applied at 130 N at a rate of 1 Hz, 5 mm from the central axis of the implant. The percentage of removal torque loss (%RTL) before and after dynamic cyclic loading was calculated and statistically analyzed using SPSS version 20. As a result of this study, it was stated that screw loosening increased with increasing abutment angle and neck length. *In vitro* studies have indicated that tapered and non-tapered abutments provide adequate resistance to maximum bending forces and fatigue testing. However, better coverage, fewer micro voids, and stability were observed in conical supports. Additionally, this study indicated that compared to angled abutments, the conical hybrid connection is more biomechanically stable when used with straight abutments.

Parnia *et al*.[34] compared the experience factor in manually tightening of implant abutments, observing instructors and postgraduate students as they made implant abutment connections. In the study, they measured the tightening values with the help of a torque meter. It was observed that male practitioners applied more torque than females, and professors applied more than students. Additionally, an increase in clamping force was observed as age progressed.

Seloto *et al*.[35] looked at the effect of sealing gel use on the vertical compliance of the implant abutment interface and determined that the maximum gap value before mechanical loading with gel use was 5.55 µm and after mechanical loading was 4.59 µm. Differences in measurement points and gel application make these values different from those in our study.

The compatibility of the implant body – abutment – screw combination is not only one of the parameters related to the superstructure success of implant-supported prostheses but also affects the survival time of the implant body in the bone. For this reason, the connection compatibility and evaluation of microgaps that will arise due to this connection have been investigated using many methods, from finite element analysis to the evaluation of microorganism leakage, some of which can be seen in the discussion section of this *in vitro* study. In addition, after prosthetic applications are completed and implant-supported prostheses are used, screw loosening and fractures are perhaps the most difficult prosthetic complications to compensate for. Therefore, selecting designs with the highest durability during use will enhance user comfort and safety. The use of a single connection type and manual compression by a single researcher are among the limitations of this study. Nevertheless, our *in vitro* study, which examined the most important parameters related to the oral survival of implant systems and tested them in a large sample group, is likely to be clinically informative.

CONCLUSION

Within the limitations of this study,
1. Considering both the connection screw and the abutment, the loosening as a result of the first tightening with the torque wrench is greater than with the manually tightened, and the gap value increases.
2. Tightening a second time after preload significantly reduced the gap values, especially when a torque wrench was used. Therefore, tightening the implants using a torque wrench after preload plays an important role in preventing screw loosening.

REFERENCES

1. Karunagaran S, Markose S, Paprocki G, Wicks R. A systematic approach to definitive planning and designing single and multiple unit implant abutments. J. Prosthodont 2014;23:639-48.

2. Ramalho I, Witek L, Coelho PG, Bergamo E, Pegoraro LF, Bonfante EA. Influence of abutment fabrication method on 3D fit at the implant-abutment connection. Int J Prosthodont 2020;33:641-7.

3. Huang Y, Wang J. Mechanism of and factors associated with the loosening of the implant abutment screw: A review. J Esthet Restor Dent 2019;31:338-45.

4. Cibirka RM, Nelson SK, Lang BR, Rueggeberg FA. Examination of the implant-abutment interface after fatigue testing. J Prosthet Dent 2001;85:268-75.

5. Michalakis KX, Calvani PL, Muftu S, Pissiotis A, Hirayama H. The effect of different implant-abutment connections on screw joint stability. J Oral Implantol 2014;40:146-52.

6. Sakamoto K, Homma S, Takanashi T, Takemoto S, Furuya Y, Masao Y, Yajima Y. Influence of eccentric cyclic loading on implant components: comparison between external joint system and internal joint system. Dent Mater J 2016;35:929-37.

7. Pjetturson BE, Zarauz C, Strasding M, Sailer I, Zwahlen M, Zembic A. A systematic review of the influence of the implant-abutment connection on the clinical outcomes of ceramic and metal implant abutments supporting fixed implant reconstructions. Clin Oral Implants Res 2018;29:160–83.

8. Sailer I, Sailer T, Stawarczyk B, Jung R, Hammerle H. In vitro study of the influence of the type of connection on the fracture load of zirconia abutments with internal and external implant-abutment connections. Int J Oral Maxillofac Implants 2009;24:850-8.

9. Truninger TC, Stawarczyk B, Leutert CR, Sailer TR, Hammerle CHF, Sailer I. Bending moments of zirconia and titanium abutments with internal and external implant-abutment connections after aging and chewing simulation. Clin Oral Implants Res 2012;23:12-8.

10. Gracis S, Michalakis K, Vigolo P, Von Steyern PY, Zwahlen M, Sailer I. Internal vs. external connections for abutments/ reconstructions: a systematic review. Clin Oral Implants Res 2016;23:202-16.

11. Coppedê AR, De Mattos MG, Rodrigues RC, Ribeiro RF. Effect of repeated torque/mechanical loading cycles on two different abutment types with internal tapered connections: An *in vitro* study. Clin Oral Implants Res 2009;20:624-32.

12. Shafie HR, Martyna S. Clinical and Laboratory Manual of Dental Implant Abutments. 1st ed. Hoboken NJ: Wiley-Blackwell; 2014; p.23-24.

13. Bozkaya D, Muftu S, Muftu A. Evaluation of load transfer characteristics of five different implants in compact bone at different load levels by finite elements analysis. J Prosthet Dent 2004;92:523-30.

14. Chun HJ, Shin HS, Han CH, Lee SH. Influence of implant abutment type on stress distribution in bone under various loading conditions using finite element analysis. Int J Oral Maxillofac Implants 2006;21:195-202.

15. Maeda Y, Satoh T, Sogo M. In vitro differences of stress concentrations for internal and external hex implant-abutment connections: a short communication. J Oral Rehabil 2006;33:75-8.

16. Sarfaraz H, Paulose A, Shenoy KK, Hussain A. A three-dimensional finite element analysis of a passive and friction fit implant abutment interface and the influence of occlusal table dimesion on the stress distribution pattern on the implant and surrounding bone. J Indian Prosthodont Soc 2015;15:3.

17. Karl M, Taylor TD. Parameters determining micromotion at the implant-abutment interface. Int J Oral Maxillofac Implants 2014;29:1338-47.

18. Norton MR. Assessment of cold welding properties of the internal conical interface of two commercially available implant systems. J Prosthet Dent 1999;81:159-66.

19. Cho SC, Small PN, Elian N, Tarnow D. Screw loosening for standard and wide diameter implants in partially edentulous cases: 3- to 7- year longitudinal data. Implant Dent 2004;13:245-50.

20. Moris ICM, Faria ACL, Ribeiro RF, Rodrigues RCS. Torque loss of different abutment size before and after cyclic loading. Int J Oral Maxillofac Implants 2015;30:1256-61.

21. Hirayama PMA, Bohner LOL, Marotti J, Steagall W, Lagana DC, Tortamano P. Influence of Abutment Surface Treatments on Screw Loosening of Morse Taper Implants. Implant Dent 2017;26:718-22.

22. DE Kok IJ, Duqum Is, Katz LH, Cooper LF. Management of implant/prosthodontic complications. Dent Clin North Am 2018;2:217-31.

23. Nithyapriya S, Ramesh A. S, Kirubakaran A, Mani J, Raghunathan J. Systematic analysis of factors that cause loss of preload in dental implants. J Indian Prosthodont Soc 2018;18:189-95.

24. Pardal-Peláez B., Montero J. Preload loss of abutment screws after dynamic fatigue in single implant-supported restorations. A systematic review. J Clin Exp Dent 2017;9:1355-61.

25. Gupta S, Gupta H, Tandan A. Technical complications of implant- causes and management: A comprehensive review. Natl J Maxillofac Surg 2015; 6:3-8.

26. Bulaqi HA, Barzegar A, Paknejad M, Safari H. Assessment of preload, remaining torque, and removal torque in abutment screws under different frictional conditions: A finite element analysis. J Prosthet Dent 2019;121:e1-7.

27. Satpathy M, Jose RM, Duan Y, Girrigs JA. Effect of abutment screw preload and preload simulation techniques on dental implant lifetime. JADA found Sci 2022;1:1-18.

28. Gratton DG, Aquilino SA, Stanford CM. Micromotion and dynamic fatigue properties of the dental implant-abutment interface. J Prosthet Dent 2001;85:47-52.

29. Kourtis S, Damanaki M, Kaitatzidou S, Kaitatzidou A, Roussou V. J esthet Restor Dent 2017;29:233-46.

30. Development of a peak insertion torque prediction model for parallel-walled dental implants. Medical Engineering and Physics 2025;138:1-10.

31. Lang LA, Kang B, Wang RF, Lang BR. Finite element analysis to determine implant preload. J Prosthet Dent 2003;90:539-46.

32. Shetty M, Krishna Prasad D, Shetty NH, Jaiman R. Implant abutment connection: Biomechanical Perspectives. NUJHS 2014;4:47-53.

33. El-Sheikh MAY, Mostafa TMN, El-Sheikh MM. Effect of different angulations and collar lengths of conical hybrid implant abutment on screw loosening after dynamic cyclic loading. Int J Implant Dent 2018;4:1-12.

34. Parnia F, Yazdani J, Fakour P, Mahboub F, Pakdel SMV. Comparison of the maximum hand-generated torque by professors and postgraduate dental students for tightening the abutment screws of dental implants. J Dent Res Dent Clin Dent Prospects 2018;12:190-5.

35. Seloto CB, Strazzi-Sahyon, HB, dos Santos, PH, Assunção VG. Effectiveness of Sealing Gel on Vertical Misfit at the Implant-Abutment Interface and Preload Maintenance of Screw-Retained Implant-Supported Prostheses. Int J Oral Maxillofac Implants 2020;35:479-84.

36. Binon PP. Implants and components: Entering the new millennium. Int J Oral Maxillofac Implants 2000;15: 76-94.

37. Meng JC, Everts JE, Qian F, Gratton DG (2007). Influence of connection geometry on dynamic micromotion at the implant-abutment interface. Int J Prosthodont;20: 623-5.

Ön Yüklemenin Farklı İmplant Abutmentlerindeki Vida Gevşemesine Etkisi

ÖZET

Amaç: Bu çalışmanın amacı; uygun ön yüklemenin yapıldığı veya yapılmadığı durumlarda implant-abutment bağlantısının mekanik davranışını karşılaştırmaktır.

Gereç ve Yöntemler: Bu çalışmada çapı 3.5 mm olan toplam 54 adet kemik seviyesi implant kullanılmıştır. Her grup, her biri manuel ve tork anahtarıyla sıkılan alt gruplara ayrılmış ve ilk üçü kontrol grubu olmak üzere toplam 6 grup test edilmiştir. Manuel sıkma aynı araştırmacı tarafından maksimum kişisel kuvvetle, el tornavidası ile sıkma ise aynı araştırmacı tarafından 30 Ncm değerinde gerçekleştirilmiştir. Bağlantı uyumunun mikro-BT kullanılarak değerlendirildiği örnek ölçüm değerleri elde edilmiştir

Bulgular: Vida ile implant gövdesi arasındaki toplam boşluk hacmi, tek sıkılan örneklere göre (minimum 0.32 mm^3) ikinci kez sıkılan örneklerde önemli ölçüde azalmıştır (minimum 0.20 mm^3). Bununla birlikte açılı abutment grubu dışında, manuel veya tork anahtarıyla ikinci kez sıkma arasında bir fark gözlenmemiştir.

Sonuç: Ön yüklemeden sonra ikinci kez sıkma, özellikle tork anahtarı kullanıldığında boşluk değerlerini önemli ölçüde azalttı. Bu nedenle, ön yüklemeden sonra implantları tork anahtarı kullanarak ve tekrarlayarak sıkmak klinik olarak hasta ağızında vida gevşemesini dolayısıyla vida kırıkları gibi büyük klinik problemleri önlemede önemli bir rol oynar.

Anahtar Kelimeler: Dental İmplant; Ön yükleme; Vida Gevşemesi

DOI: https://doi.org/10.54617/adoklinikbilimler.1555752

Original Research Article

Effect of Energy Drinks on Color Stability and Surface Roughness of Nanohybrid and Micro-Hybrid Resin Composites

Sevim Atılan Yavuz*, Ayşe Tuğba Ertürk Avunduk, Gökçe Yıldız, Esra Cengiz Yanardağ

Department of Restorative Dentistry, Faculty of Dentistry, Mersin University, Mersin, Türkiye

ABSTRACT

Aim: This study was to evaluate the color stability and surface roughness of conventional resin composites after immersion with two different energy drinks.

Materials and Methods: 66 disc specimens (6 x 2 mm) were prepared from micro-hybrid (G-ænial Posterior) and nano-hybrid (Clearfil Majesty Esthetic) resin composites. Post-polymerization was conducted by storing all specimens in distilled water at 37 °C for 24 hours. Baseline color and surface roughness (Ra) measurements were performed, after which the specimens were randomly divided into three groups (n=11/subgroup) according to the immersion solution used: Group 1 (distilled water), Group 2 (Red Bull), and Group 3 (Burn). After 7 days of immersion, final measurements were recorded. Color variations (ΔE_{00}) were determined using a spectrophotometer and the CIEDE2000 formula before and after the immersion. Data were subjected to ANOVA analysis (α = 0.05).

Results: There were no statistically significant differences in color stability between the nanohybrid and micro-hybrid resin composites ($p > 0.05$). Both resin composites exhibited color changes exceeding the AT threshold (> 1.8) and the PT threshold (> 0.8). The highest ΔE_{00} values were found in the specimens exposed to Red Bull. Specimens in distilled water showed ΔE_{00} values below the AT threshold (< 1.8). In terms of Ra values, significant differences were noted between the materials in both the Ra0 and Ra1 measurement intervals ($p < 0.001$ and $p = 0.002$). The Clearfil Majesty Esthetic specimens had the highest surface roughness, with Red Bull resulting in the greatest Ra values.

Conclusion: Over the 1-week immersion period, all tested solutions led to increased color changes and surface roughness in the restorative materials.

Keywords: Color stability; Energy drink; Resin composite; Surface roughness

Citation: Atılan Yavuz S, Ertürk Avunduk AT, Yıdız G, Cengiz Yanardağ E. Effect of Energy Drinks on Color Stability and Surface Roughness of Nanohybrid and Micro-Hybrid Resin Composites. ADO Klinik Bilimler Dergisi 2026;15(2):86-94

Editor: Sinem Akgül, Gazi University, Ankara, Türkiye.

INTRODUCTION

Resin composites serve as esthetic restorative materials for both anterior and posterior applications. The size and quantity of fillers significantly influence the physical and mechanical properties of these composites. Despite ongoing advancements by manufacturers to enhance these properties, resin composites remain vulnerable to chemical degradation.[1] This degradation can adversely affect surface roughness, leading to increased susceptibility to staining.[2]

The quality of the surface of resin composite restorations is critical for their long-term clinical success. Increased surface roughness can promote plaque accumulation, resulting in undesirable stained restorations and potential failure.[3] Factors effecting the clinical performance of resin composites include filler content, particle size, instruments used, finishing techniques, and environmental influences in the oral cavity. Notably, composites with smaller filler sizes tend to exhibit smoother surfaces. Nanotechnology-based composites, which incorporate nanofillers, are designed to enhance clinical outcomes compared to their microhybrid counterparts, thanks to the inclusion of sub-micrometer particles that improve optical and physical properties.[4]

Received: 09.27.2024; Accepted: 02.03.2026
**Corresponding author: Dr. Sevim Atılan Yavuz*
Department of Restorative Dentistry, Faculty of Dentistry, Mersin University, Mersin, Türkiye
E-mail:dtsevimatilan@gmail.com

Recently, energy drink consumption has surged, particularly among adults aged 18 to 35, who often seek these beverages for energy and fatigue relief. Energy drinks typically contain caffeine, taurine, glucuronolactone, vitamin B, and citric acid, the latter contributing to their low pH.[5] This acidic environment can compromise restorative dental materials by leaching fillers from the resin matrix, resulting in increased surface roughness. Furthermore, the synthetic dyes in these drinks can negatively impact the color stability of various resin restorative materials through both adsorption and absorption processes.[6]

Based on our knowledge, little information is available about the effect of energy drinks on the color stability and structural effects of resin composites. Given the routine consumption of acidic beverages like energy drinks, this study aimed to evaluate the impact of various energy drinks on the color change and surface roughness of micro-hybrid and nano-hybrid resin composites. The null hypotheses tested in this study were: i) There is no difference in color change among resin composites when exposed to different energy drinks; ii) There is no difference in surface roughness among resin composites due to different energy drinks.

MATERIALS AND METHODS

This study adhered to the ethical principles outlined in the Declaration of Helsinki and received approval from the Clinical Research Ethics Committee of Mersin University (no. 2024/885).

The study examined two independent variables: types of resin composites and various energy drinks. The dependent variables were color change and surface roughness. Sample size calculations were performed using G*Power software (Version 3.1.9.4, Heinrich Heine University, Düsseldorf, Germany), with a significance level of 0.05 and a power of 80%, resulting in the required sample size of 66 specimens. A flowchart of the study design is presented in Figure 1.

1. Specimen preparations

A total of 66 standardized disc specimens (6 x 2 mm) were prepared using a Teflon mold, creating 33 specimens for each restorative material: microhybrid resin composite (G-ænial Posterior (GP), GC Dental Products, Alsip, IL, USA) and nanohybrid resin com-

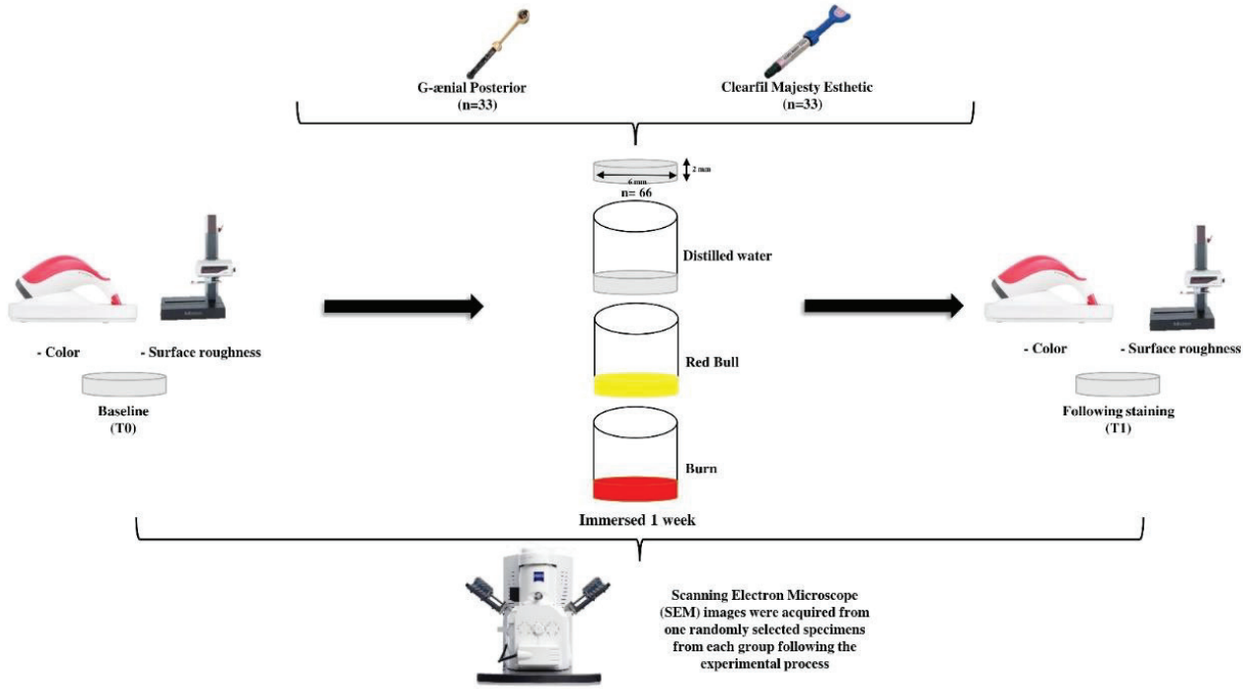

Figure 1. Flow chart of the study.

posite (Clearfil Majesty Esthetic (CME), Kuraray, Okayama, Japan). A glass plate and a Mylar strip were employed to ensure uniform thickness and consistent distance from the light-curing tip during polymerization. Specimens were polymerized with a light emitting diode (LED) light-curing unit (SmartLite Pro, Dentsply, Germany) at a light intensity of 1200 mW/cm² for 20 seconds. After polymerization, specimens were polished with aluminum oxide-impregnated discs (SofLex, 3M ESPE, St. Paul, MN, USA), immersed in distilled water for post-polymerization, and stored at 37 °C for 24 hours. Specimens were then divided into three groups (n = 11) based on immersion solutions: Group 1 (distilled water), Group 2 (Red Bull GmbH, pH ≈ 3.54), and Group 3 (Burn, The Coca-Cola Co., pH ≈ 2.67). Details regarding the manufacturers and compositions of the restorative materials and energy drinks are provided in Table 1.

2. Immersion solutions preparation

A pH meter (Hanna Instruments, Padova, Italy) was used to measure the pH levels of energy drinks. Specimens were immersed in containers ensuring full exposure to the staining solution. To minimize evaporation, solutions were sealed throughout the study. Specimens were maintained in an incubator at 37 °C, except during solution changes and measurements.

3. Color assessment process

Colorimetric evaluations were conducted at baseline (T0) and after immersion in energy drinks (T1) using a digital spectrophotometer (Vita Easyshade V; Vita Zahnfabrik, Bad Säckingen, Germany). Measurements were taken in triplicate, and mean values were recorded according to Commission Internationale de l'Eclairage (CIE) parameters. The spectrophotometer was calibrated before each test group measurement. Color differences (ΔE_{00}) were calculated using the CIEDE2000 formula:[7]

$$\Delta E_{00} = \left[\left(\frac{\Delta L}{k_L S_L}\right)^2 + \left(\frac{\Delta C}{k_C S_C}\right)^2 + \left(\frac{\Delta H}{k_H S_H}\right)^2 + R_T\left(\frac{\Delta C}{k_C S_C}\right)\left(\frac{\Delta H}{k_H S_H}\right)\right]^{1/2}$$

The parameters kL, kC, and kH serve as correction terms for experimental variations and were standardized to 1.0 in this study. CIEDE2000 values were assessed based on (PT) and (AT) thresholds of 0.8 and 1.8, respectively.[8]

Table 1. Composition and manufacturer information of restorative materials and energy drinks used in the study.

Product	Manufacturer	Composition	Code
G-ænial Posterior (A2) (Micro-hybrid composite resin)	GC, Dental Products, Alsip, IL, USA	UDMA, methacrylate monomers, ytterbium trifluoride, prepolymerized fillers, fluoroaluminosilicate, silica, camphorquinone and amine	GP
Clearfil Majesty Esthetic (A2) (Nano-hybrid composite resin)	Kuraray Noritake Dental, Tokyo, Japan	Bis-GMA, silanated barium glass filler, silanated silica filler, camphroquinone and pre-polymerized organic filler	CME
Red Bull	Red Bull GmbH, Austria	Water, sucrose, glucose, acidifier sodium citrates, carbon dioxide, taurine (0.4%), glucuronolactone (0.24%), caffeine (0.03%), inositol, vitamins (niacin, pantothenic acid, B6, B12), flavourings, and colours (caramel, riboflavin).	-
Burn	The Coca-Cola Company, Atlanta, Georgia	Carbonated water, sucrose, citric acid, taurine (0.4%), acidity regulator: sodium citrate, coloring agents: E163, E150d, preservatives: potassium sorbate, sodium benzoate, flavor, caffeine (0.03%), inositol, vitamins [nicotinamide (B3), d-calcium pantothenate, pyridoxine hydrochloride (B6), cyanocobalamin (B12)], seed extract of guarana (0.005%), antioxidants (ascorbic acid)	-

Abbreviations: Bis-GMA: bisphenol A glycerolate dimethacrylate; UDMA: urethane dimethacrylate.

4. Surface roughness assessment process

Surface roughness (Ra) was evaluated using a contact mode profilometer (Mitutoyo, Surftest SJ-410, Japan). The measuring distance was 4 mm and a cut-off value of 0.8 mm. Measurements were taken at three different locations for each specimen at baseline (T0) and following immersion (T1), with mean Ra values calculated. A Ra threshold of 0.2 µm was established.[9]

5. Experimental groups

After baseline measurements, specimens were randomly divided into three subgroups (n=11):

- Group 1: Control (Distilled water, no staining)
- Group 2: Immersed in Red Bull energy drink at 37°C for seven days
- •Group 3: Immersed in Burn energy drink at 37°C for seven days

The color and surface roughness measurements were repeated after staining (T1) process.

6. Scanning Electron Microscope (SEM) analysis

Two additional specimens from each material (GP and CME) were prepared for SEM analysis to represent Group 1 (control), Group 2 (Red Bull), and Group 3 (Burn). Specimens were sputter-coated with palladium and examined using a SEM (EVO 18; Zeiss, Wetzlar, Germany) at Mersin University Advanced Technology Education Research and Application Center, under specific magnification (x 5000) and voltage settings.

7. Statistical analysis

Data were analysed with the Statistical Package for the Social Sciences (SPSS Inc., Version 23, Chicago, IL, USA). The data's conformity to a normal distribution was evaluated using the Kolmogorov-Smirnov and Shapiro-Wilk tests. The mean values and standard deviations (SD) were compared using two-way ANOVA and Tukey's post hoc test at $p < 0.05$.

RESULTS

Table 2 displays the mean ΔE_{00} values of the restorative materials following immersion in various energy drinks. As the statistical analysis that there was no significant difference between the mean ΔE_{00} values according to the materials ($p > 0.05$). There was a statistically significant difference between the mean ΔE_{00} values according to the solutions ($p = 0.001$). The ΔE_{00} values of the staining groups (Red Bull and Burn) were obtained as 4.11 and 3.54. The control group was significantly different from the others. The mean ΔE_{00} value of the GP was 3.49 and 2.75 of the CME. The highest ΔE_{00} values was obtained with 6.34 of the GP*Red Bull interaction, while the lowest value was obtained with 0.71 of the GP*control group. In general, the color change of all interactions (except GP*control group) was exceeded the AT threshold (> 1.8) and PT threshold (> 0.8).

The mean Ra values and SD of the restorative materials are shown in Table 3. A statistically significant difference was observed between Ra0 and Ra1 values according to the material ($p < 0.001$ and $p = 0.002$). The total Ra0 and Ra1 values of the GP

Table 2. Descriptive statistics and multiple comparison results of ΔE_{00} according to restorative materials and solutions.

	ΔE_{00}		
	Restorative Materials		
Solutions	**GP**	**CME**	**Total**
Distilled water	$0.71\pm0.29^{A, a}$	$2.56\pm1.38^{B, b}$	1.64 ± 1.36^{a}
Red Bull	$6.34\pm4.50^{B, b}$	$2.03\pm1.18^{A, a}$	4.11 ± 3.89^{b}
Burn	3.41 ± 1.80^{b}	3.66 ± 1.28^{b}	3.54 ± 1.52^{b}
Total	3.49±3.58	2.75±1.42	

Abbreviations: GP: G-ænial Posterior; CME: Clearfil Majesty Esthetic
A, b: Values indicated by different small letters on the same column are statistically significantly different
A, B: Values indicated by different big letters on the same line are statistically significantly different
* Two-way ANOVA, Tukey's post hoc test

Table 3. Descriptive statistics and multiple comparison results of Ra according to restorative materials and solutions.

		Ra		
		Restorative Materials		
Solutions		**GP**	**CME**	**Total**
Distilled water	Ra0	0.14±0.09^{A}	0.66±0.66^{B}	0.40±0.53
	Ra1	0.47±0.52	0.62±0.68	0.55±0.59^{y}
Red Bull	Ra0	0.13±0.12	0.29±0.19^{a}	0.21±0.18^{a}
	Ra1	0.36±0.45^{A}	1.40±1.04$^{B, b}$	0.88±0.89$^{b, x}$
Burn	Ra0	0.18±0.14^{A}	0.59±0.34^{B}	0.39±0.33
	Ra1	0.20±0.19^{A}	0.97±0.95^{B}	0.58±0.77^{y}
Total	Ra0	0.15±0.12$^{A, a}$	0.51±0.46^{B,a}	
	Ra1	0.34±0.41$^{A, b}$	0.92±0.90^{B,b}	

Abbreviations: GP: G-ænial Posterior; CME: Clearfil Majesty Esthetic
a, b: Values indicated by different small letters on the same column are statistically significantly different
x, y: Values indicated by different small letters on the same column are statistically significantly different (for total Ra1 values of staining solutions)
A, B: Values indicated by different big letters on the same line are statistically significantly different
* Two-way ANOVA, Tukey's post hoc test

(0.15 and 0.34) were significantly higher than CME (0.51 and 0.92). There was a statistically significant difference between the mean Ra1 values according to the solutions (p = 0.002). The Ra1 values of the groups were 0.55, 0.88, and 0.58, respectively. Red Bull group was statistically different from the others. Regardless of the restorative material used, the Ra1 value of all energy drinks was significantly higher than the Ra0 value in Group 2, and similar in Group 1 and Group 3. While the highest Ra1 values was obtained with 1.40 in CME*Red Bull interaction, the lowest Ra0 values was in GP*Red Bull interaction.

Figure 2 presents SEM images of each restorative material (GP and CME). The SEM micrographs of the CME specimens treated with Red Bull exhibited increased surface porosity (Figure 2.e). Furthermore, the CME specimens showed more alterations compared to GP, particularly after immersion in Red Bull and Burn (Figure 2e-b and Figure 2f-c, respectively).

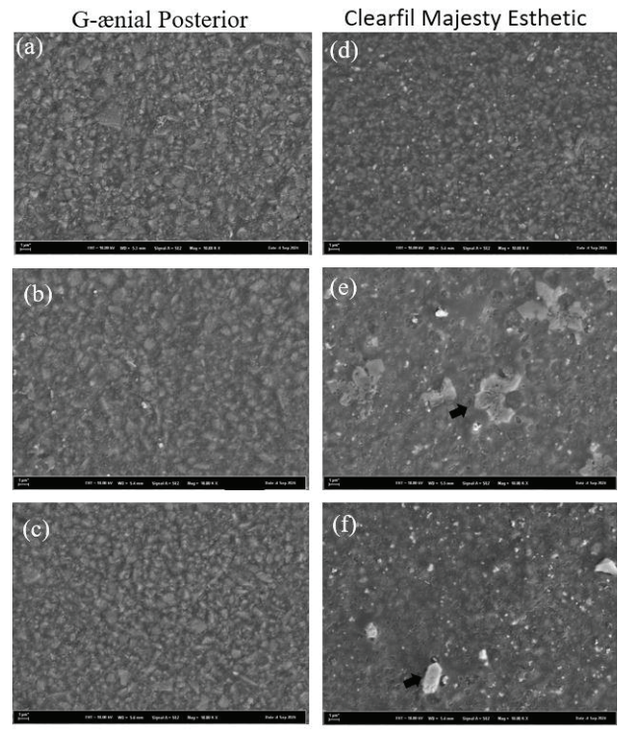

Figure 2. SEM images of the experimental groups a) Distilled water*G-ænial Posterior b) Red Bull*G-ænial Posterior c) Burn*G-ænial Posterior d) Distilled water*Clearfil Majesty Esthetic e) Red Bull*Clearfil Majesty Esthetic f) Burn*Clearfil Majesty Esthetic.

DISCUSSION

Dental resin composites can easily stain from food and beverages in the oral cavity, primarily due to the interaction between external colorants and the

resin. Colorants can either adhere to the surface or penetrate the resin matrix, resulting in discoloration that negatively effects esthetics.[10] Moreover, exposure to acidic staining solutions may alter the mechanical, physical, and esthetic properties of these restorative materials.[11] This study aimed to investigate how various energy drinks effect the color stability and surface roughness of micro-hybrid and nano-hybrid resin composites. The first hypothesis was supported, as the restorative materials showed comparable color changes after immersion in energy drinks.

The results indicated that all resin composites tested exhibited significant color changes beyond clinically AT (> 1.8). Among the materials, the micro-hybrid composite (GP) was more susceptible to color change than the nano-hybrid composite (CME). This aligns with previous findings indicating that nano-hybrid composites generally show better resistance to staining.[12] The resin matrix's type and composition influence its hydrophilicity, which is crucial for long-term color stability. Factors like filler size and distribution also effect surface roughness, polishability, and water absorption.[13] While a higher filler-to-resin ratio could lower water absorption and staining susceptibility, the size of the fillers remains debated, especially when comparing micro-hybrid and nano-hybrid composites. In nano-hybrid composites, smaller particles may break off during polishing, creating fewer voids than in micro-hybrids.[14] Thus, it's expected that the nano-hybrid composite with smaller particle size would show less color change in this study.

The color stability of resin composites was evaluated by immersing them in two energy drinks (Red Bull and Burn) and distilled water as a control for one week. Previous reviews noted that immersion periods in studies varied greatly, from 1 to 365 days, with many using a 7-day duration, which typically led to notable color changes that exceeding the PT and AT.[15,16] Based on these findings, a 7-day immersion protocol was adopted for the specimens in the present study.

The study's findings demonstrated that both energy drinks produced substantial discoloration. This effect is attributed to the low pH values of the beverages, which soften the resin matrix and enhance pigment uptake.[5] Our study contradicts the findings of Erdemir *et al*.[8], as Red Bull exhibited a numerically higher, yet statistically nonsignificant, color change compared to Burn. These discrepancies are likely attributable to the extended immersion durations of 1 and 3 months applied in Erdemir *et al*.[17] experimental protocol.

In the present study, the highest ΔE_{00} value (6.34) was observed in the GP*Red Bull group. In contrast to our findings, a previous investigation evaluating the effects of various acidic fruit juices on microhybrid and nanohybrid resin composites reported greater color stability in the microhybrid material.[18] This inconsistency between the two studies is likely attributable to differences in the types of beverages and their respective pH levels.[18] Additionally, bisphenol A glycerolate dimethacrylate (Bis-GMA) based resin matrices are known to exhibit increased water sorption due to their hydrophilic characteristics, resulting in reduced stain resistance compared with other methacrylate monomers such as urethane dimethacrylate (UDMA).[19] In the present study, the statistically significant difference observed between the two restorative materials in distilled water is therefore attributed to the presence of Bis-GMA within the monomer composition of CME.

In the present study, the surface roughness of the micro-hybrid and nano-hybrid restorative materials were evaluated following exposure to acidic energy drinks, which are widely consumed. The two tested resin composites demonstrated significant changes in surface roughness after one week of immersion in the solutions. It is known that the surface roughness of the resin composites were effected to the filler type and size, type of resin matrix, and staining agent.[17] In the literature it has been reported that resin composites with smaller particle sizes exhibit lower surface roughness.[20] Although it was expected that a nanohybrid resin composite would show higher surface roughness than a microhybrid, in the current study, nano-hybrid CME had higher surface roughness than micro-hybrid GP. Sideridou *et al*.[21] reported that UDMA-based resins containing carbamate linkages exhibit less water sorption than Bis-GMA-based resins, containing highly polar hydroxyl groups. Contrary to expectations, it is thought that the higher surface roughness of CME is due to the Bis-GMA in its structure and the presence of UDMA in the structure of GP, which shows lower

water absorption compared to Bis-GMA. And also, the previous studies were shown that glass filler particles tend to fall out from the material and the matrix component decomposes due to acidic environment.[22,23] Although CME has a nanohybrid structure, it has shown higher surface roughness, which can be attributed to the glass filler content.

Because many energy drinks exhibit pH values of 3.0 or lower, prolonged exposure has the potential to erode both tooth enamel and resin composite surfaces.[24] In accordance with previous literature, the results of the present study demonstrated that all energy drinks increased the surface roughness of the restorative materials; however, a statistically significant difference was observed only for Red Bull.[23,25] Consequently, the second null hypothesis—asserting that surface roughness would not differ among resin composites exposed to various energy drinks—was partially rejected. Although increased surface roughness was anticipated primarily in specimens exposed to the lower-pH beverage Burn (pH 2.67), Red Bull (pH 3.54) unexpectedly produced greater surface roughness in our study.

In dentistry, measurement devices such as contact profilometry, laser profilometry, SEM, and 3-dimensional (3D) optical profilometry are used for quantitative and qualitative measurement of surface roughness. However, after the contact profilometer, which provides quantitative findings, supporting it with qualitative data obtained from the SEM device increases the accuracy of surface roughness. As in many studies in the literature, the data obtained with the profilometer in the current study was supported and detailed by SEM images (Figure 2).[26,27] Considering the mean values obtained, it is seen that the highest surface roughness is in Figure 2.e in the SEM images, which supports the numerical data.

The resin composites tested in this in-vitro study do not represent all the experimental conditions to which restorative materials may be exposed in the complex oral environment. Therefore, the present study confirmed that acidic energy drinks had a detrimental effect on the color change and surface roughness of composite resin restorative materials, however it remained to be known if the durability of restorative materials would be thus adversely affected in the oral environment. Moreover, no mechanical assessment of the effect energy drinks on resin composites exists. Further studies are needed to investigate the long-term clinical and in-vitro performance of restorative materials against energy drinks.

CONCLUSION

Within the limitations of this study, it was concluded that all tested solutions increased the restorative materials' color change and surface roughness over a 1-week immersion period. Despite showing similar values, the nano-hybrid resin composite (CME) showed slightly lower color change than the micro-hybrid resin composite (GP). SEM analysis showed that before and after staining, regardless of solutions, micro-hybrid resin composite (GP) showed lower surface roughness than nano-hybrid resin composite (CME). Red Bull energy drink caused the greatest increase in both parameters of resin composites.

ACKNOWLEDGMENTS

The authors thank Seher Kuru, Mersin University Advanced Technology Education Research and Application Center, for SEM images.

CONFLICTS OF INTEREST STATEMENT

The authors declared that there is no conflict of interest.

REFERENCES

1. e Silva MLdA, da Cunha Medeiros FDS, Meireles SS, Duarte RM, Andrade AKM. The effect of drinks on color stability and surface roughness of nanocomposites. Eur J Dent; 2014;8:330-6.

2. Van Groeningen G, Jongebloed W, Arends J. Composite degradation *in vivo*. Dent Mater; 1986;2:225-7.

3. Zhang L, Yu P, Wang X-Y. Surface roughness and gloss of polished nanofilled and nanohybrid resin composites. J Dent Sci 2021;16:1198-203.

4. Antonson SA, Yazici AR, Kilinc E, Antonson DE, Hardigan PC. Comparison of different finishing/polishing systems on surface roughness and gloss of resin composites. J Dent 2011;39:e9-e17.

5. Erdemir U, Yildiz E, Eren MM, Ozel S. Surface hardness evaluation of different composite resin materials: influence of sports and energy drinks immersion after a short-term period. J Appl Oral Sci 2013;21:124-31.

6. Iazzetti G, Burgess J, Gardiner D, Ripps A. Color stability of fluoride-containing restorative materials. Oper Dent 2000;25:520-5.

7. Sharma G, Wu W, Dalal EN. The CIEDE2000 color-difference formula: Implementation notes, supplementary test data, and mathematical observations. Color Research & Application: Endorsed by Inter-Society Color Council, The Colour Group (Great Britain), Canadian Society for Color, Color Science Association of Japan, Dutch Society for the Study of Color, The Swedish Colour Centre Foundation, Colour Society of Australia, Centre Français de la Couleur 2005;30:21-30.

8. Paravina RD, Pereira Sanchez NA, Tango RN. Harmonization of color measurements for dental application. Color Res Appl 2020;45:1094-100.

9. Devlukia S, Hammond L, Malik K. Is surface roughness of direct resin composite restorations material and polisher-dependent? A systematic review. J Esthet Restor Dent 2023;35:947-67.

10. Faraoni JJ, Quero IB, Schiavuzzo LS, Palma-Dibb RG. Color stability of nanohybrid composite resins in drinks. Brazilian J Oral Sci 2019;18:e191601-e191601.

11. Al-Haj Ali S, Alsulaim H, Albarrak M, Farah R. Spectrophotometric comparison of color stability of microhybrid and nanocomposites following exposure to common soft drinks among adolescents: An *in vitro* study. Eur Arch Paediatr Dent 2021;22:675-83.

12. Al-Shami AM, Alshami MA, Al-Kholani AI, Al-Sayaghi A-AM. Color stability of nanohybrid and microhybrid composites after immersion in common coloring beverages at different times: a laboratory study. BDJ open 2023;9:39.

13. Ferooz M, Bagheri R, Jafarpour D, Burrow M. Physical properties of nanohybrid and microhybrid resin composites subjected to an acidic environment: a laboratory study. Oper Dent 2020;45:E105-E113.

14. Turssi CP, Ferracane JL, Serra MC. Abrasive wear of resin composites as related to finishing and polishing procedures. Dent Mater 2005;21:641-8.

15. Paolone G, Formiga S, De Palma F, Abbruzzese L, Chirico L, Scolavino S, *et al*. Color stability of resin-based composites: Staining procedures with liquids—A narrative review. J Esthet Restor Dent 2022;34:865-87.

16. Ozkanoglu S, Akin E. Evaluation of the effect of various beverages on the color stability and microhardness of restorative materials. Niger J Clin Pract 2020;23:322-8.

17. Erdemir U, Yıldız E, Eren MM. Effects of sports drinks on color stability of nanofilled and microhybrid composites after long-term immersion. J Dent 2012;40:e55-e63.

18. Meshki R, Rashidi M. Effect of natural and commercially produced juices on colour stability of microhybrid and nanohybrid composites. BDJ open 2022;8:11.

19. Villalta P, Lu H, Okte Z, Garcia-Godoy F, Powers JM. Effects of staining and bleaching on color change of dental composite resins. J Prosthet Dent 2006;95:137-42.

20. Rodrigues-Junior S, Chemin P, Piaia P, Ferracane J. Surface roughness and gloss of actual composites as polished with different polishing systems. Oper Dent 2015;40:418-29.

21. Sideridou I, Tserki V, Papanastasiou G. Study of water sorption, solubility and modulus of elasticity of light-cured dimethacrylate-based dental resins. Biomaterials 2003;24:655-65.

22. Han L, Okamoto A, Fukushima M, Okiji T. Evaluation of flowable resin composite surfaces eroded by acidic and alcoholic drinks. Dent Mater J 2008;27:455-65.

23. Kitchens M, Owens B. Effect of carbonated beverages, coffee, sports and high energy drinks, and bottled water on the *in vitro* erosion characteristics of dental enamel. J Clin Pediatr Dent 2007;31:153-9.

24. Al-Samadani KH. Effect of energy drinks on the surface texture of nanofilled composite resin. J Contemp Dent Pract 2013;14:830-5.

25. Bagheri R, Tyas MJ, Burrow MF. Subsurface degradation of resin-based composites. Dent Mater 2007;23:944-51.

26. Avunduk ATE, Delikan E. Effect of effervescent C vitamins on the surface roughness and color stability of composite resins: A SEM study. J Biotechnol and Strategic Health Res 2023;7:43-53.

27. Oglakci B, Kucukyildirim B, Özduman Z, Eliguzeloglu Dalkilic E. The effect of different polishing systems on the surface roughness of nanocomposites: contact profilometry and SEM analyses. Oper Dent 2021;46:173-87.

Enerji İçeceklerinin Nanohibrit ve Mikro-Hibrit Rezin Kompozitlerin Renk Değişimi ve Yüzey Pürüzlülüğü Üzerindeki Etkileri

ÖZET

Amaç: Bu çalışmanın amacı enerji içeceklerinin nano-hibrit ve mikro-hibrit rezin kompozitlerin renk değişimi ve yüzey pürüzlülüğü üzerindeki etkilerini değerlendirmektir.

Gereç ve Yöntemler: Her bir rezin kompozit [G-ænial Posterior (mikro-hibrit) ve Clearfil Majesty Esthetic (nano-hibrit)] için 33 örnek (6 x 2 mm) hazırlandı. Post-polimerizasyon için tüm numuneler, 24 sa 37 °C'de distile suda bekletildi. Renk ve yüzey pürüzlülüğünün (Ra) başlangıç ölçümlerinin ardından, numuneler test edilen solüsyonlara göre rastgele üç gruba (n = 11/grup) Grup 1 (distile su), Grup 2 (Red Bull) ve Grup 3 (Burn) dağıtıldı. Numuneler 1 hf boyunca enerji içeceği çözeltilerine daldırıldı. ΔE_{00} değerleri test prosedüründen önce ve sonra CIEDE2000 formülü kullanılarak bir spektrofotometre ile hesaplandı. Yüzey pürüzlülüğü ölçümleri tekrarlandı. İki yönlü varyans analizi ve Tukey'in post-hoc testi yapıldı. Anlamlılık düzeyi $p < 0.05$ olarak kabul edildi.

Bulgular: Nanohibrit ve mikro-hibrit rezin kompozitler arasında istatistiksel bir fark tespit edilmedi ($p > 0.05$). İki rezin kompozitin

renk değişimi AT (> 1.8) ve PT eşiğinin (> 0.8) üzerindeydi. En yüksek ΔE_{00}, Red Bull ile muamele edilen numunelerde gözlendi. Distile suda ΔE_{00} değerleri AT eşiğinin altında kalmıştır (< 1.8). Ra değerlerine göre, hem Ra0 hem de Ra1 zaman periyotlarında restoratif materyaller arasında anlamlı farklılıklar görüldü (p = 0.000 ve p = 0.002). En yüksek yüzey pürüzlülüğü Clearfil Majesty Esthetic numunelerinde gözlendi. Red Bull enerji içeceği en yüksek Ra değerlerine neden oldu.

Sonuç: Test edilen tüm solüsyonlar, 1 hf daldırma süresi boyunca restoratif materyallerin renk değişimini ve yüzey pürüzlülüğünü artırmıştır.

Anahtar Kelimeler: Renk stabilitesi; Enerji içeceği; Rezin kompozit; Yüzey pürüzlülüğü

DOI: https://doi.org/10.54617/adoklinikbilimler.1801099

Original Research Article

Influence of Material Type, Thickness, and Cement Type on Optical Properties of CAD/CAM Laminate Restorations

Lena Bal[1*], **Nihan Gönülol**[2]

[1]*Department of Restorative Dentistry, Faculty of Dentistry, Ankara Medipol University, Ankara, Türkiye*
[2]*Department of Restorative Dentistry, Faculty of Dentistry, 19 Mayıs University, Samsun, Türkiye*

ABSTRACT

Aim: The long-term success of laminate restorations depends not only on their mechanical strength but also on the stability of their optical properties. This study aimed to evaluate the effects of CAD/CAM material type, thickness, and cement type on color change (ΔE00) and translucency parameter differences (ΔTP) of laminate restorations after UV aging.

Materials and Methods: A total of 200 specimens were prepared from five different CAD/CAM materials (CEREC feldspathic block, Cerasmart block, Vita Enamic block, Lava Ultimate block, and Grandio CAD/CAM block) and two thicknesses (0.7 mm and 1.2 mm). Specimens were divided according to cement type (dual-cure and light-cure). Color measurements (L*, a*, b*) were performed before and after UV aging, and color and translucency differences (ΔE_{00} and ΔTP) were calculated using the CIEDE2000 formula. UV aging was applied as an artificial aging procedure and was not included as an independent variable in the statistical analysis. Data were analyzed using three-way ANOVA according to material type, thickness, and cement type ($p < 0.05$).

Results: Material type significantly influenced color changes (ΔE_{00}) and the translucency parameter differences (ΔTP). Among the tested groups, the CEREC block (1.1 ± 0.3) demonstrated the least color change. In contrast, the Lava Ultimate block (12.7 ± 0.5) exhibited the most significant color change ($p < 0.05$). The lowest ΔTP differences were observed for Lava Ultimate block (-0.2 ± 0.2), Vita Enamic (-0.3 ± 0.4), and Cerasmart (-0.1 ± 0.4) ($p < 0.05$).

Conclusion: All groups exhibited color changes that exceeded both the perceptibility and clinical acceptability thresholds. Changes observed after UV aging indicated a decrease in translucency. Among the evaluated factors, material type was identified as the most critical factor affecting ΔE_{00} values, while specimen thickness was the main determinant of ΔTP.

Keywords: Computer-Aided Design; Cosmetic Dentistry; Dental Laminates; Prosthodontics

Citation: Bal L, Gönülol N. Influence of Material Type, Thickness, and Cement Type on Optical Properties of CAD/CAM Laminate Restorations. ADO Klinik Bilimler Dergisi 2026;15(2):95-104

Editor: Yeliz Kılınç, Gazi University, Ankara, Türkiye

INTRODUCTION

With the continuous evolution of aesthetic standards and the increasing adoption of digital systems for anterior laminate restorations, the optical properties of CAD/CAM glass-based blocks have become increasingly significant. Consequently, pre-sintered feldspathic ceramics, such as the CEREC block (Dentsply Sirona, Germany), which exhibit high color stability, are widely preferred for anterior restorations. Over time, the integration of resin components to enhance flexibility and strength has further improved the color stability of ceramics, resulting in the development of novel CAD/CAM glass-based materials.[1]

Hybrid ceramic blocks, such as the Vita Enamic (VITA Zahnfabrik, Germany) polymer-infiltrated ceramic network, are particularly noteworthy for their unique structure, in which polymer particles infiltrate a ceramic framework. In contrast, Cerasmart (GC, Japan) and Lava Ultimate (3M ESPE, USA) blocks, both classified as resin nanoceramic structures, differ from hybrid ceramics because their resin matri-

Received: 10.13.2025; Accepted: 03.12.2026
**Corresponding author: Dr. Lena Bal*
Department of Restorative Dentistry, Faculty of Dentistry, Ankara Medipol University, Eti, Celal Bayar Blvd, No:88/1, Çankaya, Ankara, Türkiye
E-mail: lena.almasifar@ankaramedipol.edu.tr

ces are reinforced by embedding glass and ceramic fillers. Among advanced CAD/CAM restorative materials, Grandio blocks (VOCO, Germany) stand out for their nanohybrid composition, high particulate and filler load, superior flexural strength and wear resistance, polishability, and improved aesthetic qualities.[2]

The optical properties of laminate restorations, which are essential for achieving aesthetic success, are strongly influenced by the color compatibility, stability, and polishability of CAD/CAM blocks. Additionally, factors such as surface roughness, restoration thickness, and the cementation technique used play crucial roles in both the optical performance and long-term clinical success of these materials. To determine clinical success, *in vitro* studies are often conducted to simulate clinical and intraoral conditions and assess the optical behavior of restorative materials.[2, 3]

One widely used accelerated aging protocol for assessing the color stability of dental materials, particularly those intended for the anterior region, is ultraviolet (UV) exposure. [2, 3] This has been evaluated through both visual and instrumental methods in some studies.[4] The cementation materials used for laminates may statistically affect their optical characteristics. Therefore, the present study aimed to evaluate the effects of CAD/CAM material type, thickness, and cement type on the color change (ΔE_{00}) and translucency parameter (ΔTP) of laminate restorations after UV aging.

The null hypothesis was that CAD/CAM material type, specimen thickness, and cement type would not have a statistically significant effect on color change (ΔE_{00}) and translucency parameter differences (ΔTP) of laminate restorations after UV aging.

MATERIALS AND METHODS

Based on the effect size (f = 0.06) reported by Arocha *et al*.[5], power analysis was performed using G*Power 3.1 (Heinrich-Heine University, Düsseldorf, Germany). With α = 0.05 and power = 0.80, the minimum required sample size was calculated as 10 specimens per group. In total, 200 specimens were prepared, with 40 from each CAD/CAM block.

Two hundred specimens of 12 × 14 mm were sectioned with a low-speed precision saw (IsoMet 4000, Buehler, Lake Bluff, IL, USA) under water cooling at two thicknesses (0.7 mm and 1.2 mm) to assess the optical properties. Four hybrid CAD/CAM blocks were used, including Cerasmart block (CS), Vita Enamic block (VE), Lava Ultimate block (LU), and Grandio block (GR), and one feldspathic block, CEREC Feldspathic block (CE). All blocks used were high-translucency (HT) and shade A2. Detailed material information is provided in Table 1.

Specimens were polished with 600-, 1200-, and 2000-grit silicon carbide papers (MetaServ, Buehler, Lake Bluff, IL, USA) under water cooling to ensure baseline roughness and surface standardization. For resin-containing specimens, an additional 20-second polishing step was performed using Sof-Lex discs (3M ESPE, St. Paul, MN, USA) at four grit levels (coarse, medium, fine, and extra-fine). Glazing of the CE group was performed following the manufacturer's recommendations. Thereafter, all specimens were immersed in distilled water (St. Kearny, USA) and ultrasonically cleaned for 10 minutes.

A digital caliper (Electronic Digital Caliper, Shan, China; accuracy of ±0.1 mm) was used to measure the thickness of each specimen. Before cementation, the back surfaces of the resin nano-ceramic blocks were sandblasted with 50-μm Al_2O_3 at 0.15 MPa using a sandblasting device (Hager & Werken, Duisburg, Germany). The back surfaces of the hybrid ceramic and feldspathic blocks were etched with 9% hydrofluoric acid (Porcelain Etch, Ultradent, South Jordan, UT, USA) for 60 seconds, rinsed, and treated with ceramic primer (Calibra Silane, Dentsply Sirona, Charlotte, NC, USA) for 10 seconds, followed by air drying.[6] A universal adhesive (G-Premio Bond, GC, Tokyo, Japan) was then applied, gently air-dried for 5 seconds, and light-cured with an LED device (Elipar S10, 3M ESPE, St. Paul, MN, USA) at 1200 mW/cm^2 for 10 seconds.

Two different cements (dual-cure (DC) (Calibra Ceram; Dentsply Sirona, USA) and light-cure (LC) (Calibra Veneer; Dentsply Sirona, USA)) were applied to the subgroups, and the specimens were pressed onto pre-prepared glass plates. Resin cement was light-cured from the outer surface for 20 s to simulate clinical conditions. The final thickness was verified with a digital caliper (Electronic Digital Caliper, Shan, China), ensuring that any reduction

Table 1. Materials and compositions used in the study.

Materials	Compositions	Materials Type	Manufacturer
Cerasmart (CS)	Bis-MEPP, UDMA, DMA 71%, Silica (20 nm), barium glass (300 nm)	Resin nano ceramic	GC, Japan (Lot no: not mentioned)
Cerec (CE)	ZrO2, HfO, Yb2O3 >99 (by weight), Al (OH)3	Feldspar ceramic	Dentsply Sirona, Germany (Lot no: not mentioned)
Lava Ultimate (LU)	Bis-GMA, UDMA, bis-EMA, TEGDMA, 80% SiO2 (20 nm), ZrO2 (4-11 nm)	Resin nano ceramic	3M ESPE, USA (Lot no: not mentioned)
Vita Enamic (VE)	UDMA, TEGDMA, 86% feldspathic porcelain	Hybrid ceramic	VITA Zahnfabrik, Germany (Lot no: not mentioned)
Grandio (GR)	BisGMA, TEGDMA, Urethane-BisGMA, Silica, barium- aluminum borosilicate	Nano-ceramic hybrid	VOCO, Germany (Lot no: not mentioned)
Calibra Ceram Dual Cure (DC)	Urethane Dimethacrylate; Di- and Tri-Methacrylate resins; Phosphoric acid modified acrylate resin, Barium Boron FluoroAluminoSilicate Glass; Organic Peroxide Initiator; Camphorquinone (CQ) Photoinitiator; Phosphene Oxide Photoinitiator; Accelerators; Butylated Hydroxy Toluene; UV Stabilizer; Titanium Dioxide; Iron Oxide; Hydrophobic Amorphous Silicon Dioxide. Particles of inorganic filler range from 16nm to 7µm, average particle size 3.8µm, total filler 46.3%by volume.	Dual-Cure Resin Cement	Dentsply Sirona, USA (Lot no: not mentioned)
Calibra veneer Light Cure (LC)	Dimethacrylate Resins; Camphorquinone (CQ), Photoinitiator; Stabilizers; Glass Fillers; Fumed silica; Titanium Dioxide; Pigments. Particles of inorganic filler range from 0.02 to 1.3µm, total filler 44.9% by volume.	Light Cure Resin Cement	Dentsply Sirona, USA (Lot no: not mentioned)

after polishing was compensated following cementation (±0.15 mm). The thickness of the cement layer ranged from 0.1 to 0.2 mm. Although lot numbers could not be recorded, all materials were obtained from the same commercial packaging to minimize potential batch-related variability.

For baseline color measurements of CAD/CAM materials, a spectrophotometer (Vita Easyshade, VITA Zahnfabrik, Bad Säckingen, Germany) was used under standardized lighting on a white background simulating dental tissue, in compliance with ISO 7491. Measurements were taken three times at room temperature (23 ± 1 °C), and mean values for L_1*, a_1*, b_1*, C_1, and h_1 were recorded.[7] A schematic illustration of the study design is presented in Figure 1.

To evaluate the translucency parameter (TP) the same specimens were used. Measurements were repeated on a black background.[8] After the initial color assessment, specimens were mounted on aluminum dies and subjected to accelerated UV aging (BGD 856, Biuged Guangzhou Co., Ltd., Guangzhou, China) for 300 hours with a total energy of 150 kJ/m^2. Aging was conducted at 10 cm from the light source under conditions of 50-60 °C and 95-50% humidity. A single cycle comprised 8 hours of light exposure and an additional 4 hours of light exposure combined with water/steam spray.[3] The UV aging device is shown in Figure 2. UV aging was applied to the same specimens following baseline measurements to simulate long-term clinical conditions. Color and translucency differences (ΔE_{00} and ΔTP) were calculated based on the measurements obtained before and after aging. Therefore, UV aging was not considered an independent variable but rather a procedure to induce optical changes.

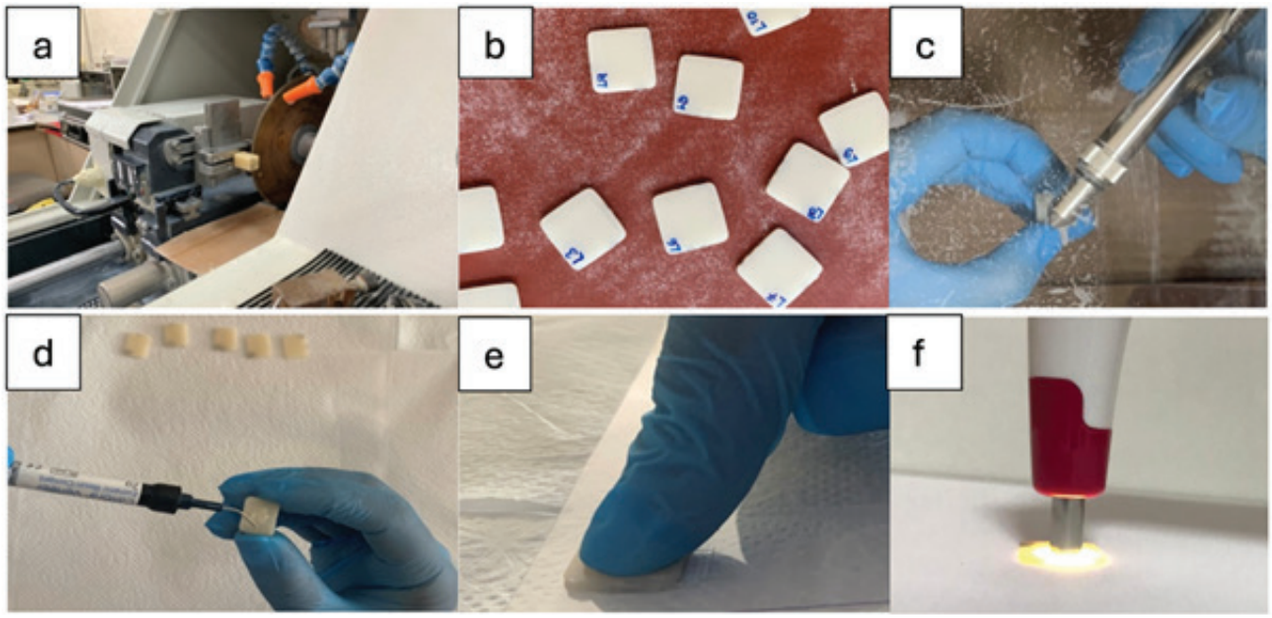

Figure 1. A schematic illustration of the study. a) CAD/CAM blocks were sectioned to predetermined thicknesses using a precision cutting device.b) The prepared specimens were subjected to a standardized grinding and polishing protocol to achieve surface standardization.c) The specimens were conditioned using pretreatment procedures appropriate to their material composition.d) Following surface pretreatment, luting cement was applied to the intaglio surfaces of the specimens.e) The specimens were pressed onto pre-prepared glass plates to ensure uniform cement thickness.f) Color measurements of the specimens were performed using a spectrophotometer before and after aging.

Figure 2. UV aging device, used for the aging procedure in the study.

After UV aging, a second set of color measurements was taken, recording L_2*, a_2*, b_2*, C_2, and h_2 values. Color differences (ΔE_{00}) were calculated using the CIEDE2000 color difference evaluation system according to the following formula:

$$\Delta E_{00} = [(\frac{\Delta L'}{K_L S_L})^2 + (\frac{\Delta C'}{K_C S_C})^2 + (\frac{\Delta H'}{K_H S_H})^2 + R_r(\frac{\Delta C'}{K_C S_C})(\frac{\Delta H'}{K_H S_H})]^{1/2}$$

The CIEDE2000 system was also used to calculate the TP. TP values were obtained from L*, a*, and b* measurements on black and white backgrounds before and after UV aging, and ΔTP was calculated as $TP_{uv} - TP_{00}$.

$$TP_{00} = \sqrt{\left(\frac{L'_B - L'_W}{K_L S_L}\right)^2 + \left(\frac{C'_B - C'_W}{K_C S_C}\right)^2 + \left(\frac{H'_B - H'_W}{K_H S_H}\right)^2 + R_T\left(\frac{C'_B - C'_W}{K_C S_C}\right)\left(\frac{H'_B - H'_W}{K_H S_H}\right)}$$

Data were analyzed using IBM SPSS Statistics 23 (IBM Corp., Armonk, NY, USA). The normality of data distribution was assessed using the Kolmogorov-Smirnov test, and homogeneity of variances was evaluated using Levene's test. When the assumptions of normality and homogeneity were satisfied, parametric tests were applied. Color change (ΔE_{00}) and translucency parameter difference (ΔTP) were considered as separate outcome variables. A three-way ANOVA was performed to evaluate the effects of material type, thickness, and cement type on ΔE_{00} and ΔTP values. Post hoc multiple comparisons were conducted using Tukey's honestly significant difference (HSD) test when significant differences were detected. Results were expressed as mean ± standard deviation (SD), and the level of statistical significance was set at $p < 0.05$. No additional ANOVA models were applied.

RESULTS

This study evaluated the color change (ΔE_{00}) and translucency parameter changes (ΔTP) of CAD/CAM blocks according to cement type, block thickness, and material type. Both the material type and thickness significantly influenced ΔE_{00} and ΔTP ($p < 0.001$). Among the tested groups, the feldspathic ceramic block (CE) showed the least color change, while the resin nanoceramic block (LU) showed the greatest ($p < 0.001$). In contrast, LU, VE, and CS block specimens demonstrated the lowest ΔTP (-0.5), whereas CE had the highest (-0.8). The statistical significance and mean ΔE_{00} and ΔTP values for different thicknesses and cements are detailed in Tables 2 and 3.

Negative values indicate a decrease in translucency. Thickness had a statistically significant effect on ΔTP ($p < 0.001$). The mean ΔTP was -0.8 ± 0.6 for specimens with a thickness of 0.7 mm and -0.4 ± 0.4 for those with a thickness of 1.2 mm. The lowest ΔTP was observed in the CS group at 1.2 mm (-0.2 ± 0.3), whereas the highest was found in the CE group at 0.7 mm (-1.2 ± 0.7). Moreover, the interaction between block type and thickness significantly influenced ΔTP values ($p = 0.002$).

Table 2. Mean ± SD ΔE_{00} values according to materials, thicknesses, and cementation techniques.

	Thickness	Dual Cure	Light Cure	M1
Group CS	0.7	10.1 ± 0.6 $^{a}_{-C}$	10.3 ± 0.3 $^{a}_{-C}$	10.2 ± 0.5 $_{C}$
	1.2	7.2 ± 0.3 $^{a}_{-FG}$	7.4 ± 0.2 $^{a}_{-EF}$	7.3 ± 0.3 $_{E}$
	M2	8.7 ± 1.5 $^{a}_{-BC}$	8.8 ± 1.5 $^{a}_{-B}$	8.8 ± 1.5 $_{B}$
Group CE	0.7	3.0 ± 0.5 $^{a}_{-J}$	8.4 ± 0.4 $^{a}_{-D}$	5.7 ± 2.8 $_{G}$
	1.2	1.1 ± 0.3 $^{a}_{-K}$	2.5 ± 0.7 $^{a}_{-J}$	1.8 ± 0.9 $_{J}$
	M2	2.0 ± 1.0 $^{a}_{-G}$	5.4 ± 3.1 $^{a}_{-D}$	3.7 ± 2.8 $_{C}$
Group LU	0.7	12.5 ± 0.4 $^{a}_{-A}$	12.9 ± 0.6 $^{a}_{-A}$	12.7 ± 0.5 $_{A}$
	1.2	7.8 ± 0.4 $^{a}_{-DFE}$	8.1 ± 0.2 $^{a}_{-DE}$	7.9 ± 0.4 $_{D}$
	M2	10.1 ± 2.4 $^{a}_{-A}$	10.5 ± 2.5 $^{a}_{-A}$	10.3 ± 2.4 $_{A}$
Group VE	0.7	4.2 ± 0.5 $^{a}_{-I}$	5.7 ± 0.6 $^{a}_{-H}$	5.0 ± 1.0 $_{H}$
	1.2	2.3 ± 0.1 $^{a}_{-J}$	2.5 ± 0.2 $^{a}_{-J}$	2.4 ± 0.2 $_{I}$
	M2	3.3 ± 1.0 $^{a}_{-F}$	4.1 ± 1.7 $^{a}_{-E}$	3.7 ± 1.5 $_{C}$
Group GR	0.7	11.2 ± 0.5 $^{a}_{-B}$	10.0 ± 0.6 $^{a}_{-C}$	10.6 ± 0.8 $_{B}$
	1.2	6.6 ± 0.2 $^{a}_{-G}$	6.6 ± 0.4 $^{a}_{-G}$	6.6 ± 0.3 $_{F}$
	M2	8.9 ± 2.4 $^{a}_{-B}$	8.3 ± 1.8 $^{a}_{-C}$	8.6 ± 2.1 $_{B}$
Mean Value	0.7	8.2 ± 3.9 $^{a}_{-B}$	9.5 ± 2.4 $^{a}_{-A}$	8.8 ± 3.3
	1.2	5.0 ± 2.8 $^{a}_{-D}$	5.4 ± 2.5 $^{a}_{-C}$	5.2 ± 2.6
	M	6.6 ± 3.7	7.4 ± 3.2	7.0 ± 3.5

Subscript uppercase letters indicate significant differences among groups within the same column (α = 0.05). Identical letters indicate no significant difference.M1: Represents the mean ΔE_{00} values of specimens prepared using different cementation techniques at the same thickness. M2: Represents the mean ΔE_{00} values of specimens prepared with different thicknesses using the same cementation technique. Negative values indicate a decrease in translucency. Cerasmart (CS), Cerec (CE), Lava Ultimate (LU), Vita Enamic (VE), Grandio (GR).

Table 3. Mean ± SD ΔTP values according to materials, thicknesses, and cementation techniques.

		Dual Cure	Light Cure	M1
Group CS	0.7	-0.7 ± 0.5 $_{BC}$	-0.8 ± 0.6 $_{BC}$	-0.8 ± 0.5 $_{BC}$
	1.2	-0.1 ± 0.4 $_{A}$	-0.3 ± 0.2 $_{A}$	-0.2 ± 0.3 $_{A}$
	M2	-0.4 ± 0.6 $_{B}$	-0.6 ± 0.5 $_{B}$	-0.5 ± 0.5 $_{B}$
Group CE	0.7	-1.1 ± 0.6 $_{C}$	-1.3 ± 0.8 $_{C}$	-1.2 ± 0.7 $_{C}$
	1.2	-0.3 ± 0.2 $_{AB}$	-0.5 ± 0.4 $_{AB}$	-0.4 ± 0.3 $_{AB}$
	M2	-0.7 ± 0.6 $_{A}$	-0.9 ± 0.7 $_{A}$	-0.8 ± 0.7 $_{A}$
Group LU	0.7	-0.6 ± 0.5 $_{AB}$	-0.6 ± 0.4 $_{AB}$	-0.6 ± 0.4 $_{AB}$
	1.2	-0.2 ± 0.2 $_{AB}$	-0.3 ± 0.3 $_{AB}$	-0.3 ± 0.3 $_{AB}$
	M2	-0.4 ± 0.4 $_{B}$	-0.5 ± 0.3 $_{B}$	-0.5 ± 0.4 $_{B}$
Group VE	0.7	-0.3 ± 0.4 $_{AB}$	-0.8 ± 0.5 $_{AB}$	-0.6 ± 0.5 $_{AB}$
	1.2	-0.5 ± 0.4 $_{AB}$	-0.5 ± 0.3 $_{AB}$	-0.5 ± 0.4 $_{AB}$
	M2	-0.4 ± 0.4 $_{B}$	-0.7 ± 0.4 $_{B}$	-0.5 ± 0.4 $_{B}$
Group GR	0.7	-0.8 ± 0.4 $_{AB}$	-0.6 ± 0.7 $_{AB}$	-0.7 ± 0.5 $_{AB}$
	1.2	-0.6 ± 0.4 $_{AB}$	-0.7 ± 0.5 $_{AB}$	-0.6 ± 0.4 $_{AB}$
	M2	-0.7 ± 0.4 $_{AB}$	-0.6 ± 0.6 $_{AB}$	-0.6 ± 0.5 $_{AB}$
Mean Value	0.7	-0.7 ± 0.5	-0.8 ± 0.6	-0.8 ± 0.6
	1.2	-0.4 ± 0.4	-0.5 ± 0.4	-0.4 ± 0.4
	M	-0.5 ± 0.5	-0.7 ± 0.5	-0.6 ± 0.5

Different superscript lowercase letters indicate significant differences between Dual Cure and Light Cure within the same row ($p < 0.05$). Different subscript uppercase letters indicate significant differences among groups within the same column ($p < 0.05$). Identical letters indicate no significant difference. M1: Represents the mean ΔTP values of specimens prepared using different cementation techniques at the same thickness. M2: Represents the mean ΔTP values of specimens prepared with different thicknesses using the same cementation technique. Cerasmart (CS), Cerec (CE), Lava Ultimate (LU), Vita Enamic (VE), Grandio (GR).

DISCUSSION

The findings obtained after UV aging demonstrated that CAD/CAM material type, specimen thickness, and cement type significantly influenced color change (ΔE_{00}) and translucency parameter differences (ΔTP) of laminate restorations. Material type and thickness were identified as the primary factors influencing both ΔE_{00} and ΔTP values, while the effect of cement type was comparatively limited. Accordingly, the null hypothesis was rejected.

Resin-based CAD/CAM materials are generally more susceptible to discoloration, primarily due to their inherent water absorption, which allows pigments to be absorbed from the oral environment. The organic polymer matrix in composite resins has been identified as the leading cause of this instability. Advances in CAD/CAM technology have thus focused on reducing the organic content of resin-based and polymer-infiltrated ceramics to improve long-term color stability. [9] Furthermore, translucency in resin-based materials is highly dependent on filler particle size, resin matrix composition, reinforcement strategies, and the use of infiltrating monomers with different refractive indices. Notably, smaller filler particles (~20 nm) promote more effective light transmission, thereby improving translucency.[10, 11]

In contrast, ceramic-based CAD/CAM materials displayed superior resistance to discoloration and better maintenance of translucency. In particular, the feldspathic ceramic (CEREC feldspathic group) demonstrated the most stable color performance in this study. These results align with those of Li *et al*.[12], who noted that the glass matrix composition and pre-sintering processes of ceramic blocks significantly influence their color stability. This correlation underscores the importance of microstructural features in ceramics for their optical durability under aging conditions.

The hybrid ceramic structure of the Vita Enamic block, composed of feldspathic ceramic and aluminum oxide–reinforced urethane dimethacrylate (UDMA) with triethylene glycol dimethacrylate (TEGDMA),

contributed to its favorable color stability. The comparable ceramic-rich structures of Vita Enamic and CEREC may explain the similarity in their ΔE_{00} values. Although CEREC and Vita Enamic blocks exhibited differences in TP values, their ΔE_{00} values were closely aligned, suggesting that cementation exerted minimal influence on discoloration. This discrepancy indicates that translucency and color stability are not always directly correlated. While TP is primarily influenced by filler particle size, matrix composition, and the refractive index mismatch between the resin and ceramic phases, color stability is more strongly associated with the ceramic network's chemical durability and the reduced presence of hydrophilic resin components. [13] In a recent *in vitro* study [14], it was demonstrated that both Vita Enamic and Lava Ultimate CAD/CAM blocks exhibited color changes beyond clinical acceptance after immersion in staining solutions such as tea and grape juice. Notably, Vita Enamic and Lava Ultimate showed higher ΔE_{00} values compared to more stable ceramic groups such as Vita Suprinity and Crystal Ultra. These findings were further corroborated by another study, which showed that Lava Ultimate experienced significantly greater discoloration across all beverage groups and storage periods than Vita Enamic. Moreover, an *in vivo* study [15] comparing Vita Enamic and Cerasmart over one year of service reported that both materials remained within the clinically acceptable limit of $\Delta E_{00} < 3.3$. However, Vita Enamic showed slightly higher light and hue shifts.

Lava Ultimate block, classified as a resin nano-ceramic, is composed of nanoparticles (approximately 80% ceramic, 20% silica, composite, zirconia) embedded within a matrix. While this structure enhances mechanical properties, the hydrophilic nature of the resin phase, particularly due to its monomer composition, facilitates the penetration of colorants. As a result, Lava Ultimate is more prone to discoloration than ceramic-dominant CAD/CAM materials. [15] The high translucency of Lava Ultimate is primarily attributed to its nanofiller particles, which are smaller than the wavelength of visible light and therefore reduce scattering and absorption. Similar findings were reported by Turgut *et al*.[16], who demonstrated that smaller filler size and homogeneous distribution improve light transmission and translucency in resin-based ceramics.

The monomeric composition of CAD/CAM materials has a critical impact on their optical performance. UDMA has been shown to provide superior resistance to color changes compared to bisphenol A-glycidyl methacrylate (Bis-GMA), owing to its lower water absorption and superior solubility profile. This reduced hydrophilicity minimizes pigment uptake, thereby enhancing long-term color stability.[17-19] In contrast, TEGDMA, commonly used as a diluent monomer, is more hydrophilic and prone to water absorption.[20] This property increases the likelihood of pigment penetration and contributes to discoloration over time. Therefore, CAD/CAM blocks with a higher proportion of UDMA and reduced contents of Bis-GMA and TEGDMA demonstrate superior resistance to staining and better maintain their aesthetic properties in the long term. [20, 21] The discoloration observed in resin nano-ceramic CAD/CAM blocks such as Lava Ultimate is likely linked to the presence of Bis-GMA, whereas the UDMA in Vita Enamic enhances its color stability. Comparative studies have reported ΔE_{00} values exceeding clinical acceptability thresholds ($\Delta E_{00} > 2.24$) for nano-ceramic resin and resin nano-ceramic materials. In contrast, Vita Enamic shows better performance, particularly due to its hybrid ceramic structure, consisting of ~86% inorganic ceramic and 14-26% polymer matrix. [22]

Cementation remains a debated issue in studies evaluating the discoloration of CAD/CAM materials.[23] The complex interaction among material thickness, translucency, and cement shade can either enhance or reduce discoloration. In the present study, the dual-cure cement achieved the lowest ΔE_{00} values, indicating superior color stability compared to light-cure cements. Amine-free dual-cure formulations exhibit improved long-term stability due to the absence of tertiary amines, which are prone to yellowing. In contrast, traditional dual-cure systems with benzoyl peroxide/amine initiators may display more discoloration than light-cure cements. [24, 25] Moreover, dual-cure systems offer handling advantages, such as an extended gel phase (up to 45 seconds), which facilitates easier removal of excess cement, an advantage particularly noted for self-adhesive systems. [26]

Modern dual-cure formulations incorporate alternative activators such as organic peroxides, cam-

phorquinone-amine mixtures, phosphine oxide photoinitiators, and UV stabilizers, all of which enhance color stability over time. The incorporation of UV stabilizers in modern resin cements, combined with the UV aging protocol applied in this study, likely enhanced the accuracy of the results by better simulating long-term clinical conditions. In contrast, thermal cycling systems, in which cements remain in continuous contact with water, often overestimate discoloration and introduce variability, representing a limitation of some earlier investigations.[2,3]

Discoloration and aging are strongly associated with the degradation of unreacted amine initiators within the resin matrix. Under UV irradiation, these residual amines undergo photodegradation, producing yellowish chromophores that reduce optical stability and intensify discoloration. Previous studies [26, 27] have confirmed that tertiary amine photoinitiators are particularly susceptible to this degradation pathway, which contributes to the long-term aesthetic deterioration of resin-based materials.

Thickness is another crucial factor for optical performance. Awad *et al*.[1], demonstrated that translucency is significantly influenced by both thickness and surface treatments. More recent studies have confirmed that reduced thickness increases light transmission but simultaneously enhances the impact of background color. Alharbi *et al*.[28], also reported that surface treatments, such as glazing and polishing, alter light scattering patterns, thereby affecting translucency. Similarly, Çömlekoğlu *et al*.[29], found that cement shade and thickness had minimal influence on ΔE_{00} in the cervical and middle thirds but significantly impacted the incisal region, where light transmission is greater. In this study, thinner laminates (0.7 mm) enhanced cement-related discoloration, whereas thicker laminates (1.2 mm) reduced this effect by attenuating light transmission. Accordingly, thicker specimens demonstrated diminished color perception changes despite similar cement conditions. [30-32]

To address the limitations of this study, different aging protocols, such as hydrochloric acid and thermal cycling, could be compared to provide a more comprehensive understanding of material performance. Newly developed materials on the market could also be included in future studies. Finally, since this study was *in vitro*, corroborating the findings with future *in vivo* studies under clinical conditions is necessary.

CONCLUSION

All CAD/CAM materials showed color changes exceeding clinically acceptable thresholds after UV aging, accompanied by a reduction in translucency. Among the evaluated variables, material type and specimen thickness were the most influential factors affecting optical properties, while the effect of cement type was limited.

REFERENCES

1. Awad D, Stawarczyk B, Liebermann A, Ilie N. Translucency of esthetic dental restorative CAD/CAM materials and composite resins with respect to thickness and surface roughness. J Prosthet Dent 2015;113:534-40.

2. Turgut S, Kılınç H, Bağış B. Effect of UV aging on translucency of currently used esthetic CAD-CAM materials. J Esthet Restor Dent 2019;31:147-52.

3. Kilinc H, Turgut S. Optical behaviors of esthetic CAD-CAM restorations after different surface finishing and polishing procedures and UV aging: an *in vitro* study. J Prosthet Dent 2018;120:107-13.

4. Paravina RD, Ghinea R, Herrera LJ, Bona AD, Igiel C, Linninger M, *et al*. Color difference thresholds in dentistry. J Esthet Restor Dent 2015;27:1-9.

5. Arocha MA, Basilio J, Llopis J, Di Bella E, Roig M, Ardu S. *et al*. Colour stainability of indirect CAD-CAM processed composites vs conventionally laboratory processed composites after immersion in staining solutions. J Dent 2014;42:831-8.

6. Campos F, Almeida C, Rippe M, De Melo R, Valandro L, Bottino M. Resin bonding to a hybrid ceramic: effects of surface treatments and aging. Oper Dent 2016;41:171-8.

7. Kim-Pusateri S, Brewer JD, Davis EL, Wee AG. Reliability and accuracy of four dental shade-matching devices. J Prosthet Dent 2009;101:193-9.

8. Paravina RD, Powers JM. Esthetic color training in dentistry. St Louis: Mosby; 2004.

9. Egilmez F, Ergun G, Cekic-Nagas I, Vallittu PK, Lassila LVJ. Does artificial aging affect mechanical properties of CAD/CAM composite materials? J Prosthodont Res 2018;62:65-74.

10. Varvara EB, Gasparik C, Ruiz-López J, Aghiorghiesei AI, Culic B, Dudea D. Color and translucency compatibility among various resin-based composites and layering strategies. Dent J 2025;13:173.

11. Paolone G, Baldani S, De Masi N, Mandurino M, Collivasone G, Scotti N, *et al*. Translucency of bulk-fill composite materials: a systematic review. J Esthet Restor Dent 2024;36:995-1009.

12. Li RW, Chow TW, Matinlinna JP. Ceramic dental biomaterials and CAD/CAM technology: state of the art. J Prosthodont Res 2014;58:208-16.

13. Gawriołek M, Sikorska E, Ferreira LF, Costa AI, Khmelinskii I, Krawczyk A, *et al*. Color and luminescence stability of selected dental materials *in vitro*. J Prosthodont 2012;21:112-22.

14. Yerliyurt K, Sarıkaya I. Color stability of hybrid ceramics exposed to beverages in different combinations. BMC Oral Health 2022;22:180.

15. Mahrous AI, Salama AA, Shabaan AA, Abdou A, Radwan MM. Color stability of two different resin matrix ceramics: randomized clinical trial. BMC Oral Health 2023;23:665.

16. Turgut S, Bagis B. Effect of resin cement and ceramic thickness on final color of laminate veneers: an *in vitro* study. J Prosthet Dent 2013;109:179-86.

17. Hampe T, Wiessner A, Frauendorf H, Alhussein M, Karlovsky P, Bürgers R, *et al*. Monomer release from dental resins: the current status on study setup, detection and quantification for *in vitro* testing. Polymers 2022;14:1790.

18. Paolone G, Mandurino M, De Palma F, Mazzitelli C, Scotti N, Breschi L, *et al*. Color stability of polymer-based composite CAD/CAM blocks: a systematic review. Polymers 2023;15:464.

19. Mousdraka MG, Gerasimidou O, Nikolaidis AK, Gogos C, Koulaouzidou EA. Evaluation of color stability of UDMA-based dental composite resins after exposure to conventional cigarette and aerosol tobacco heating system. J Compos Sci 2025;9:352.

20. Stawarczyk B, Sener B, Trottmann A, Roos M, Ozcan M, Hämmerle CH. Discoloration of manually fabricated resins and industrially fabricated CAD/CAM blocks versus glass-ceramic: effect of storage media, duration, and subsequent polishing. Dent Mater J 2012;31:377-83.

21. Eldwakhly E, Ahmed DRM, Soliman M, Abbas MM, Badrawy W. Color and translucency stability of novel restorative CAD/CAM materials. Dent Med Probl 2019;56:349-56.

22. Acar O, Yilmaz B, Altintas SH, Chandrasekaran I, Johnston WM. Color stainability of CAD/CAM and nanocomposite resin materials. J Prosthet Dent 2016;115:71-5.

23. Turgut S, Bagis B. Colour stability of laminate veneers: an *in vitro* study. J Dent 2011;39:57-64.

24. Yang Y, Wang Y, Yang H, Chen Y, Huang C. Effect of aging on color stability and bond strength of dual-cured resin cement with amine or amine-free self-initiators. Dent Mater J 2022;41:17-26.

25. Hardan L, Bourgi R, Hernández-Escamilla T, Piva E, Devoto W, Lukomska-Szymanska M, *et al*. Color stability of dual-cured and light-cured resin cements: a systematic review and meta-analysis of *in vitro* studies. J Prosthodont 2024;33:212-20.

26. Kilinc E, Antonson SA, Hardigan PC, Kesercioglu A. The effect of ceramic restoration shade and thickness on the polymerization of light- and dual-cure resin cements. Oper Dent 2011;36:661-9.

27. Favarão J, Oliveira D, Zanini M, Rocha M, Correr-Sobrinho L, Sinhoreti M. Effect of curing-light attenuation on color stability and physical and chemical properties of resin cements containing different photoinitiators. J Mech Behav Biomed Mater 2021;113:104-10.

28. Alharbi G, Al Nahedh HN, Al-Saud LM, Shono N, Maawadh A. Effect of different finishing and polishing systems on surface properties of universal single shade resin-based composites. BMC Oral Health 2024;24:197.

29. Çömlekoğlu ME, Paken G, Tan F, Dündar-Çömlekoğlu M, Özcan M, Akan E, *et al*. Evaluation of different thickness, die color, and resin cement shade for veneers of multilayered CAD/CAM blocks. J Prosthodont 2016;25:563-9.

30. Doğu Kaya B, Öztürk S, Şenol AA, Kahramanoğlu E, Yılmaz Atalı P, Tarçın B. Effect of CAD-CAM block thickness and translucency on the polymerization of luting materials. BMC Oral Health 2024;24:1384.

31. Zheng S, Chen H, Lin Q, Zhu S. Effect of dentin conditioners on dentin bond strength: a systematic review and meta-analysis. J Prosthet Dent 2024;132:509-11.

32. Radeesujalitkul P, Sripetchdanond J, Srisawasdi S. Influence of ceramic translucency, ceramic thickness, and resin cement shades on the color of CAD-CAM lithium disilicate veneers. J Dent Assoc Thai 2024;74:180-7.

CAD/CAM Lamina Restorasyonlarda Materyal Tipi, Kalınlık ve Siman Türünün Optik Özellikler Üzerindeki Etkisi

ÖZET

Amaç: Lamina restorasyonların uzun dönem klinik başarısı, yalnızca mekanik dayanımlarına değil; aynı zamanda renk stabilitesi ve translüsentlik gibi optik özelliklerinin korunmasına da bağlıdır. Bu çalışmada, UV yaşlandırma sonrası CAD/CAM materyal tipi, kalınlık ve siman türünün lamina restorasyonların renk değişimi (ΔE_{00}) ve translüsensi parametresi değişimleri (ΔTP) üzerindeki etkilerinin değerlendirilmesi amaçlanmıştır.

Gereç ve Yöntemler: Toplam 200 örnek, beş farklı CAD/CAM materyalinden (CEREC feldspatik blok, Cerasmart blok, Vita Enamic blok, Lava Ultimate blok ve Grandio CAD/CAM blok) ve iki farklı kalınlıkta (0.7 mm ve 1.2 mm) hazırlandı. Örnekler, simantasyon türüne göre (dual-cure ve light-cure) gruplara ayrıldı. Renk ölçümleri (L*, a*, b*) UV yaşlandırma öncesi ve sonrası gerçekleştirildi; renk ve translüsensi farkları (ΔE_{00} ve ΔTP) CIEDE2000 formülü kullanılarak hesaplandı. UV yaşlandırma, bir yaşlandırma prosedürü olarak uygulanmış olup istatistiksel analizde bağımsız değişken olarak değerlendirilmemiştir. Veriler, materyal tipi, kalınlık ve siman türüne göre üç yönlü ANOVA kullanılarak analiz edildi ($p < 0.05$).

Bulgular: Materyal tipi, ΔE_{00} ve ΔTP değerlerini istatistiksel

olarak anlamlı düzeyde etkiledi. Gruplar arasında en düşük renk değişimi CEREC'te (1.1 ± 0.3) izlenirken, en yüksek renk değişimi Lava Ultimate'te (12.7 ± 0.5) saptandı ($p < 0.05$). En düşük ΔTP değerleri ise Lava Ultimate (-0.2 ± 0.2), Vita Enamic (-0.3 ± 0.4), ve Cerasmart (-0.1 ± 0.4) gruplarında saptandı ($p < 0.05$).

Sonuç: Tüm gruplarda, algılanabilirlik ve klinik olarak kabul edilebilirlik eşiklerinin üzerinde renk değişimi saptandı. UV yaşlandırma sonrasında elde edilen bulgular, translüsensinin azaldığını ortaya koymuştur. Değerlendirilen faktörler arasında, CAD/CAM materyal tipi ΔE_{00} değerlerini etkileyen en kritik faktör olarak belirlenirken, örnek kalınlığı ΔTP değerlerinin temel belirleyicisi olarak bulundu.

Anahtar Kelimeler: Bilgisayar Yardımlı Tasarım; Kozmetik Diş Hekimliği; Diş Laminatları; Prostodonti

DOI: https://doi.org/10.54617/adoklinikbilimler.1826596

Original Research Article

Effects of Build Orientation and Post-polymerization Method on the Mechanical Properties of a 3D-printed Permanent Resin Material

Selin Çelik Öge[1]*, Ezgi Sonkaya Akburak[2]

*[1]*Department of Prosthetic Dentistry, Faculty of Dentistry, Çukurova University, Adana, Türkiye*
[2]Department of Restorative Dentistry, Faculty of Dentistry, Çukurova University, Adana, Türkiye

ABSTRACT

Aim: The purpose of this study was to investigate how different build orientations and post-polymerization protocols influence the microhardness and biaxial flexural strength (BFS) of 3D-printed permanent resin material.

Materials and Methods: Ninety disc-shaped specimens were manufactured using a digital light processing (DLP) 3D printer at three build orientations (0°, 45°, 90°). Specimens were post-processed using either a desktop curing unit (FC) or a handheld polywave light emitting diode (LED) light-curing unit (LCU). Microhardness (VHN) was measured using a Vickers microhardness tester, and BFS was evaluated using a piston-on-three-ball test. Two-way ANOVA and Tukey HSD tests were used for statistical analysis (α = .05).

Results: The post-polymerization method significantly affected BFS ($p < .001$), with the LCU group exhibiting higher strength (336.8 ± 81.6 MPa) than the FC group (255.2 ± 83.3 MPa). Build orientation also had a significant influence on BFS ($p < .001$); the 0° groups showed higher values than the 45° and 90° groups. Microhardness was significantly influenced by the post-polymerization method ($p = .04$), whereas build orientation had no significant effect on VHN values (p=63).

Conclusion: Both build orientation and post-polymerization method influenced the mechanical behavior of the 3D-printed resin, particularly its BFS. The handheld polywave LCU provided superior flexural performance compared with the desktop curing unit, suggesting that it may serve as a reliable alternative for post-polymerization of 3D-printed dental materials. Optimizing printing and post-polymerization parameters is essential to enhance the mechanical reliability of additively manufactured restorations.

Received: 11.20.2025; Accepted: 02.28.2026
**Corresponding author: Dr. Selin Çelik Öge*
Department of Prosthetic Dentistry, Faculty of Dentistry, Çukurova University 01380, Balcalı/Sarıçam, Adana, Türkiye
E-mail: dtselincelik@gmail.com

Keywords: Flexural strength; Hardness tests; Polymerization; Three-dimensional printing

Citation: Çelik Öge S, Sonkaya Akburak E. Effects of Build Orientation and Post-polymerization Method on the Mechanical Properties of a 3D-printed Permanent Resin Material. ADO Klinik Bilimler Dergisi 2026;15(2):105-113

Editor: Yeliz Kılınç, Gazi University, Ankara, Türkiye

INTRODUCTION

The continuous progress of computer-aided design and manufacturing (CAD/CAM) systems has substantially reshaped various areas of dental practice, especially in prosthodontics and restorative dentistry. Subtractive and additive manufacturing -also known as milling and 3D printing- constitute the fundamental methods of these technologies.[1] While subtractive manufacturing (SM) offers standardized material quality through milling of industrially prefabricated blocks, it is limited by material waste and geometric constraints.[2,3] In contrast, additive manufacturing (AM) enables layer-by-layer fabrication with minimal waste, allowing efficient production of intricate designs and multiple units simultaneously.[4–6]

The dental AM workflow comprises three main phases: digital design, printing, and post-processing. Among the printing parameters, build orientation is one of the most critical factors influencing the internal structure and mechanical behavior of printed objects.[7] The orientation of the layers relative to the direction of applied forces affects not only the bonding strength between layers but also the surface quality, dimensional accuracy, and overall durability of the printed restoration.[8] Variations in build angle can

therefore lead to anisotropic properties, resulting in differences in flexural strength and surface hardness depending on the printing direction.[9,10]

Following the printing process, post-processing steps such as cleaning and post-polymerization have a significant impact on the mechanical and biological performance of printed resins.[11] The post-polymerization process is generally conducted using light sources that emit at specific wavelengths to advance the polymerization of the printed material from its initial green state to a completely cured, stable form.[11–13] In the literature, desktop post-polymerization devices are commonly used for this purpose, offering controlled light intensity and exposure time that ensure sufficient polymerization.[14–16] Recently, the utilization of portable light-curing units (LCUs) has been suggested as an effective choice, providing mobility, decreased processing time, and possibility for chairside applications.[11,12]

Conventional LCUs emit light within a wavelength range that matches the absorption spectrum of camphorquinone, the primary photoinitiator in most resin-based materials.[17] In recent years, advanced polywave light-emitting diode (LED) LCUs capable of emitting multiple wavelength bands have been developed to effectively activate different photoinitiator systems.[18,19] Such devices may also be applicable for the post-polymerization of 3D-printed resins, potentially offering a practical, time-efficient, and chairside alternative to traditional desktop curing units.[12,20]

Therefore, the aim of this study was to evaluate the effects of two key parameters -build orientation and post-processing protocols- on the mechanical properties of 3D-printed permanent resin material. The null hypothesis was that neither the use of different polymerization devices nor variations in build orientation would significantly affect the mechanical properties -microhardness and biaxial flexural strength- of the 3D-printed resin material.

MATERIALS AND METHODS

In this *in vitro* study, a total of 90 disc-shaped specimens (14 × 1.8 mm) were printed from a permanent crown resin with nanoceramic fillers (Power Resin C&B Ceramic; Dentafab, Türkiye) (Table 1). An a priori power analysis (G*Power 3.1; Düsseldorf University, Germany) was performed for a two-way ANOVA including both main effects and their interaction. Assuming a medium-to-strong effect size (Cohen's f = 0.35), an α level of 0.05, and a statistical power of 0.80, a minimum of 15 specimens per subgroup was required.

Specimens were designed using CAD software (Exocad, Germany), exported in STL format, and processed in Dentafab platform software (Dentafab, Türkiye). Discs were positioned to avoid contact during printing. Three print build orientations were used: 0°, 45°, and 90°, with 30 specimens printed per orientation in separate batches. Printing was performed using a digital light processing (DLP) printer (SEGA LFP-PRO; Dentafab, Türkiye) with a 50 µm layer thickness and a 385 nm light source.

All 90 printed specimens were randomly assigned (https://www.randomizer.org) into two post-polymerization groups: a control group (FC) using a desktop curing unit (Form Cure; Formlabs, USA) and an experimental group (LCU) using a handheld polywave LED light-curing unit (Valo; Ultradent Products, USA). Each group contained 15 discs per build orientation (0°, 45°, 90°). The study design was presented in Figure 1.

Specimens in the FC group were ultrasonically

Table 1. 3D-printed resin used in the study.

Material	Type	Composition	Manufacturer	Lot Number
Power Resin C&B Ceramic	3D-printed nanoceramic-filled permanent crown resin	Esterification products of 4,4'-isopropylidenediphenol, ethoxylated and 2-methylprop-2-enoic acid (50–55%), ethyl phenyl (2,4,6-trimethylbenzoyl) phosphinate (1–5%), dental glass (20–30%)	Dentafab, 3BFAB Technology, Türkiye	MD1108250818004

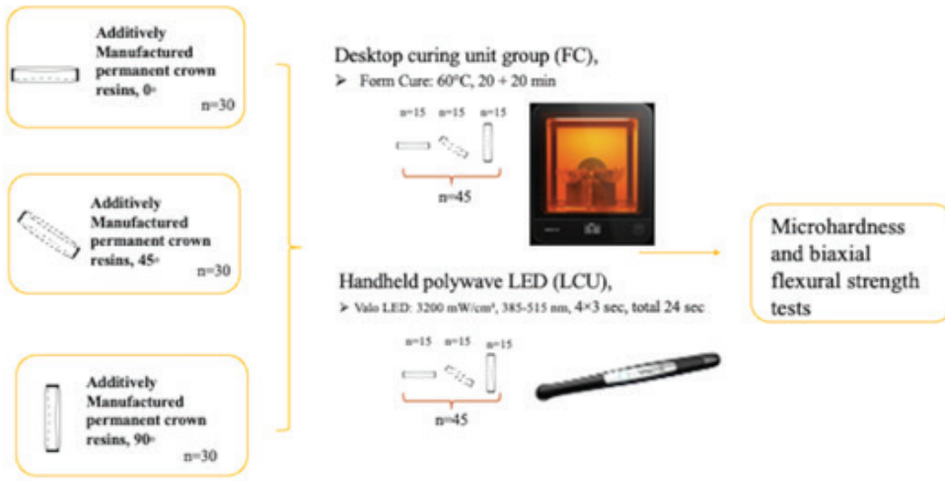

Figure 1. Study design.

cleaned (Form Wash; Formlabs, USA) in 99% isopropyl alcohol for 5 minutes and dried with compressed air. Curing was performed in a desktop curing unit at 60°C for 20 minutes on each side (supports in place for the first cycle, removed for the second), following the manufacturer's instructions. For the LCU group, specimens were cleaned in 99% isopropyl alcohol for 5 minutes, air-dried, and polymerized using a handheld polywave LED LCU from both top and bottom surfaces in four cycles of 3 seconds each (total exposure: 24 seconds) in Xtra Power mode, following the protocol described by Kim *et al*.[12], who reported improved microhardness and biaxial flexural strength with bidirectional light curing for a total of 24 seconds. The device emitted a broad wavelength spectrum (385–515 nm) with an irradiance of 3200 mW/cm². After every five specimens, irradiance was verified using a radiometer (Model 100; Demetron/Kerr, Danbury, USA) to ensure consistency.

All specimens were kept in distilled water at 37 °C for 24 hours prior to testing. The upper and lower surfaces were sequentially polished under continuous water flow using silicon carbide abrasives in 800-, 1200-, and 2000-grit sequences. Specimen dimensions were verified with a digital caliper (Micrometers 293-82130; Mitutoyo).

Vickers microhardness was measured using a microhardness tester (HMV-2000; Shimadzu Corporation, Japan) with a 300-gf load applied for 15 seconds. Indentations were made with a 10 μm diamond tip at 0.25 mm spacing along a 5.6 mm test line. Measurements were taken from three regions of each specimen at 45° intervals, and the average of these readings was used for analysis. Vickers hardness number (VHN, kg/mm²) was calculated according to the formula:

$$VHN = 1854.4 \times P / d^2$$

where P is the applied load (g) and d is the mean diagonal length of the indentation (mm).

Biaxial flexural strength (BFS) of the specimens was determined using a piston-on-three-ball setup in accordance with ISO 6872 standards.[21] For each test, three supporting steel spheres were positioned 120° apart on an 11-mm diameter circle. The specimens were loaded until fracture in a universal testing machine (Testometric M270, UK) at a crosshead speed of 1 mm/min, using a flat-ended piston with a 1.5-mm diameter. To prevent any influence of the Vickers indentations on subsequent biaxial flexural strength testing, the surface containing the microhardness indentations was always positioned facing upward during the BFS test, away from the critical tensile zone. The BFS value (σ, MPa) was then calculated using the following formula:

$$BFS = -0.2387P(X-Y) / b^2$$

$$X = (1+v)\ln(r_2/r_3)^2 + [(1-v)/2](r_2/r_3)^2$$

$Y = (1+v)[1 + \ln(r_1/r_3)^2] + (1-v)(r_1/r_3)^2$, in this equation, r_1 corresponds to the radius of the supporting circle (5.5 mm), r_2 represents the radius of the loading piston (0.75 mm), and r_3 denotes the radius of the test specimen. The specimen thickness is expressed

as b, the Poisson's ratio was taken as 0.25, and P refers to the fracture load recorded in Newtons.

All statistical evaluations were performed in SPSS version 25.0 (IBM Corp., Armonk, NY, USA). Data normality was assessed with the Shapiro–Wilk test, while variance homogeneity was confirmed through Levene's test. Since the assumptions for parametric testing were satisfied, a two-way analysis of variance (ANOVA) was conducted to evaluate the effects of post-polymerization method (two levels: FC and LCU) and build orientation (three levels: 0°, 45°, and 90°) as fixed factors, as well as their interaction, on microhardness and biaxial flexural strength. When significant effects were detected, pairwise comparisons were performed using Tukey's honestly significant difference (HSD) post hoc test. The significance level was set at $\alpha = 0.05$.

RESULTS

The mean and standard deviation values of VHN and BFS for each post-polymerization group (FC and LCU) are descriptively presented in Table 2. The LCU group exhibited slightly higher VHN values (22.8 ± 1.4) compared to the FC group (22.2 ± 1.6). The LCU group (336.8 ± 81.7 MPa) showed higher BFS values than the FC group (255.2 ± 83.4 MPa).

Mean VHN and BFS values according to build orientation are descriptively summarized in Table 3. The specimens printed at 0° (366.9 ± 83.4 MPa) exhibited a higher BFS value than those printed at 45° (269.1 ± 76.3 MPa) and 90° (252.1 ± 71.6 MPa).

The effects of build orientation and post-polymerization method on subgroups' VHN and BFS values, along with pairwise comparisons based on Tukey's HSD test, are presented in Table 4. The specimens printed at LCU-0° (23.7 ± 1.19) exhibited a higher VHN value than those printed at LCU-90° (21.9 ± 0.5) and FC-0° (21.1 ± 1.5). For BFS, the highest values were obtained in the LCU-0° group (402. ± 71.6 MPa), followed by FC-0° (331.8 ± 81.4 MPa), while the lowest mean value was recorded in the FC-45° group (214.7 ± 47.2 MPa).

The two-way ANOVA revealed the effects of the post-polymerization method (two levels: FC and LCU) and build orientation (three levels: 0°, 45°, and 90°), as well as their interaction, on the outcome variables VHN and BFS. Complete ANOVA outputs, including degrees of freedom and F statistics, are presented in Table 5. The post-polymerization method significantly affected both VHN ($p = .04$) and BFS ($p < .001$), whereas build orientation significantly influenced BFS ($p < .001$) but not VHN ($p = .63$). A significant interaction between post-polymerization method and build orientation was observed for VHN ($p < .001$), whereas no significant interaction was found for BFS ($p = .38$). The interaction effects are illustrated in Figures 2 and 3.

Table 2. Mean (±SD) values of VHN and BFS according to post-polymerization method.

	VHN Mean ± SD	BFS (MPa) Mean ± SD
FC	22.2 ± 1.6	255.2 ± 83.4
LCU	22.8 ± 1.4	336.8 ± 81.7

VHN, Vickers hardness number; BFS, biaxial flexural strength; MPa, megapascals; SD, standard deviation; FC, desktop polymerization unit group; LCU, light curing unit group.

Table 3. Mean (±SD) VHN and BFS values according to build orientation.

	VHN Mean ± SD	BFS (MPa) Mean ± SD
0°	22.5 ± 1.9	366.9 ± 83.4
45°	22.6 ± 1.4	269.1 ± 76.3
90°	22.3 ± 1.3	252.1 ± 71.6

VHN, Vickers hardness number; BFS, biaxial flexural strength; MPa, megapascals; SD, standard deviation.

Table 4. Mean (±SD) subgroups' VHN and BFS values according to build orientation and post-polymerization method with Tukey HSD pairwise comparisons.

Group	0°	45°	90°
VHN			
FC	21.1 ± 1.5^{c}	22.7 ± 1.2^{ab}	22.5 ± 1.6^{ab}
LCU	23.7 ± 1.1^{b}	22.5 ± 1.5^{abc}	21.9 ± 0.5^{ac}
BFS (MPa)			
FC	331.8 ± 81.4^{C}	214.7 ± 47.2^{A}	219.2 ± 59.6^{AB}
LCU	402 ± 71.6^{D}	323.5 ± 59^{C}	285 ± 68.8^{BC}

Different lowercase letters within each row indicate statistically significant differences in microhardness ($p < .05$). Different uppercase letters within each row indicate statistically significant differences in BFS ($p < .05$). VHN, Vickers hardness number; BFS, biaxial flexural strength; MPa, megapascals; SD, standard deviation; FC, desktop polymerization unit group; LCU, light curing unit group.

Table 5. Results of two-way ANOVA evaluating the effects of post-polymerization method, build orientation, and their interaction on VHN and BFS.

	df	F (VHN)	p (VHN)	F (BFS)	p (BFS)
Post-polymerization method	1	4.34	.04	34.93	<.001
Build Orientation	2	0.47	.63	26.82	<.001
Interaction (Post-polymerization method × Build orientation)	2	12.80	<.001	0.98	.38
Error	84	—	—	—	—

VHN, Vickers Hardness Number; BFS, biaxial flexural strength; df, degrees of freedom; F, F statistic obtained from two-way ANOVA.

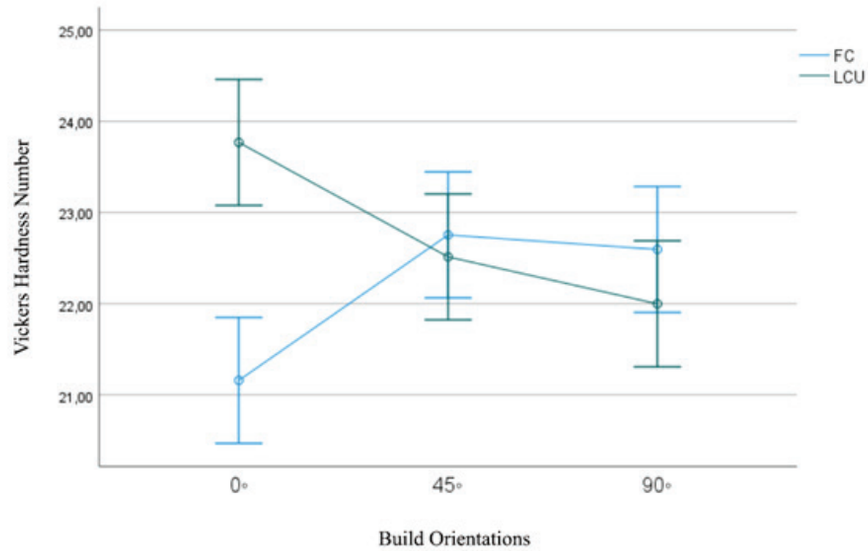

Figure 2. Interaction plot showing the combined effects of build orientation and post-polymerization method on Vickers microhardness (VHN). Error bars represent 95% confidence intervals ($p < 0.001$).

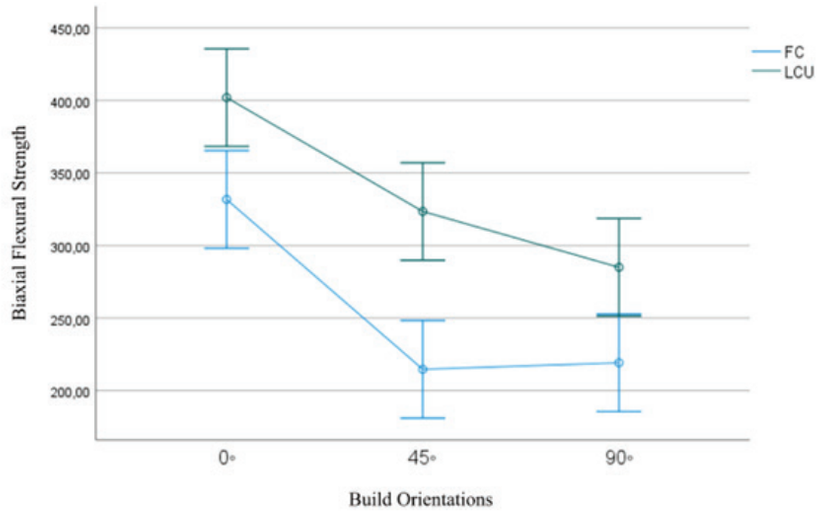

Figure 3. Interaction plot showing the combined effects of build orientation and post-polymerization method on biaxial flexural strength (BFS). Error bars represent 95% confidence intervals (p = 0.38).

DISCUSSION

Based on the findings of this study, the null hypotheses were partially rejected. Both the post-polymerization method and build orientation significantly influenced the biaxial flexural strength of the 3D-printed resin material, whereas microhardness was significantly affected by the post-polymerization method but not by build orientation.

The results of this study demonstrated that build orientation significantly influenced the BFS value of the 3D-printed permanent resin material, with specimens printed at 0° exhibiting the highest BFS values, followed by those printed at 45° and 90°. These findings suggest that build orientation plays a dominant role in determining flexural performance. Similar trends have been documented in previous studies, where specimens printed parallel to the build platform demonstrated superior mechanical strength compared with those fabricated at oblique or vertical angles.[8,22] This behavior can be attributed to the anisotropic structure inherent to layer-by-layer fabrication. When the layers are aligned parallel to the direction of the applied load, as in the 0° orientation, stress is distributed more uniformly across the printed planes, resulting in higher resistance to fracture. In contrast, the 45° and 90° orientations expose the interlayer interfaces to tensile stresses, leading to premature crack initiation and reduced mechanical performance.[8,23] However, some studies have reported opposite findings, indicating that specimens printed at 90° exhibited superior mechanical properties compared with those printed at 0°.[9,24] Such discrepancies may be attributed to several factors, including the type of 3D printer, the resin's chemical composition, the post-polymerization protocol, and the mechanical testing parameters employed. These variations across studies highlight the complexity of additive manufacturing and emphasize the importance of further investigating the influence of build orientation on the mechanical performance of 3D-printed dental materials.

In the present study, no statistically significant differences in microhardness were observed among the groups, regardless of build orientation. This finding is consistent with the results of de Castro *et al*.[9], who also reported that the printing direction had no significant effect on the surface hardness of 3D-printed resins. One possible explanation for this behavior is that surface hardness is primarily governed by the outermost cured layers, which receive sufficient light exposure during printing and post-polymerization, leading to a similar degree of polymerization across orientations. Because the adhesive strength between successive printed layers is lower than the strength within each layer, the influence of orientation tends to manifest more clearly in flexural strength rather than in hardness.[24]

The two-way ANOVA revealed significant main effects of both post-polymerization method and build orientation on BFS ($p < .001$). However, no significant interaction was detected between these factors ($p = .38$), indicating that the superiority of the LCU was independent of build orientation. The present study demonstrated that the post-polymerization technique significantly influenced the flexural properties of the printed resin, with the LCU group exhibiting superior BFS values compared to the FC group. This finding may be attributed to the enhanced irradiance and extensive wavelength spectrum of the polywave LED LCU device, which may efficiently activate various photoinitiator systems and enhance the degree of cross-linking inside the polymer matrix. Recent studies similarly reported that high-intensity or polywave LCUs can achieve mechanical performance comparable to, or in some cases superior to, traditional desktop post-polymerization units under appropriate conditions.[11,12] Bayarsaikhan *et al*.[11] reported that a VALO handheld LCU produced flexural strength values comparable to those from several commercial post-polymerization chambers, indicating that high-intensity LCUs can attain enough polymerization in reduced exposure durations. Similarly, Kim *et al*.[12] indicated that increasing the number of LCU curing cycles enhanced both microhardness and biaxial flexural strength, and that the performance of a handheld LCU was equivalent to that of a normal desktop curing unit when both surfaces of the printed disk were sufficiently irradiated. Based on these findings, the 24-second light-curing protocol used in the present study was selected from scientific evidence rather than arbitrarily. Kim *et al*.[12] demonstrated that bidirectional irradiation for a total of 24 seconds produced consistently high VHN values across both surfaces while also yielding superior BFS compared with shorter exposure durations. This balanced polymerization is essential for achieving reliable mechanical performance throughout the thickness of additively manufactured resin materials while maintaining clinical practicality.

In terms of microhardness, the post-polymerization method significantly affected VHN values, whereas build orientation alone did not produce a significant main effect. However, the significant interaction between the post-polymerization method and build orientation indicates that the influence of the curing device depends on the printing geometry. This is reflected by the LCU-0° subgroup, which exhibited the highest microhardness among all groups. This finding suggests that the effectiveness of light-curing is not determined solely by the light source itself, but also by how light transmission is modulated by the internal layer configuration of the printed material. Differences in optical pathways and energy distribution across build orientations may explain why certain geometric configurations benefit more from high-intensity polywave irradiation. Overall, these results indicate that contemporary polywave LCUs may serve as a practical alternative to conventional desktop post-polymerization units.

One of the limitations of this study is that only a single resin material and one type of 3D printing technology were evaluated, which restricts the generalizability of the findings to other resin compositions or printing systems. Another limitation is that the specimens were not exposed to any aging procedures, which could alter the mechanical properties and better simulate intraoral conditions. In addition, although the degree of conversion is a critical determinant of the physical behavior of photopolymerized resins, this parameter was not assessed in the present study. Further studies should investigate different 3D printing technologies and resin formulations, incorporate artificial aging protocols, and evaluate the degree of conversion using Fourier-transform infrared (FTIR) or Raman spectroscopy to provide a more comprehensive understanding of how polymerization efficiency influences mechanical performance.

CONCLUSION

Within the limitations of this study, both build orientation and post-polymerization method were found to influence the mechanical performance of the 3D-printed permanent resin material. While build orientation significantly affected biaxial flexural strength, it had no impact on microhardness. The handheld polywave LED LCU produced biaxial flexural strength values superior to those of the desktop curing unit, indicating that it may serve as an effective alternative for post-polymerization of 3D-printed dental materials. These findings highlight the importance of optimizing printing and post-

processing parameters to enhance the mechanical reliability of additively manufactured restorations.

REFERENCES

1. Alghazzawi TF. Advancements in CAD/CAM technology: Options for practical implementation. J Prosthodont Res 2016;60:72-84.

2. Azari A, Nikzad S. The evolution of rapid prototyping in dentistry: a review. Rapid Prototyp J 2009;15:216-25

3. Revilla-León M, Özcan M. Additive Manufacturing Technologies Used for Processing Polymers: Current Status and Potential Application in Prosthetic Dentistry. J Prosthodont 2019;28:146-58.

4. Lerner H, Nagy K, Pranno N, Zarone F, Admakin O, Mangano F. Trueness and precision of 3D-printed versus milled monolithic zirconia crowns: An *in vitro* study. J Dent 2021;113.

5. Van Noort R. The future of dental devices is digital. Dent Mater 2012;28:3-12.

6. Kessler A, Hickel R, Reymus M. 3D printing in dentistry-state of the art. Oper Dent 2020;45:30-40.

7. Mudhaffer S, Haider J, Satterthwaite J, Silikas N. Effects of print orientation and artificial aging on the flexural strength and flexural modulus of 3D printed restorative resin materials. J Prosthet Dent 2025;133:1345-57.

8. Casucci A, Verniani G, Sami Haichal W, Manfredini D, Ferrari M, Ferrari Cagidiaco E. Influence of Printing Angulation on the Flexural Strength of 3D Printed Resins: An In Vitro Study. Appl Sci 2024;14:10067.

9. de Castro EF, Nima G, Rueggeberg FA, Giannini M. Effect of build orientation in accuracy, flexural modulus, flexural strength, and microhardness of 3D-Printed resins for provisional restorations. J Mech Behav Biomed Mater 2022;136:105479.

10. Sfondrini MF, Gariboldi F, Cerri M, Todaro C, Pascadopoli M, Casiraghi G, *et al*. Influence of Printing Orientation on the Flexural Strength of Different Light-Cured Resins Manufactured with Two 3D Printers: In Vitro Study. Materials 2025;18:3029.

11. Bayarsaikhan E, Gu H, Hwangbo NK, Lim JH, Shim JS, Lee KW, *et al*. Influence of different postcuring parameters on mechanical properties and biocompatibility of 3D printed crown and bridge resin for temporary restorations. J Mech Behav Biomed Mater 2022;128:105127.

12. Kim RJY, Kim DH, Seo DG. Post-polymerization of three-dimensional printing resin using a dental light curing unit. J Dent Sci 2024;19:945-51.

13. Kang MJ, Lim JH, Lee CG, Kim JE. Effects of Post-Curing Light Intensity on the Mechanical Properties and Three-Dimensional Printing Accuracy of Interim Dental Material. Materials (Basel) 2022;15:6889.

14. Bayarsaikhan E, Lim JH, Shin SH, Park KH, Park YB, Lee JH, *et al*. Effects of Postcuring Temperature on the Mechanical Properties and Biocompatibility of Three-Dimensional Printed Dental Resin Material. Polymers (Basel) 2021;13:1180.

15. Kim JH, Kwon JS, Park JM, Lo Russo L, Shim JS. Effects of postpolymerization conditions on the physical properties, cytotoxicity, and dimensional accuracy of a 3D printed dental restorative material. J Prosthet Dent 2024;132:241-50.

16. Alharbi S, Alshabib A, Algamaiah H, Aldosari M, Alayad A. Influence of Post-Printing Polymerization Time on Flexural Strength and Microhardness of 3D Printed Resin Composite. Coatings 2025;15:230.

17. Guarneri JAG, Price RB, Maucoski C, Arrais CAG. The dark art of light curing in dentistry. J Dent 2024;150:105375.

18. Elsharawy RM, Elawsya ME, AbdAllah AM, ElEmbaby AES. Polymerization efficiency of different bulk-fill resin composites cured by monowave and polywave light-curing units: a comparative study. Quintessence Int (Berl) 2024;55:264-72.

19. Santini A, Gallegos IT, Felix CM. Photoinitiators in dentistry: a review. Prim Dent J 2013;2:30-3.

20. Çelikel P, Şengül F, Büyüksefil M, Aslan İnce N, Şimşek Derelioğlu S. Üç Boyutlu Yazıcılarda Kullanılan İki Farklı Reçine Materyalinde Farklı Polimerizasyon Cihazlarının Yüzey Sertliğine Etkisi: İn Vitro Çalışma. Turkiye Klinikleri J Dent Sci 2024;30:67-73.

21. ISO 6872:2015 - Dentistry — Ceramic materials. Accessed May 7, 2025. https://www.iso.org/standard/59936.html

22. Diken Turksayar AA, Donmez MB, Olcay EO, Demirel M, Demir E. Effect of printing orientation on the fracture strength of additively manufactured 3-unit interim fixed dental prostheses after aging. J Dent 2022;124:104155.

23. Zohdi N, Yang RC. Material Anisotropy in Additively Manufactured Polymers and Polymer Composites: A Review. Polymers 2021;13:3368.

24. Alharbi N, Osman R, Wismeijer D. Effects of build direction on the mechanical properties of 3D-printed complete coverage interim dental restorations. J Prosthet Dent 2016;115:760-7.

3D Baskılı Kalıcı Rezin Materyalin Mekanik Özellikleri Üzerinde Basım Açısı ve Post-Polimerizasyon Yönteminin Etkileri

ÖZET

Amaç: Bu çalışmanın amacı, farklı basım açıları ve post-polimerizasyon protokollerinin, 3D baskı ile üretilmiş kalıcı rezin materyalin mikrosertlik ve çift eksenli eğilme direnci (BFS) üzerindeki etkilerini değerlendirmektir.

Gereç ve Yöntemler: Doksan adet disk şeklinde örnek, dijital ışıkla şekillendirme (DLP) tipi bir 3D yazıcı kullanılarak üç farklı baskı açısında (0°, 45°, 90°) üretildi. Örnekler, ya masaüstü bir polimerizasyon cihazı (FC) ya da taşınabilir poliwave ışık yayan diyot (LED) esaslı bir ışık cihazı (LCU) ile kürlendi. Mikrosertlik (VHN), Vickers mikrosertlik test cihazı ile; BFS ise piston-üç-bilye testi kullanılarak değerlendirildi. İstatistiksel analiz için iki yönlü ANOVA ve Tukey HSD testleri uygulandı (α = .05).

Bulgular: Post-polimerizasyon yöntemi BFS üzerinde anlamlı bir etki gösterdi (p < .001); LCU grubu (336.8 ± 81.6 MPa), FC grubuna (255.2 ± 83.3 MPa) kıyasla daha yüksek BFS değerleri sergiledi. Basım açısı da BFS üzerinde anlamlı bir etki oluşturdu (p < .001); 0° basım açısındaki örnekler, 45° ve 90° gruplarından daha yüksek direnç gösterdi. Mikrosertlik değerleri post-polimerizasyon yönteminden anlamlı düzeyde etkilenmiştir (p = .04), ancak basım açısının mikrosertlik üzerinde anlamlı bir etkisi bulunmamıştır (p = .63).

Sonuç: Hem basım açısı hem de post-polimerizasyon yöntemi, 3D baskılı rezin materyalin mekanik davranışını, özellikle BFS değerlerini etkilemiştir. Taşınabilir poliwave LCU, masaüstü polimerizasyon cihazına kıyasla daha yüksek eğilme direnci sağlamış olup, 3D baskılı dental materyallerin post-polimerizasyon işlemi için güvenilir bir alternatif olabileceğini göstermektedir. 3D baskı restorasyonlarının mekanik güvenilirliğini artırmak için baskı ve post-polimerizasyon parametrelerinin optimize edilmesi önemlidir.

Anahtar Kelimeler: Sertlik testleri; Mekanik kavramlar; Polimerizasyon; Üç boyutlu üretim

DOI: https://doi.org/10.54617/adoklinikbilimler.1876759

Original Research Article

Comparison of Mean Mandibular Dental Arch Dimensions and Preformed Copper Nickel Titanium Archwire Dimensions: A Retrospective Study

Berrak Çakmak*, Tuba Tortop

Department of Orthodontics, Faculty of Dentistry, Gazi University, Ankara, Türkiye

ABSTRACT

Aim: Selection of an appropriate archwire form is critical for maintaining the natural dental arch and ensuring post-treatment stability. Preformed copper-nickel-titanium (CuNiTi) archwires are widely used in contemporary orthodontics and are often designed with broader arch forms. This study aimed to determine the average mandibular dental arch dimensions to compare them with those of preformed CuNiTi archwires.

Materials and Methods: Three-dimensional intraoral scans of 44 individuals with untreated class I malocclusion and minimal crowding/diastema were evaluated. Mandibular intercanine and intermolar widths, as well as canine and molar arch depths, were measured using a bracket slot point-based reference system. Eleven commonly used preformed CuNiTi archwires from five manufacturers were selected, and their corresponding dimensions were measured. Differences between individual dental arch measurements and corresponding archwire dimensions were analyzed using one-sample t-tests, with $p < 0.05$ as the level of statistical significance.

Results: All evaluated preformed CuNiTi archwires differed significantly from the natural mandibular intercanine width ($p < 0.05$). In the intermolar region, Cu Nitanium ProForm – Lower, Cu Nitanium DL-X - Universal, and Tanzo Mid Form III archwires showed no significant difference from the natural mandibular width ($p > 0.05$), whereas the remaining archwires demonstrated significant discrepancies.

Conclusion: None of the evaluated archwires matched the intercanine width, and limited compatibility was observed in the intermolar region. These findings suggest that dimensional discrepancies are mainly concentrated in the intercanine region, emphasizing the importance of individualized archwire selection to preserve mandibular arch stability.

Received: 01.29.2026; Accepted: 04.21.2026
**Corresponding author: Dr. Berrak Çakmak*
Department of Orthodontics, 1st Street, Bişkek Street, Building No: 4, Ankara, 06490, Türkiye
E-mail: berrak@gazi.edu.tr

Keywords: Archwire, Arch form; CuNiTi; Mandibular arch, Transverse dimension

Citation: Çakmak B, Tortop T. Comparison of mean mandibular dental arch dimensions and preformed copper nickel titanium archwire dimensions: A retrospective study. ADO Klinik Bilimler Dergisi 2026;15(2):114-121

Editor: Yeliz Kılınç, Gazi University, Ankara, Türkiye

INTRODUCTION

Selecting an ideal archwire form during orthodontic treatment is critical to treatment success.[1] The archwire form determines the final arrangement of the teeth and contributes to the post-treatment stability of the dentoalveolar structures.[2] Thus, it plays a decisive role in achieving proper tooth alignment, long-term stability, preventing relapse, and achieving favorable esthetic outcomes.[3,4] On this basis, it is recommended that the archwire form selected at the beginning of orthodontic treatment closely approximates the patient's natural dental arch form.[5-8]

Orthodontic arch wires vary according to their material properties and treatment purposes. Today, copper-nickel-titanium (CuNiTi) wires stand out as a compatible option for self-ligating bracket systems, enhancing treatment effectiveness through their low friction and continuous activation.[9] Designed with the philosophy of dental expansion, CuNiTi wires are generally produced in wider arch forms than conventional wires, allowing for easier transverse arch expansion.[9,10] However, the long-term stability and relapse potential of transverse expansion produced by broader arch forms, particularly in the mandibular dental arch, remain a subject of debate.[11-13] This issue is further complicated by well-documented variations in dental arch morphology influenced by eth-

nic background, genetic factors, and environmental factors.[14-17]

Determining the average dental arch dimensions of the Turkish population and evaluating their compatibility with preformed CuNiTi archwire forms is clinically relevant. Selecting an archwire that closely matches the patient's natural arch form may reduce unnecessary transverse forces during orthodontic treatment, allow more controlled tooth movement, and contribute to improved post-treatment stability.[18,19]

Although several studies have evaluated the compatibility between natural dental arch dimensions and preformed archwires, most have focused on conventional NiTi archwires.[20-21] In contrast, preformed CuNiTi archwires, despite their widespread clinical use and their tendency to be manufactured with broader, expansion-oriented arch forms, have received limited attention in this context. Furthermore, data regarding their compatibility with mandibular arch dimensions in the Turkish population are scarce. Considering that dental arch morphology may vary across populations, evaluating this compatibility in a population-specific manner is of clinical importance.

Therefore, the aim of this study was to determine the average arch dimensions and compare them with those of different preformed CuNiTi archwire forms. The null hypothesis was that there would be no statistically significant difference between the dimensions of preformed CuNiTi archwires and the natural mandibular arch.

MATERIALS AND METHODS

Ethical approval for the study was obtained from the Gazi University Ethics Committee on September 23, 2025 (approval number: 2025-1584). Sample size was calculated using G*Power (version 3.1.9.4; Heinrich-Heine-University, Düsseldorf, Germany). A sample size estimation for a one-sample t-test (two-tailed) was performed, using the intermolar width difference of 2.62 mm reported by Oda *et al*.[14] as the reference value for the difference between the mean of measurements of each natural distance against the single preformed material measurement. As no prior data were available to estimate the standard deviation, a medium effect size (Cohen's d = 0.50) was assumed according to Cohen's criteria.[22] With a significance level of α = 0.05 and a statistical power of 0.90, the required sample size was calculated as 42 participants.

The study material consisted of pretreatment intraoral three-dimensional scan images and clinical records of 44 individuals (22 females and 22 males; age range: 18-29 years; mean age: 24.6±2.8 years) who received treatment at the Department of Orthodontics, Faculty of Dentistry, Gazi University, between January 2018 and January 2025, and met the inclusion criteria.

The inclusion criteria were as follows: having a skeletal and dental class I relationship with overbite/overjet between 2 and 4 mm, exhibiting less than 2 mm of crowding or diastema, and no anterior or lateral cross-bite, and having permanent dentition. Individuals with missing, supernumerary, restored, impacted teeth, a history of orthodontic treatment, pronounced facial asymmetry, craniofacial syndromes, systemic diseases, poor-quality 3D intraoral scan images, and incomplete clinical records were excluded from the study.

The 3D intraoral scan files were printed at true 1:1 scale, and all measurements were manually obtained from the printed models using a digital caliper. In accordance with the protocol described by Oda *et al*.,[14] reference bracket thickness values were incorporated for the central incisors, canines, and first molars. Standardized thickness values of 1.34 mm for the central incisors, 0.75 mm for the canines, and 0.73 mm for the first molars were applied perpendicular to the buccal midpoint of each tooth on the two-dimensional printed images in the mesiodistal direction. This procedure enabled the determination of the bracket slot point (BSP), which represents the estimated position of the archwire. Using the BSP as a reference, transverse arch widths (intercanine and intermolar) and sagittal arch depths (canine and molar depths) were measured separately for the anterior and posterior segments (Figure 1). The BSP-based measurement approach was preferred because it represents the estimated position of the archwire within the bracket slot, thereby providing a clinically relevant reference for evaluating archwire-arch compatibility rather than relying solely on anatomical landmarks.

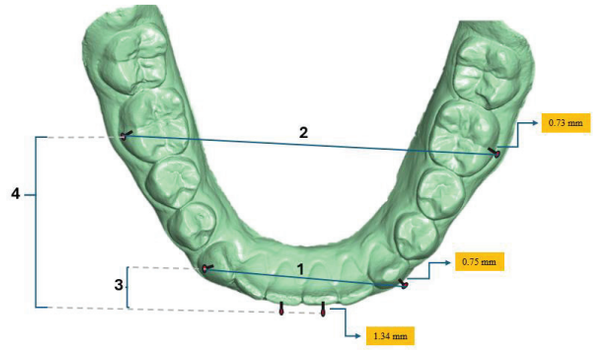

Figure 1. Arch widths and depths measured using the BSP as a reference: 1. Intercanine width 2. Intermolar width, 3. Canine depth 4. Molar depth.

To identify the archwires included in the analysis, manufacturers' local representatives were contacted to determine the most commonly used products in clinical practice. Based on this information, eleven preformed archwires from five different international manufacturers were selected for dimensional evaluation (Table 1). Archwire measurements were obtained using millimeter graph paper, with each wire positioned so that its midline coincided with a predefined reference line. Intercanine and intermolar widths were then recorded at levels corresponding to the previously established mean canine and molar arch depths (Figure 2).

All measurements were taken by the same examiner (BÇ), who has 8 years of orthodontic experience. To assess intra-examiner reliability, measurements

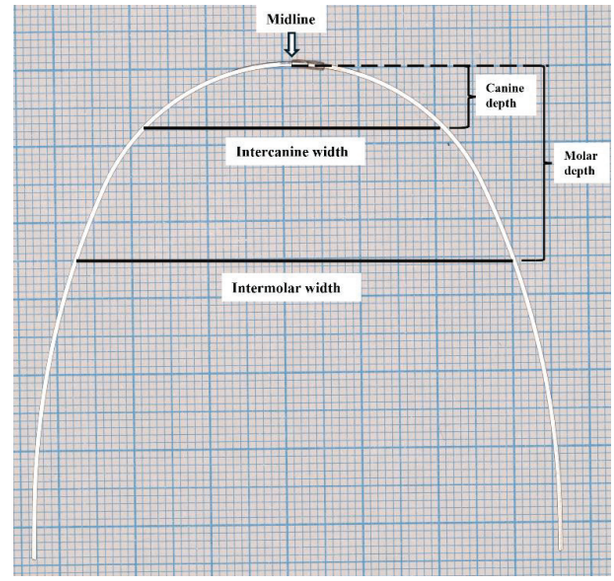

Figure 2. Measurement of the archwire dimensions on graph paper.

were repeated by the same examiner (BÇ) on a randomly selected subset of 22 individuals from the sample after a two-week interval.

Statistical analysis

Data analysis was performed using SPSS software (version 31.0; IBM Corp., Armonk, NY, USA). Descriptive statistics were calculated and expressed as mean ± standard deviation (SD). Intra-examiner reliability was assessed using intraclass correlation coefficients (ICC).

Table 1. Preformed archwires evaluated in the study and their manufacturers.

CuNiTi Archwire	Manufacturer
M5 Thermal CuNiTi Trueform I - Lower	G&H Orthodontics (Franklin, IN, USA)
M5 Thermal CuNiTi Europa II - Lower	G&H Orthodontics (Franklin, IN, USA)
Damon CuNiTi - Universal	Ormco (Glendora, CA, USA)
CuNiTi Broad arch small - Lower	Ormco (Glendora, CA, USA)
CuNiTi Large - Lower	Ormco (Glendora, CA, USA)
Tanzo Mid Form III - Lower	American Orthodontics (Sheboygan, WI, USA)
Tanzo Mid VLP large - Universal	American Orthodontics (Sheboygan, WI, USA)
Cu Nitanium ProForm - Lower	Ortho Organizer (Carlsbad, CA, USA)
Cu Nitanium DL-X - Universal	Ortho Organizer (Carlsbad, CA, USA)
Orthoshape Damon - Universal	IMD (Wuxi, Jiangsu, P.R. China)
Orthoshape Natural - Lower	IMD (Wuxi, Jiangsu, P.R. China)

The normality of the data distribution was evaluated using the Shapiro-Wilk test. For each preformed archwire, the difference between individual dental arch measurements and the corresponding archwire dimension was calculated. One-sample t-tests were performed to determine whether the mean difference significantly deviated from zero. The level of statistical significance was set at $p < 0.05$.

RESULTS

The ICC was 0.999 for intercanine distance, 0.999 for intermolar distance, 0.955 for canine depth, and 0.998 for molar depth, indicating excellent intraexaminer reliability for each measurement.

Descriptive statistics of the dental arch measurements were presented in Table 2. The mean intercanine width was 29.81 ± 1.49 mm, and the mean intermolar width was 52.82 ± 2.39 mm. The mean canine depth was 6.45 ± 0.59 mm, whereas the mean molar depth was 28.61 ± 1.55 mm.

Differences between the mandibular arch dimensions and preformed archwire dimensions are presented in Table 3. All evaluated preformed CuNiTi archwires differed significantly from the natural mandibular intercanine width ($p < 0.05$). In the intermolar region, Cu Nitanium ProFor-Lower, Cu Nitanium DL-X-Universal, and Tanzo Mid Form III showed no significant difference from the natural width ($p > 0.05$). In contrast, M5 Thermal CuNiTi Europa II-Lower, Damon CuNiTi-Universal, CuNiTi Large-Lower, Tanzo Mid VLP Large-Universal, Orthoshape Damon-Universal, and Orthoshape Natural-Lower exhibited significantly greater intermolar widths, whereas M5 Thermal CuNiTi Trueform I-Lower and CuNiTi Broad Arch Small-Lower were significantly narrower ($p < 0.05$).

Table 2. Descriptive statistics of natural dental arch measurements.

Measurements	Min-Max	X̄±SD
Intercanine width (mm)	25.9-33.8	29.81±1.49
Intermolar width (mm)	48.38-58.08	52.82±2.39
Canine depth (mm)	5.10-7.7	6.45±0.59
Molar depth (mm)	25.4-31.7	28.61±1.55

Min: Minimum, Max: Maximum, X̄: Mean, SD: Standard deviation

Table 3. Comparison between natural mandibular arch dimensions and preformed CuNiTi archwire dimensions.

CuNiTi Archwire	Intercanine width (mm)	Intermolar width (mm)	ΔIntercanine width (mm)±SD	p	ΔIntermolar width (mm)±SD	p
M5 Thermal CuNiTi Trueform I - Lower	32.50	50.20	-2.69±1.49	<0.001*	2.62±2.39	<0.001*
M5 Thermal CuNiTi Europa II - Lower	32.50	54.20	-2.69±1.49	<0.001*	-1.38±2.39	<0.001*
Damon CuNiTi - Universal	34.40	60.30	-4.59±1.49	<0.001*	-7.48±2.39	<0.001*
CuNiTi Broad arch small - Lower	34.50	51.50	-4.69±1.49	<0.001*	1.32±2.39	<0.001*
CuNiTi Large - Lower	35.80	54.30	-5.99±1.49	<0.001*	-1.48±2.39	<0.001*
Tanzo Mid Form III - Lower	31.80	52.40	-1.99±1.49	<0.001*	0.42±2.39	0.25
Tanzo Mid VLP large - Universal	33.80	59.60	-3.99±1.49	<0.001*	-6.78±2.39	<0.001*
Cu Nitanium ProForm - Lower	33.30	52.50	-3.49±1.49	<0.001*	0.32±2.39	0.379
Cu Nitanium DL-X - Universal	36.40	52.50	-6.59±1.49	<0.001*	0.32±2.39	0.379
Orthoshape Damon - Universal	35.20	59.80	-5.39±1.49	<0.001*	-6.98±2.39	<0.001*
Orthoshape Natural - Lower	33.40	53.70	-3.59±1.49	<0.001*	-0.88±2.39	0.019*

Δ=|Mean dental arch measurement- Archwire measurement| (mm), SD: Standard deviation

*p<0.05

Positive values indicate wider dental arch compared to the archwire; negative values indicate wider archwire compared to the dental arch.

DISCUSSION

In this study, the average mandibular arch dimensions were determined, and their dimensional compatibility with commonly used CuNiTi archwires was retrospectively evaluated. The main finding of our study is that all evaluated pre-shaped CuNiTi archwires differed significantly from the natural intercanine width of the studied population, whereas limited dimensional compatibility was observed in the intermolar region. This situation highlights that the discrepancy between commercial archwires and natural mandibular morphology is mainly localized to the anterior segment rather than uniformly distributed throughout the arch.

In the present study, only individuals with untreated skeletal and dental class I malocclusion and minimal crowding or spacing were included in order to establish reference values that accurately represent the natural mandibular arch form. This selection was based on previous findings by Uysal *et al*.[23,24] who demonstrated that mandibular arch widths vary according to malocclusion type, being reduced in class II division 1 and division 2 malocclusions and increased in class III malocclusion compared with normal occlusion. Therefore, inclusion of other malocclusion types could have introduced morphological variability unrelated to natural arch form. As noted by Little,[25] significant alterations to the mandibular intercanine width often lead to post-treatment relapse, highlighting the importance of using the pretreatment arch form for archwire selection. Unlike the maxilla, which allows for greater biomechanical expansion through various appliances, the mandible's dimensions are largely dictated by the underlying cortical bone and the positioning of the canines. Therefore, the mandibular arch serves as the limiting factor in determining the final occlusal relationship. For this reason, the mandibular arch was chosen for evaluation in the present study.

Mandibular dental arch dimensions in individuals with class I malocclusion have been reported in several studies conducted on Turkish populations. Celebi *et al*.[17] evaluated 34 class I malocclusion subjects and reported mean intercanine width of 28.96 mm, intermolar width of 48.97 mm, canine depth of 6.33 mm, and molar depth of 25.63 mm. In a study of 40 individuals with class I malocclusion, Şen Yılmaz *et al*.[20] reported an intercanine width of 29.67 mm and an intermolar width of 52.35 mm, while the mean canine depth was 6.08 mm and the molar depth was 26.85 mm. In contrast, Olmez and Doğan[21] reported slightly narrower transverse dimensions in a larger sample of 200 subjects with class I malocclusion: an intercanine width of 27.89 mm, an intermolar width of 48.00 mm, a canine depth of 5.36 mm, and a molar depth of 26.79 mm. In the present study, which also included individuals with class I malocclusion, the mean intercanine width (29.81 mm) and intermolar width (52.82 mm) were within the ranges reported in previous studies. Similarly, the mean canine depth (6.45 mm) and molar depth (28.61 mm) were generally comparable to those reported in the literature. Although minor numerical differences were observed among studies, these variations appear limited and are likely related to differences in sample size and measurement protocols rather than clinically meaningful differences in mandibular dental arch morphology.

The current literature shows significant differences in the fit of preformed arch wires across populations. Al-Barakati *et al*.[26] obtained gender-specific results in the Saudi Arabian population; they identified Ormco Orthos Large and RMO Ovoid forms as the most compatible models for men, and 3M Unitek Orthoform LA and RMO Normal forms for women. Oda *et al*.,[14] studying the Japanese population, emphasized that among commercial wires, Ormco Orthos and Ormco Vari-Simplex Large models gave the closest results to the natural arch form, but that preformed wires generally remained significantly narrower than the natural arches of Japanese individuals in both the canine and molar regions. In contrast, Hedayati *et al*.,[27] studying the Iranian population, stated that Iranians mostly have a "tapered" arch form and that most commercially available wires are too wide for this population, with 3M Unitek (Orthoform) models performing relatively better in this group. In the Indian region, Bhowmik *et al*.[28] found that rectangular NiTi wires compatible with the 3M Unitek (MBT) system excessively widened the intercanine width in Indian women and men (average 7.15 mm and 6.28 mm, respectively), warning that this could increase the risk of recurrence. Ahmed *et al*.,[29] studying the Pakistani population, found that commercial wires were too narrow in the molar region and too wide in the premolar region of Pakistani individuals, proving

that standard wires do not offer a “universal” solution in this population. Şen Yılmaz *et al*.,[20] in their study on the Turkish population, found that commercially available wires did not perfectly match the mandibular arch dimensions of Turkish individuals, but among the wires examined, RMO Europa II was the most successful in terms of overall fit (especially in intermolar width), while RMO Bioform III was more suitable for intercanine spacing. In the present study, Cu Nitanium ProForm - Lower, Cu Nitanium DL-X - Universal, and Tanzo Mid Form III archwires showed no significant difference from the natural mandibular intermolar width. In contrast, Damon CuNiTi, Orthoshape Damon, and Tanzo Mid VLP Large archwires demonstrated significantly greater intermolar widths, whereas M5 Thermal CuNiTi Trueform I and CuNiTi Broad Arch Small were significantly narrower than the natural posterior arch dimension.These findings show that the mismatch between preformed archwires and the natural mandibular arch is region-dependent rather than uniform. While posterior compatibility may be achieved with certain archwires, clinically relevant discrepancies are mainly concentrated in the anterior segment. Therefore, archwire selection should be individualized according to population characteristics and patient-specific arch morphology, rather than based solely on the manufacturer or arch form category.

While advantages such as low friction and continuous activation of CuNiTi wires enhance clinical efficacy,[10] our study highlights the drawbacks of using these wires with a one-size-fits-all approach. The average values obtained in our study, it is critical for clinicians to individualize the arch wire form to the patient’s original form at the start of treatment, or to choose the form closest to the population average from among the available forms.

An original aspect of the present study is its specific focus on preformed CuNiTi archwires. Although several studies[11,20,21] in the literature have compared conventional NiTi archwire forms with natural dental arch dimensions, CuNiTi archwires, despite their widespread clinical use, have received limited attention. Given that CuNiTi archwires are commonly designed with broader arch forms based on an expansion-oriented philosophy, their dimensional compatibility with natural dental arches warrants separate evaluation.

A limitation of the present study is that the sample consisted exclusively of individuals with untreated class I occlusion. Although this approach allowed the evaluation of natural arch dimensions, it may limit the generalizability of the findings. Although the sample included an equal number of male and female participants, sex-based analyses were not performed to avoid reduced statistical power. Future studies with larger samples should investigate potential sex-related differences in archwire compatibility. One limitation of the present study is also the use of printed models instead of direct digital measurements. However, this approach was preferred because currently available three-dimensional software does not provide a validated and standardized method for applying the BSP protocol with fixed bracket thickness values. Future advances in digital orthodontic analysis may enable fully three-dimensional implementation of this method. One limitation of the present study is also its cross-sectional design, which precludes direct evaluation of treatment-induced changes and long-term stability. Future longitudinal studies assessing treatment outcomes and relapse rates in relation to archwire-arch compatibility would further clarify the clinical implications of these findings.

CONCLUSION

None of the evaluated preformed CuNiTi archwires were compatible with the natural mandibular intercanine width. However, several archwires demonstrated dimensional compatibility in the intermolar region. These findings indicate that discrepancies between commercial archwire forms and natural mandibular arch morphology are primarily localized to the anterior segment rather than the posterior region. Therefore, selection of archwire form should be individualized, particularly in the canine region, to preserve the original arch morphology and minimize the risk of relapse. The null hypothesis was rejected, because significant and region-specific differences were observed between the dimensions of preformed CuNiTi archwires and the natural mandibular arch dimensions. Future studies with larger sample sizes and different malocclusion types will help determine the most suitable archwire.

DECLARATION OF COMPETING INTEREST

The authors have no conflicts of interest relevant to this article.

REFERENCES

1. Su Y, Zhang J, Ma H, Zheng X. A novel method to define personalized post-orthodontic treatment dental arch form. BMC Oral Health 2025;25:1587.

2. Ronay V, Miner RM, Will LA, Arai K. Mandibular arch form: the relationship between dental and basal anatomy. Am J Orthod Dentofacial Orthop 2008;134:430-8.

3. Garg H, Khatria H, Kaldhari K, Singh K, Purwar P, Rukshana R. Intermolar and ıntercanine width changes among class I and class II malocclusions following orthodontic treatment. Int J Clin Pediatr Dent 2021;14:S4-S9.

4. Braun S, Hnat WP, Leschinsky R, Legan HL. An evaluation of the shape of some popular nickel titanium alloy preformed arch wires. Am J Orthod Dentofac Orthop 1999;116:1-12.

5. Haddadpour S, Motamedian SR, Behnaz M, Asefi S, Bagheban AA, Abdi AH, *et al*. Agreement of the clinician's choice of archwire selection on conventional and virtual models. Angle Orthod 2019;89:597-604.

6. Motamedi AK, Dadgar S, Teimouri F, Aslani F. Stability of changes in mandibular intermolar and intercuspid distances following orthodontic treatment. Dent Res J (Isfahan) 2015;12:71-5.

7. McNamara C, Drage KJ, Sandy JR, Ireland AJ. An evaluation of clinicians' choices when selecting archwires. Eur J Orthod 2010;32:54-9.

8. Pentagna BB, Degan VV, Godoi APT, Correr AB, Correr ARC, Menezes CC. Does the initial surface roughness of different CuNiTi wires affect the frictional resistance?. Braz Dent J 2023;34:129-35.

9. Major PW, Toogood RW, Badawi HM, Carey JP, Seru S. Effect of wire size on maxillary arch force/couple systems for a simulated high canine malocclusion. J Orthod 2014;41:285-91.

10. George AM, Babu H, Arvind P, Muthuswamy Pandian S, Subramaniam A. Effects of broad arch form wires on arch development with passive self-ligating and conventional brackets: a cone beam tomographic study. APOS Trends Orthod (in press). doi: 10.25259/APOS_130_2024

11. Mughal AT, Jan A, Akhtar O, Ghaffar F, Shafique HZ, Shahid R. Comparison of preformed archwires with average natural arch forms. J Pak Med Assoc 2021;71:2495-500.

12. Gardner SD, Chaconas SJ. Posttreatment and postretention changes following orthodontic therapy. Angle Orthod 1976;46:151-61.

13. Kahl-Nieke B, Fischbach H, Schwarze CW. Treatment and postretention changes in dental arch width dimensions: a long-term evaluation of influencing cofactors. Am J Orthod Dentofacial Orthop 1996;109:368-78.

14. Oda S, Arai K, Nakahara R. Commercially available archwire forms compared with normal dental arch forms in a Japanese population. Am J Orthod Dentofac Orthop 2010;137:520-27.

15. Lombardo L, Coppola P, Siciliani G. Comparison of dental and alveolar arch forms between different ethnic groups. Int Orthod 2015;134:462-88.

16. Lombardo L, Fattori L, Molinari C, Mirabella D, Siciliani G. Dental and alveolar arch forms in a Caucasian population compared with commercially available archwires. Int Orthod 2013;11:389-421.

17. Celebi AA, Keklik H, Tan E, Ucar FI. Comparison of arch forms between Turkish and North American. Dental Press J Orthod 2016;21:51-8.

18. Allan D, Woods MG. Arch-dimensional changes in non-extraction cases with finishing wires of a particular material, size and arch form. Aust Orthod J 2015;31:26-36.

19. Fleming PS, Dibiase AT, Lee RT. Arch form and dimensional changes in orthodontics. Prog Orthod 2008;9:66-73.

20. Şen Yılmaz B, Erkan S, Sunal Aktürk E, Yaradanakul K. Comparison of the nickel titanium alloy archwires' dimensions with the mean arch dimensions of a Turkish sample. Meandros Med Dent J 2022;23:46-52.

21. Olmez S, Dogan S. Comparison of the arch forms and dimensions in various malocclusions of the Turkish population. Open J Stomatol 2011;1:158-64.

22. Cohen, J. Statistical power analysis for the behavioral sciences (2nd ed.). Routledge, 1988.

23. Uysal T, Memili B, Usumez S, Sari Z. Dental and alveolar arch widths in normal occlusion, class II division 1 and class II division 2. Angle Orthod 2005;75:941-7.

24. Uysal T, Usumez S, Memili B, Sari Z. Dental and alveolar arch widths in normal occlusion and Class III malocclusion. Angle Orthod 2005;75:809-13.

25. Little RM. Stability and relapse of dental arch alignment. Br J Orthod 1990;17:235-41.

26. Al-Barakati RG, Alqahtani ND, AlMadi A, Albarakati SF, ALKofide EA. Evaluation of the fit of preformed nickel titanium arch wires on normal occlusion dental arches. Saudi Dent J 2016;28:18-23.

27. Hedayati Z, Fakhri F, Moshkel Gosha V. Comparison of commercially available arch wires with normal dental arch in a group of Iranian population. J Dent (Shiraz) 2015;16:106-12.

28. Bhowmik SG, Hazare PV, Bhowmik H. Correlation of the arch forms of male and female subjects with those of preformed rectangular nickel-titanium archwires. Am J Orthod Dentofacial Orthop 2012;142:364-73.

29. Ahmed M, Shaikh A, Fida M. Evaluation of conformity of preformed orthodontic archwires and dental arch form. Dental Press J Orthod 2019;24:44-52.

Ortalama Mandibular Dental Ark Boyutları ile Önceden Şekillendirilmiş Bakır Nikel-Titanyum Ark Tellerinin Boyutlarının Karşılaştırılması: Retrospektif Bir Çalışma

ÖZET

Amaç: Uygun ark teli formunun seçimi, doğal dental arkın korunması ve tedavi sonrası stabilitenin sağlanması açısından kritik öneme sahiptir. Önceden şekillendirilmiş bakır-nikel-titanyum (CuNiTi) ark telleri güncel ortodontik uygulamalarda yaygın olarak kullanılmakta ve çoğunlukla daha geniş ark formlarına sahip olacak şekilde üretilmektedir. Bu çalışmanın amacı, ortalama mandibular dental ark boyutlarını belirlemek ve bunları önceden şekillendirilmiş CuNiTi ark telleri ile karşılaştırmaktır.

Gereç ve Yöntemler: Minimal çapraşıklık veya diastemaya sahip, tedavi görmemiş Sınıf I maloklüzyonlu 44 bireyin üç boyutlu intraoral taramaları değerlendirildi. Mandibular interkanin ve intermolar genişlikler ile kanin ve molar ark derinlikleri, braket slot noktasına dayalı referans sistemi kullanılarak ölçüldü. Beş farklı üreticiye ait yaygın olarak kullanılan 11 adet önceden şekillendirilmiş CuNiTi ark telinin boyutları kaydedildi. Bireysel dental ark ölçümleri ile önceden şekillendirilmiş ark teli boyutları arasındaki farklar tek örneklem t-testi ile analiz edildi ve istatistiksel anlamlılık düzeyi $p < 0.05$ olarak kabul edildi.

Bulgular: Değerlendirilen tüm önceden şekillendirilmiş CuNiTi ark telleri, doğal mandibular interkanin genişlikten anlamlı düzeyde farklı bulundu ($p < 0.05$). İntermolar bölgede ise Cu Nitanium ProForm - Lower, Cu Nitanium DL-X - Universal ve Tanzo Mid Form III ark telleri doğal mandibular genişlikten anlamlı fark göstermedi ($p > 0.05$); diğer ark tellerinde anlamlı farklılık saptandı.

Sonuç: Değerlendirilen ark tellerinin hiçbiri doğal interkanin genişlik ile uyum göstermemiş, intermolar bölgede ise sınırlı düzeyde uyumluluk gözlenmiştir. Bu bulgular, boyutsal uyumsuzlukların ağırlıklı olarak interkanin bölgede yoğunlaştığını göstermekte ve mandibular ark stabilitesinin korunması için bireyselleştirilmiş ark teli seçiminin önemini vurgulamaktadır.

Anahtar Kelimeler: Ark teli; CuNiTi; Mandibular ark; Transvers boyut

DOI: https://doi.org/10.54617/adoklinikbilimler.1914621

Case Report

Anaphylaxis in Dental Practice: Report of Two Cases

Özgür Dağal*, Zeynep Naiboğlu

Gazi University, Faculty of Dentistry, Department of Oral and Maxillofacial Surgery, Ankara, Türkiye

ABSTRACT

Introduction: Anaphylaxis is defined by the World Allergy Organization as a rapidly developing, potentially fatal systemic hypersensitivity reaction. Clinical manifestations may include cutaneous, respiratory, and cardiovascular involvement, with edema of the tongue and oropharyngeal region representing the most life-threatening presentation.

Case Report: Two anaphylactic reactions occurring after local anesthetic administration are presented. A 37-year-old male patient undergoing mandibular molar extraction and a 42-year-old female patient scheduled for implant surgery developed dyspnea, dysphagia, and acute soft-tissue edema of the pharyngeal region. Following early diagnosis and emergency intervention, both patients were stabilized and referred for further management. Subsequent allergological evaluation confirmed articaine hypersensitivity in both cases, and the planned procedures were successfully completed using mepivacaine hydrochloride as an alternative local anesthetic agent.

Conclusion: Increasing clinicians' awareness and knowledge regarding the risk of anaphylaxis in dental practice is of critical importance for patient safety.

Keywords: Anaphylaxis; Emergency treatment; Local anesthesia

Citation: Dağal Ö, Naiboğlu Z. Anaphylaxis in Dental Practice: Report of Two Cases ADO Klinik Bilimler Dergisi 2026;15(2):122-128

Editor: Sibel Elif Gültekin, Gazi University, Ankara, Türkiye

Received: 03.23.2026; Accepted: 05.01.2026
**Corresponding author: Dr. Özgür Dağal*
Gazi University Faculty of Dentistry Department of Oral and Maxillofacial Surgery Emek District, Biskek Street, 1st Avenue, No:4 Çankaya, Ankara, Türkiye
E-mail: ozgurdagal@gazi.edu.tr

INTRODUCTION

Anaphylaxis is defined by the World Allergy Organization (WAO) as a systemic hypersensitivity reaction that typically develops rapidly and has the potential to be fatal. Unlike other allergic reactions, it is not confined to a localized response; rather, it is characterized by a systemic response involving multiple organs and systems.[1-3]

Following exposure to an antigen, cutaneous and mucosal involvement (pruritus, generalized urticaria, erythema and swelling of the lips, tongue, or uvula), respiratory manifestations (dyspnea, wheezing, stridor), and hypotension or end-organ dysfunction (hypotonia, syncope, incontinence) may develop within seconds, minutes, or hours. These clinical findings constitute the diagnostic criteria for anaphylactic shock. Anaphylactic shock may follow a biphasic course and can recur within 72 hours after the initial episode has been brought under control.[2, 4]

Triggers of anaphylaxis vary by age. In early life, the most common causes are food allergies (e.g., tree nuts and seafood), whereas in adulthood, medications and insect venoms predominate. Cases in which the underlying cause cannot be identified are defined as idiopathic anaphylaxis.[3, 4] In recent years, the increasing incidence of anaphylactic shock has highlighted the importance of improving dentists' knowledge and awareness in recognizing the clinical signs of anaphylaxis and implementing effective emergency management.[5]

In dental practice, a variety of agents may precipitate anaphylaxis. Commonly prescribed antibiotics include amoxicillin, phenoxymethylpenicillin, and metronidazole, all of which may trigger allergic reactions. Amoxicillin is the antibiotic most frequently associated with anaphylaxis, and fatal anaphylactic

reactions related to this drug have been reported. Similarly, chlorhexidine is a widely used antiseptic in dentistry and may be present in toothpastes and antiseptic solutions. An increase in cases of chlorhexidine-induced anaphylaxis worldwide has been reported.[6]

Hypersensitivity reactions were first classified by Gell and Coombs into four distinct types according to their underlying immunologic mechanisms. Type I hypersensitivity is an IgE-mediated immediate reaction in which re-exposure to a sensitizing antigen triggers the rapid degranulation of mast cells and basophils, leading to the release of histamine, leukotrienes, and prostaglandins. This cascade can manifest within minutes as urticaria, angioedema, bronchospasm, or anaphylaxis. Type II hypersensitivity is a cytotoxic antibody-mediated reaction in which IgG or IgM antibodies bind to cell-surface or extracellular matrix antigens, thereby activating the complement system and culminating in tissue injury; hemolytic transfusion reactions represent a prototypical example. In Type III hypersensitivity, the deposition of antigen–antibody immune complexes within vascular walls activates the complement cascade, triggering localized inflammation and tissue damage, as classically illustrated by serum sickness. Type IV hypersensitivity, in contrast, is an antibody-independent, T lymphocyte-mediated delayed-type reaction; driven by the activation of CD4+ and CD8+ T cells, the response typically becomes apparent 48–72 hours after antigen exposure and encompasses conditions such as contact dermatitis and drug-induced delayed cutaneous reactions. In dental practice, adverse reactions to local anesthetics are most commonly attributed to Type I and Type IV hypersensitivity mechanisms.[7] In dentistry, the risk of allergic reactions to commonly used amide-type local anesthetics (e.g., lidocaine) is very low. Mepivacaine and prilocaine without epinephrine are among the amide derivatives with the lowest allergic potential. In contrast, ester-type local anesthetics carry a higher risk of allergy because they are metabolized to para-aminobenzoic acid.[6-8]

A substantial proportion of reactions attributed to local anesthetics arise not from the active anesthetic agent itself but from excipients present in the solution.[7,9] Benzoates used as preservatives in multidose vials and metabisulfites used as stabilizers in epinephrine-containing anesthetic solutions are among the main triggers of these reactions.[9]

Against the backdrop of the aforementioned considerations, the two cases presented herein exemplify the clinical manifestations and emergency management of anaphylactic reactions developing in the course of local anesthetic administration during routine dental procedures.

CASE REPORT

CASE 1

A 37-year-old male patient presented to the Department of Oral and Maxillofacial Surgery, Gazi University Faculty of Dentistry, with pain in the left posterior mandible. His medical history was unremarkable, with no known systemic disease or previous allergic reactions. Based on clinical and radiographic evaluation, extraction of tooth #38 was indicated. After obtaining informed consent from the patient, regional and infiltration anesthesia was administered articaine hydrochloride 80 mg/epinephrine 0.01 mg per 2 ml (Maxicaine®, VEM Pharmaceuticals, Turkey).

During the anesthetic onset period, the patient reported, "I cannot breathe" and "my throat is swelling." The procedure was immediately discontinued. On urgent clinical assessment, marked uvular edema was detected, and a Code Blue was activated. In parallel, the emergency medical dispatch center (112) was contacted and clearly informed that this was a suspected anaphylaxis case. Nasal oxygen was initiated at 5 L/min, the patient was placed on continuous monitoring, and intravenous access was established without delay.

Vital signs were recorded as follows: noninvasive blood pressure 110/70 mmHg, SpO_2 98%, and heart rate 100 beats/min. Airway management equipment (bag-valve mask, face mask, laryngoscope, size 7 endotracheal tube) and 1 mg epinephrine were prepared and kept readily available for emergency intervention.

Intravenous methylprednisolone (methylprednisolone sodium succinate 40 mg; Prednol-L®, Mustafa Nevzat Pharmaceuticals, Turkey) 100 mg, pheniramine hydrogen maleate (pheniramine hydrogen

maleate 45.5 mg/2 ml; Avil®, Sandoz Pharmaceuticals, Turkey) (one ampoule), and 100 mL normal saline as a rapid infusion were administered. The patient demonstrated a prompt clinical response; respiratory compromise resolved and vital signs remained stable. After a period of close clinical observation, the patient was handed over to the emergency medical team and transferred to a fully equipped healthcare facility for further evaluation and management.

Following discharge, the patient was referred to the Department of Allergy and Immunology, Gazi University Faculty of Medicine, for comprehensive allergological evaluation. Subsequent allergy workup confirmed hypersensitivity to articaine. The planned dental procedure was successfully completed at a later date using mepivacaine hydrochloride 30 mg/ml (Safecaine®, VEM Pharmaceuticals, Turkey) as an alternative local anesthetic agent.

CASE 2

A 42-year-old female patient presented to the Department of Oral and Maxillofacial Surgery, Gazi University Faculty of Dentistry, with a complaint of missing teeth. Her medical history was unremarkable, with no systemic disease and no prior history of allergic reactions.

Clinical and radiographic examination revealed complete edentulism of the maxilla, and implant surgery was planned. Informed consent was obtained from the patient for the procedure. Infiltration anesthesia was administered using a 2 ml cartridge of articaine hydrochloride 80 mg/epinephrine 0.01 mg (Maxicaine®, VEM Pharmaceuticals, Turkey). Dexamethasone 8 mg (Dekort® 8 mg/2 ml, Deva Holding, Turkey) was administered prophylactically to prevent postoperative edema, and tenoxicam 20 mg (Oksamen-L® 20 mg, Gensenta Pharmaceuticals, Turkey) was administered prophylactically for postoperative pain management.

During the anesthetic onset period, the patient reported, “I am having difficulty breathing,’’ “my throat is swelling,’’ and “I cannot swallow.’’ Urgent clinical assessment revealed marked edema of the tongue and uvula. A Code Blue was immediately activated, and the emergency medical dispatch center (112) was simultaneously contacted and explicitly informed of a suspected case of anaphylaxis. Nasal oxygen was initiated at 5 L/min, continuous monitoring was established, and intravenous access was secured. Vital signs were recorded as follows: noninvasive blood pressure 104/64 mmHg, SpO_2 97%, and heart rate 96 beats/min. Airway management equipment, including a bag-valve mask, face mask, laryngoscope, and size 7 endotracheal tube, were prepared and kept immediately available for emergency intervention, together with 1 mg epinephrine. Intravenous methylprednisolone sodium succinate (Prednol-L® 40 mg, Mustafa Nevzat Pharmaceuticals, Turkey) 100 mg, one ampoule of pheniramine hydrogen maleate 45.5 mg/2 ml (Avil®, Sandoz Pharmaceuticals, Turkey), and 100 mL of normal saline as a rapid infusion were promptly administered.

A prompt clinical response was observed; respiratory compromise resolved and vital signs remained stable. Following a period of close clinical observation, the patient was handed over to the emergency medical team and transferred to a fully equipped healthcare facility for further evaluation and management.

Following discharge, the patient was referred to the Department of Allergy and Immunology, Gazi University Faculty of Medicine, for comprehensive allergological evaluation. Allergy workup confirmed hypersensitivity to articaine; however, no allergic sensitization was detected to tenoxicam or dexamethasone, which had been administered prophylactically prior to the procedure. The planned implant surgery was subsequently completed without complication using mepivacaine hydrochloride 30 mg/ml (Safecaine®, VEM Pharmaceuticals, Turkey) as an alternative local anesthetic agent.

DISCUSSION

Anaphylaxis is a rapidly progressive and life-threatening systemic reaction that requires accurate and timely intervention. However, evidence from the current literature and real-world practice indicates that awareness and practical competency regarding anaphylaxis management among healthcare professionals remain suboptimal.[1,2,6,10] One of the main challenges in clinical practice is the variability of anaphylaxis manifestations among patients, which may complicate prompt recognition and accurate diagnosis. Although urticaria, angioedema,

respiratory distress, and hypotension are prominent in many cases, diagnosis may be delayed or incorrect when these findings are absent, atypical, or subtle.[10]

Among the clinical conditions that may be confused with anaphylaxis, panic attacks and vasovagal syncope are particularly noteworthy, as misidentification of these entities may result in unnecessary interventions or, conversely, inadequate treatment.[6,10,11] In the present case, clinical assessment was conducted systematically in accordance with the ABCDE approach.[11] Airway (A) evaluation revealed marked edema of the tongue and uvula, and this potentially life-threatening upper airway compromise was identified without delay. Breathing (B) was assessed through continuous SpO_2 monitoring, and supplemental nasal oxygen was promptly initiated. Circulation (C) was evaluated via noninvasive blood pressure and heart rate monitoring, with parameters remaining within clinically acceptable limits throughout the episode. Disability (D) assessment confirmed that the patient maintained full consciousness with no evidence of neurological deterioration. The systematic application of this framework facilitated rapid differential diagnosis, enabled timely and targeted intervention, and contributed directly to the favorable clinical outcome observed in this case. Current guidelines pertaining to emergency management in dental practice similarly emphasize the potential of structured assessment protocols to reduce clinical errors and enhance patient safety.[6,10,11]

Epinephrine remains the first-line and life-saving therapy in the management of anaphylaxis. Clinical guidelines recommend intramuscular administration, preferably into the anterolateral thigh. Nevertheless, studies have shown that many healthcare providers, particularly dentists, lack sufficient knowledge and hands-on experience regarding epinephrine administration.[6,10] This deficit may contribute to treatment delays in emergencies and adversely affect patient outcomes. In dental practice, frequent exposure to potential allergens, such as local anesthetics and latex, may increase the risk of anaphylactic reactions. For this reason, it is essential that dentists possess adequate theoretical knowledge and practical skills to recognize anaphylaxis promptly and initiate appropriate emergency management.

Toothpastes containing milk-derived protein have also been reported to cause anaphylaxis in individuals with allergy to milk and dairy products. Likewise, iodoform is included in the composition of butamben/eugenol/iodoform-containing topical dressing (Alveogyl®, Septodont®), which is used in endodontic materials and in the management of dry socket. Due to the risk of allergic reactions, its use is not recommended in individuals with allergies to procaine derived anesthetics, iodine, or iodine-containing compounds.[10]

Natural rubber latex allergy became more prevalent toward the end of the 20th century with increased glove use in healthcare settings; however, its incidence has shown a decreasing trend in recent years.[6] Latex allergy has been reported in 9.7% of healthcare workers, 7.2% of at-risk patient groups, and 4.3% of the general population.[1] Patients with spina bifida, healthcare workers, and individuals with allergies to foods such as banana, kiwi, and avocado are considered to be at increased risk. Latex-induced anaphylaxis may follow a more severe course in patients with uncontrolled asthma.[6,8] Nevertheless, despite the prevalence of latex allergy, the development of an anaphylactic reaction in dental practice is exceedingly rare, with only one case reported over the past 20 years. Recent studies indicate that latex is no longer a prominent trigger of perioperative anaphylaxis.[8]

Although anaphylaxis may arise through different mechanisms, certain biological pathways can be commonly activated, and more than one mechanism may be engaged simultaneously. IgE-mediated anaphylaxis is the most common and classical mechanism, initiated when an allergen binds to allergen-specific IgE on the surface of mast cells and basophils. This interaction activates intracellular signaling pathways, leading to the release of both preformed and newly synthesized mediators. Non–IgE-mediated anaphylaxis may occur via immunologic or non-immunologic mechanisms. Immunologic mechanisms include complement activation, the contact and coagulation systems, and IgG-mediated anaphylaxis.[7,9] Non-immunologic mechanisms are particularly associated with certain medications, alcohol, and physical exertion. In addition, direct activation of mast cells via the MRGPRX2 receptor may also contribute to the

development of anaphylactic reactions.[9, 11]

Articaine, a structurally distinctive amide-type local anesthetic characterized by a thiophene ring rather than the phenyl ring found in other amide agents such as lidocaine and mepivacaine, is the most widely used local anesthetic in dental practice. As the sole common agent administered in both cases presented herein, articaine was identified as the most probable causative trigger. True IgE-mediated hypersensitivity to amide-type local anesthetics is exceedingly rare, accounting for less than 1% of all adverse drug reactions attributable to this class; nevertheless, when such reactions do occur, articaine has been identified as one of the most frequently implicated agents within the amide group.[6,9] The proposed sensitization mechanism involves articaine functioning as a hapten — a small molecule that is not inherently immunogenic but acquires antigenic properties upon binding to serum carrier proteins, thereby eliciting allergen-specific IgE production during initial exposure. Upon subsequent re-exposure, sensitized mast cells and basophils undergo activation, triggering the release of histamine and other vasoactive mediators and culminating in the clinical manifestations of anaphylaxis.[7,12] Beyond IgE-mediated pathways, complement-mediated mast cell degranulation and pseudo-allergic mechanisms involving direct cellular activation have also been described in the setting of articaine hypersensitivity. The use of epinephrine-containing formulations in both cases warrants particular attention, as sodium metabisulfite — incorporated as a stabilizing agent in vasopressor-containing local anesthetic solutions — is a recognized trigger of hypersensitivity reactions and may contribute to such reactions either synergistically with, or independently of, the anesthetic molecule itself.[6,9] From a risk stratification perspective, patients with a prior history of drug hypersensitivity, an atopic background, or known sulfite sensitivity require heightened vigilance when articaine-containing formulations are planned; in such individuals, allergy evaluation including skin prick testing and intradermal testing is recommended prior to elective dental procedures.[6, 9, 12]

A three-step approach, comprising prevention, alert, and intervention, has been proposed for the effective management of anaphylaxis. In the prevention phase, it is essential to document the patient's medical history in detail, identify risk factors, and improve healthcare professionals' education and awareness. In the alert phase, early recognition of warning signs and close monitoring of symptoms are required. In the intervention phase, predefined emergency management protocols should be implemented promptly, and the emergency response team should be contacted without delay.[12]

Maintaining an emergency kit in dental clinics and ensuring its appropriate use are of paramount importance. The kit should be portable and readily accessible, and rapid access to an oxygen source is recommended. In addition, the kit must include a guide containing emergency telephone numbers and management protocols.[1] In the dental office emergency drug kit, the availability of 1:1,000 (1 mg/mL) epinephrine ampoules is mandatory; although prefilled 1:1,000 epinephrine syringes are available, difficulties in procuring these products have been reported.[6]

Epinephrine is the cornerstone and life-saving drug in the treatment of anaphylaxis. Delays in administration increase mortality, and failure to administer epinephrine is the most common cause of anaphylaxis-related deaths.[6,8,11,12] Epinephrine reverses peripheral vasodilation, thereby increasing blood pressure; reduces edema; produces bronchodilation; enhances myocardial contractility; and inhibits the release of histamine and leukotrienes.[6] Epinephrine should be stored in ampoule form and protected from light and heat to prevent inactivation. Each epinephrine ampoule contains a concentration of 1 mg/mL. The recommended intramuscular dose is 500 µg (0.5 mL of a 1:1,000 solution) for adults and children aged ≥12 years, 300 µg (0.3 mL) for children aged 6–12 years, and 150 µg (0.15 mL) for children under 6 years. If the clinical response is inadequate, doses may be repeated at 5-minute intervals. In addition to epinephrine, other medications are also used in the management of anaphylaxis (Table 1).[7]

The vastus lateralis muscle is considered the preferred site for intramuscular epinephrine injection. Current guidelines recommend performing aspiration; however, they do not recommend post-injection massage or skin disinfection with alcohol.[9,11]

Table 1. Medications and dose regimens for the treatment of anaphylaxis.

Medication	Dosage and Administration	Clinical Indication
Epinephrine (Adrenaline)	0.01 mg/kg (maximum 0.5 mg), administered via the IM route	First-line treatment of anaphylactic shock.
Antihistamines	Chlorpheniramine: 10 mg IV/IM, or Diphenhydramine: 25–50 mg IV/IM	Control of histamine-mediated symptoms.
Corticosteroids	Hydrocortisone: 200 mg IV, or Methylprednisolone: 1–2 mg/kg IV	Prevention of late-phase reactions and reduction of inflammation.
β2-Agonists	Salbutamol: 2.5 mg via nebulized inhalation	Treatment of bronchospasm and relief of respiratory symptoms.
Fluid Therapy	Isotonic saline (0.9% NaCl) IV	Management of hypotension and circulatory support.
Oxygen	High-flow oxygen (6–8 L/min)	Prevention of hypoxemia and respiratory support.

IV: Intravenous, IM: Intramuscular

The urgency of the patient's condition and the need for epinephrine administration should be explained promptly and clearly, and the anterolateral thigh should be prepared for injection whenever possible. Epinephrine should be drawn from a 1:1,000 ampoule into a syringe, air bubbles should be expelled, and the drug should be administered intramuscularly into the muscle in a single swift motion at a 90° angle using an appropriate needle. After injection, a brief waiting period is recommended, the needle should be safely removed, and epinephrine should be kept readily available in case repeat dosing is required.[12,13]

Although an epinephrine allergy is theoretically possible, it is extremely rare in clinical practice. Most reported cases are associated with sodium metabisulfite present in epinephrine solutions.[14] However, even in individuals with sulfite sensitivity, epinephrine administration should not be delayed when anaphylaxis occurs, as its therapeutic benefit clearly outweighs the potential risks.[15,16] In suspected anaphylaxis, help should be summoned immediately, emergency medical services (112) should be notified, and the patient should be assessed using the ABCDE approach (airway, breathing, circulation, disability, exposure).[15,17] The dental procedure should be terminated, exposure to the suspected allergen should be discontinued, and appropriate positioning and high-flow oxygen support should be provided.[6,18,19]

CONCLUSION

The key components of successful anaphylaxis management are early recognition of the severity of the clinical presentation, prompt activation of specialist/emergency assistance, and immediate initiation of epinephrine therapy without delay. Effective implementation of these goals depends not only on individual knowledge and preparedness but also on the continuity of institutional training policies. Therefore, the establishment of standardized and periodic training programs for healthcare professionals should be regarded as a sustainable strategy to enhance patient safety and improve clinical outcomes.

REFERENCES

1. Castilano A, Sternard B, Cummings ED. Pitfalls in anaphylaxis diagnosis and management at a university emergency department. Allergy Asthma Proc 2018; 39: 316–21.

2. Johnson RF, Peebles RS. Anaphylactic shock: pathophysiology, recognition, and treatment. Semin Respir Crit Care Med 2004; 25: 695–703.

3. Brown SG. The pathophysiology of shock in anaphylaxis. Immunol Allergy Clin North Am 2007; 27: 165–75.

4. María A, Verdú S, Ferreira A. Anaphylactic shock: a review of the pathophysiology and therapeutic management. Odontologia (Montevideo) 2025; 3:199-4.

5. Maher NG, de Looze J, Hoffman GR. Anaphylaxis: an update for dental practitioners. Aust Dent J 2014; 59: 142–8.

6. Hussar DA. Interactions involving drugs used in dental practice. J Am Dent Assoc 1973; 87: 349–58.

7. Soar J, Pumphrey R, Cant A. Emergency treatment of anaphylactic reactions-guidelines for healthcare providers. Resuscitation 2008; 77: 157–69.

8. Chin SM, Ferguson JW, Bajurnows T. Latex allergy in dentistry. Review and report of case presenting as a serious reaction to latex dental dam. Aust Dent J 2004; 49: 146–8.

9. Henderson S. Allergy to local anaesthetic agents used in dentistry-what are the signs, symptoms, alternative diagnoses and management options? Dent Update 2011; 38: 410–2.

10. Travers A, Taylor K. Adrenaline use: The use of pre-filled adrenaline syringes in anaphylaxis kits. Br Dent J 2019; 226: 85–6.

11. Simons FE, Ardusso LR, Bilò MB. World allergy organization guidelines for the assessment and management of anaphylaxis. World Allergy Organ J 2011; 4: 13–37.

12. Becker DE. Drug allergies and implications for dental practice. Anesth Prog 2013; 60: 188–97.

13. Sala-Cunill A, Cardona V. Definition, Epidemiology, and Pathogenesis. Current Treatment Options in Allergy 2015; 2: 207–17.

14. Ben-Shoshan M, Clarke AE. Anaphylaxis: past, present and future. Allergy 2011; 66: 1–14.

15. Khodoun M, Strait R, Orekov T. Peanuts can contribute to anaphylactic shock by activating complement. J Allergy Clin Immunol 2009; 123: 342–51.

16. Simons FE. Anaphylaxis. J Allergy Clin Immunol 2010; 125: S161–81.

17. Whyte AF, Soar J, Dodd A. Emergency treatment of anaphylaxis: concise clinical guidance. Clin Med (Lond) 2022; 22: 332–9.

18. Jevon P, Shamsi S. Management of anaphylaxis in the dental practice: an update. Br Dent J 2020; 229: 721–8.

19. McNeil BD, Pundir P, Meeker S. Identification of a mast-cell-specific receptor crucial for pseudo-allergic drug reactions. Nature 2015; 519: 237–41.

Diş Hekimliği Pratiğinde Anafilaksi: İki Olgu Sunumu

ÖZET

Giriş: Anafilaksi, Dünya Alerji Örgütü tarafından hızlı gelişen ve ölümle sonuçlanma potansiyeli taşıyan sistemik aşırı duyarlılık reaksiyonu olarak tanımlanmaktadır. Klinik bulgular kutanöz, solunum ve kardiyovasküler sistemleri etkileyerek; dil ve orofaringeal bölgede ödem gelişmesi hayatı tehdit eden klinik tablo oluşturmaktadır.

Vaka Raporu: Bu çalışmada, lokal anestezik uygulaması sonrası gelişen iki anafilaktik reaksiyon olgusu sunulmaktadır. Mandibular molar çekimi yapılan 37 yaşında erkek hasta ve implant cerrahisi planlanan 42 yaşında kadın hastada dispne, disfaji ve faringeal bölgede akut yumuşak doku ödemi gelişmiştir. Erken tanı ve acil müdahalenin ardından her iki hasta da stabilize edilerek ileri tedavi için sevk edilmiştir. Alerji değerlendirmesi her iki hastada da artikain hipersensitivitesini doğrulamış ve planlanan girişimler alternatif lokal anestezik ajan olarak mepivakain hidroklorür kullanılarak başarıyla tamamlanmıştır.

Sonuç: Diş hekimliği pratiğinde anafilaksi riskine karşı klinisyenlerin farkındalık ve bilgi düzeylerinin artırılması hasta güvenliği açısından kritik öneme sahiptir.

Anahtar Kelimeler: Anafilaksi; Acil tedavi; Lokal anestezi

DOI: https://doi.org/10.54617/adoklinikbilimler.1893329

Case Report

Management of a Maxillary Ossifying Fibroma Using a Three-Dimensional Virtual Model: A Case Report

Yusuf Ersel Arslan [1*], **Berkay Mülayim** [2], **Benay Yıldırım** [2], **Umut Tekin** [1]

[1]*Department of Oral and Maxillofacial Surgery, Gülhane Faculty of Dentistry, Health Sciences University, Ankara, Türkiye*
[2]*Department of Oral Pathology, Faculty of Dentistry, Gazi University, Ankara, Türkiye*

ABSTRACT

Introduction: Ossifying fibroma is a benign, but locally aggressive neoplasm of the maxillofacial region. It represents a fibro-osseous lesion in which normal bone tissue is replaced by cellular fibrous tissue containing mineralized material, usually detected incidentally. Treatment options range from conservative approaches such as enucleation and curettage to resection.

Case Report: We present the surgical management of an ossifying fibroma incidentally detected in the right posterior maxilla of a 48-year-old female patient with the support of three-dimensional (3D) virtual planning. Under the guidance of the virtual planning, the lesion was enucleated, and a peripheral osteotomy was performed. No recurrence was observed during the one year clinical and radiological follow-up period.

Conclusion: 3D virtual modeling can contribute to safe and precise surgery by providing spatial awareness to the surgeon and it has the potential to strengthen the informed consent process and patient–physician communication.

Keywords: Computer-assisted surgery; Image processing, computer-assisted; Imaging, three-dimensional; Patient education as topic

Received: 02.20.2026; Accepted: 05.01.2026
**Corresponding author: Dr. Yusuf Ersel Arslan*
SBU Gülhane Faculty of Dentistry, Department of Oral and Maxillofacial Surgery, Emrah mah. Etlik, Ankara, Türkiye
E-mail: yusuferselarslan@gmail.com

Citation: Arslan YE, Mülayim B, Yıldırım B, Tekin U. Management of a Maxillary Ossifying Fibroma Using a Three-Dimensional Virtual Model: A Case Report. ADO Klinik Bilimler Dergisi 2026;15(2):129-134

Editor: Yeliz Kılınç, Gazi University, Ankara, Türkiye

INTRODUCTION

Ossifying fibroma (OF) is a benign fibro-osseous neoplasm characterized by the replacement of bone tissue with fibrous stroma and varying amounts of mineralized components and typically exhibits a slow growth pattern.[1] According to the 2022 updated classification of the World Health Organization (WHO), an ossifying fibroma is defined as a mesenchymal odontogenic tumor arising from multipotent cells of the periodontal ligament.[2] These lesions are generally observed in the 2nd to 4th decades of life, show a marked predilection for women, and most commonly affect the posterior mandibular region.[3] Although maxillary involvement is less common, lesions in this region can reach advanced stages without causing noticeable symptoms because of the presence of adjacent anatomical spaces and the cancellous structure of the maxillary bone, and are often detected incidentally during routine examinations.[4]

The treatment method for ossifying fibroma is determined by the location, size, and infiltrative potential of the lesion, and it encompasses a wide surgical spectrum, ranging from conservative procedures such as enucleation and curettage to resection.[5]

Currently, 3D modeling and virtual planning technologies are frequently used to increase operational safety and surgical precision, particularly for fibro-osseous lesions with complex anatomical relationships.[6]

This case presentation aimed to highlight the role of digital planning tools in regard to surgical management by utilizing 3D modeling technology in a case of OF incidentally detected in the posterior maxilla.

CASE REPORT

A 48-year-old female patient was referred to our clinic with a lesion detected in the right posterior maxilla during routine radiographic examinations. The medical history of the patient revealed no complaints of pain, paresthesia, or swelling. Extraoral examination revealed no obvious facial asymmetry, whereas intraoral examination revealed a firm, immobile mass in the posterior region of the right maxilla extending from the distal aspect of tooth 15 to the maxillary tuberosity, causing bone expansion in both the vestibular and palatal directions (Figure 1).

Panoramic radiography revealed a well-defined, mixed radiolucent, radiopaque lesion in the right posterior maxilla (Figure 2A). Cone-beam computed tomography (CBCT) demonstrated that the lesion measured approximately 26 × 24 × 23 mm, extended superiorly into the maxillary sinus, and was in close proximity medially to the descending palatine artery (Figure 2B).

Before the surgical intervention, an incisional biopsy was performed under local anesthesia using a trephine drill for histopathological evaluation. The performed pathological examination revealed broad, acellular osteoid islands that were partially anastomosed and surrounded by cellular spindle cell stroma with brush-like edges blending into the surrounding connective tissue (Figure 3A). At higher magnification, spindle-shaped fibroblasts without cytological atypia, spherical calcification foci between them, and “osteoblastic rimming” around the bone trabeculae (osteoblast alignment) were observed, and OF was diagnosed (Figure 3B).

For surgical planning, 3D Slicer software (version 5.8.0; www.slicer.org) was used to detail the complex relationship between the lesion and surrounding

Figure 1. Intraoral view.

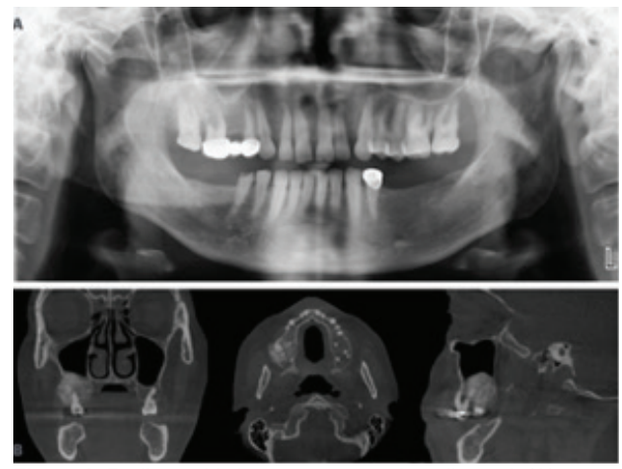

Figure 2. Radiographic images; panoramic radiograph (A) and CBCT sections (B).

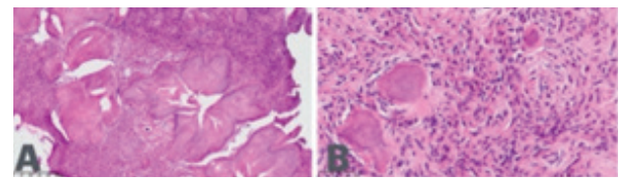

Figure 3. Histopathological images; H&E, ×100 (A) and H&E, ×400 (B).

anatomical structures, its true volume, and its margins to guide surgery. The CBCT data of the patient were imported into the software, and the craniomaxillofacial bones were automatically segmented using an artificial intelligence-based DentalSegmentator extension (3D Slicer, version 5.8.0; www.slicer.org). Because artificial intelligence could not separate the lesion from the adjacent anatomical structures, reference points were manually defined on the CBCT slices during the lesion segmentation process, and the “fill between slices” module was used. Therefore, a 3D model of the lesion was manually created (Figure 4). The surgical margins and excision strategy were designed based on a digital model obtained using a semi-automated workflow.

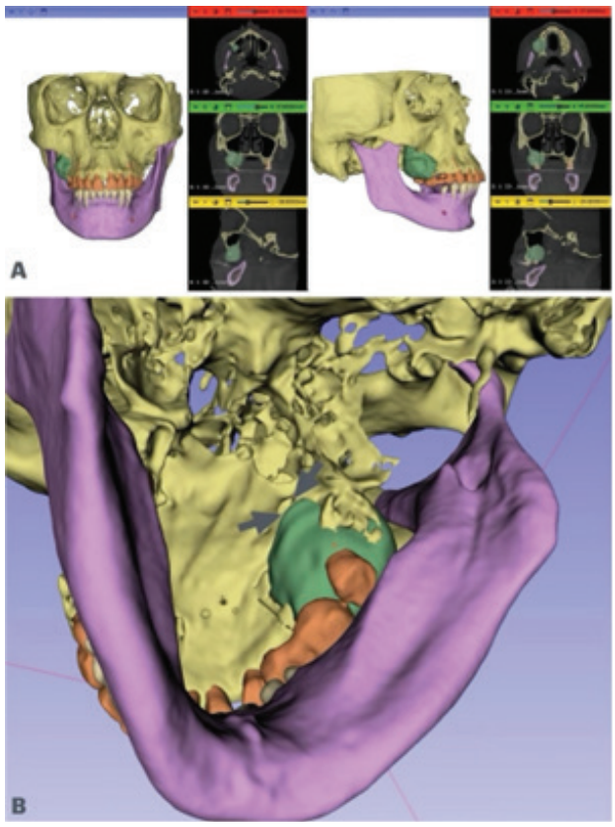

Figure 4. Three-dimensional virtual model reconstructed from CBCT data; different views of the model (A) and proximity of the lesion to the greater palatine foramen (grey arrows) (B).

Figure 5. Intraoperative views.

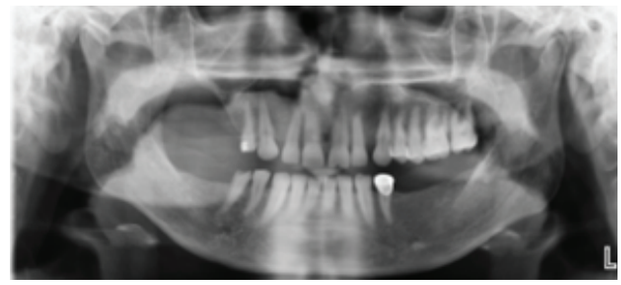

Figure 6. Panoramic radiograph at 1-year postoperative follow-up.

During the surgical procedure, teeth 16 and 17 were extracted, and the lesion was enucleated within the boundaries determined using the 3D modeling data (Figure 5). Following enucleation, peripheral osteotomy was performed on the cavity walls using appropriate burs to minimize the risk of recurrence. Perioperative observation revealed that the lesion displaced the maxillary sinus superiorly; however, the sinus membrane and bony integrity were preserved, and no perforation occurred. The descending palatine artery was also preserved. The reconstruction procedure was not considered during the initial phase. The patient was followed up for recurrence, and no signs of recurrence were detected during the year of clinical and radiological follow-up (Figure 6). Because of the potential for recurrence, the patient is still being followed up by our team. Written informed consent was obtained from the patient for the surgical procedures performed, as well as for the use of the clinical data and images included in this study for scientific publication.

DISCUSSION

Ossifying fibroma, the most common fibro-osseous lesion of the maxillofacial region, the fibrous osteoma, is a benign neoplasm that presents diagnostic challenges owing to its clinical and radiological variability.[3,7] Although the literature reports a significant predominance of mandibular over maxillary involvement (70 - 90%), lesions located in the posterior maxilla, as in the present case, can progress clinically silently and reach large sizes because of the extensive anatomical spaces and spongy bone structure of the region.[8] As in the current case, this may result in the incidental detection of the lesion during routine procedures; indeed, 31-58% of OF cases have been reported in the literature to be diagnosed incidentally.[9,10]

Because the histopathological features of benign fibro-osseous lesions are similar, a clinicoradiological correlation is essential for a definitive diagnosis.[3,7]

At the microscopic level, the osteoblastic rimming observed in our case indicates neoplastic bone formation.[11] The presence of heterogeneous osteoid structures and brush-like edges blended into the surrounding connective tissue supported this diagnosis.[12] Histological findings alone are not diagnostic; fibrous dysplasia is the main differential diagnosis.[3,9] The sharply demarcated nature of OF, presence of cortical expansion instead of bone replacement, and heterogeneous osteoid structures are important features in distinguishing OF from fibrous dysplasia.[12,13] OF may also show histological similarities with focal and florid cemento-osseous dysplasia.[9,11] Nevertheless, it is crucial to exclude malignancies, such as low-grade osteosarcoma, particularly when rapid growth, an atypical radiological pattern, or a clinically aggressive appearance is present.[5] In this context, incisional biopsy performed with a trephine drill before surgical intervention can be considered a critical step that increases diagnostic accuracy by helping clarify the biological behavior of the lesion and rule out any aggressive variants. In suspicious cases, negativity for molecular markers such as MDM2 and CDK4 may provide additional evidence in favor of benign fibro-osseous processes.[14]

In the surgical management of the present case, 3D virtual surgical planning, an approach that has been increasingly adopted in recent years, was integrated into the clinical decision-making process.[15] Although CBCT sections provide valuable information regarding lesion boundaries and adjacent structures, visualization of these data within a 3D environment allows the assessment of lesion volume, extent, and relationship to critical anatomical structures, such as the maxillary sinus and palatal vascular structures, within a single model.[16] In the literature, virtual surgical planning (VSP) workflows frequently culminate in the fabrication of physical models and surgical guides. However, these additional production stages may limit the applicability of such methods because of the need for advanced infrastructure and associated high costs. Data on the standalone use of VSP in benign tumors, without these additional stages, remain limited.[17] Virtual models can provide an overall spatial assessment without requiring each tomographic section to be examined separately, thereby facilitating the determination of surgical access strategies and the anticipation of intraoperative risks, particularly in anatomically complex regions such as the posterior maxilla.[17,18] In the present case, the proximity of the lesion to the descending palatine artery was visualized more clearly, which allowed for a more meticulous preparation process against potential bleeding complications, thereby shortening the operative time and preventing this complication through a more predictable surgery. Given the well-circumscribed fibro-osseous nature of the lesion, enucleation was planned, and a surgical cutting guide was not considered necessary. Instead, the virtual model was referred to during the intraoperative period. Intraoperative reference to the virtual plan allowed the accuracy of each step to be verified. Through the “mental navigation” provided by the virtual model, safe surgical boundaries were more easily achieved, the conservative approach was applied more confidently, and unnecessary morbidity could be avoided. Therefore, as used in this study, virtual models can enable the surgeon to access more detailed visual information instead of relying solely on the limited information provided by CBCT sections, even in situations where physical guides and models requiring advanced infrastructure or additional costs cannot be produced. This low-cost digital workflow, based solely on virtual modeling, provides an adequate visual-spatial reference source that goes beyond conventional imaging data.

Furthermore, the availability of free and easily accessible platforms, such as the software used in this study, together with the modeling method employed, represents a significant advantage that increases the applicability of this approach across different centers.[15] Automating the segmentation and modeling process with artificial intelligence-based plugins can reduce operator dependence, provide a faster workflow, and support the broader use of digital planning in surgical practice.[15]

Three-dimensional modeling can make a meaningful contribution not only to surgical planning but also to patient education and informed consent processes.[8] Although systematic reviews have confirmed that these technologies significantly facilitate understanding of the pathology and the surgical plan, the literature remains concentrated largely in fields such as urology and orthopedics, while data regarding maxillofacial surgery are still relatively limited.[19] Compared with physical models, virtual models offer

a lower-cost and more easily modifiable alternative. In the present case, they enabled the patient to understand the true dimensions of the lesion and the scope of the planned intervention more concretely, thereby minimizing the risk of a potential “expectation mismatch.” This clinical observation suggests that the integration of virtual models into consent processes in maxillofacial surgery represents a valuable area for future research, particularly given the current gap in the literature and the potential to improve both patient awareness and communication quality.

The combination of enucleation and peripheral osteotomy used as the treatment strategy in this case was a conservative approach that aimed to reduce residual lesion tissue while avoiding the morbidity of radical resections.[5] The recurrence rates in OF have been reported in the literature to vary widely (0–28%) depending on the surgical technique used, and long-term clinical and radiological follow-up is particularly important in cases located in the maxilla and adjacent to the sinus.[13] Although the absence of recurrence during one year of follow-up in this case was favorable in terms of short-term outcome, a longer follow-up is planned for a more accurate assessment of recurrence.

CONCLUSION

In conclusion, approaches supported by a free and easily accessible 3D modeling platform may contribute to surgical safety and increased patient awareness in maxillary OF cases, and may encourage the wider use of similar digital planning approaches in clinical practice.

ACKNOWLEDGEMENTS

None.

CONFLICTS OF INTEREST STATEMENT

No conflicts of interest.

REFERENCES

1. Tater J, Diajil AR. Immunohistochemical analysis of osteoclastic and osteoblastic activity in ossifying fibroma and juvenile ossifying fibroma: A comparative study. J Med Life 2023;16:1369-74.

2. Vered M, Wright JM. Update from the 5th Edition of the World Health Organization Classification of Head and Neck Tumors: Odontogenic and maxillofacial bone tumours. Head Neck Pathol 2022;16:63-75.

3. Collins LHC, Zegalie NFT, Sassoon I, Speight PM. A clinical, radiological and histopathological review of 74 ossifying fibromas. Head Neck Pathol 2023;17:433-46.

4. Bhat SV, Kumar SP, Periasamy S, Krishna VK. An uncommon presentation of ossifying fibroma in the maxilla. Cureus 2022;14:e23638.

5. Gautier B, Dugast S, Guyonvarc’h P, Longis J, Corre P, Bertin H. Ossifying fibroma and juvenile ossifying fibroma: A systematic review on clinical and radiological parameters, treatment modalities and recurrence. J Stomatol Oral Maxillofac Surg 2025;126:102185.

6. Sharaf BA, Abushehab A, Michaelcheck CE, Hussein SM, Gibreel W, Alser O, *et al*. Virtual surgical planning in craniomaxillofacial surgery: A systematic review and meta-analysis of accuracy, operative time, and cost-effectiveness. J Plast Reconstr Aesthet Surg 2025;105:305-14.

7. Kumar KAJ, Kishore PK, Mohan AP, Venkatesh V, Kumar BP, Gandla D. Management and treatment outcomes of maxillofacial fibro-osseous lesions: A retrospective study. J Maxillofac Oral Surg 2015;14:728-34.

8. Nilesh K, Punde P, Patil NS, Gautam A. Central ossifying fibroma of mandible. BMJ Case Rep 2020;13:e239286.

9. MacDonald-Jankowski DS, Li TK. Ossifying fibroma in a Hong Kong community: The clinical and radiological features and outcomes of treatment. Dentomaxillofac Radiol 2009;38:514-23.

10. MacDonald-Jankowski DS. Ossifying fibroma: A systematic review. Dentomaxillofac Radiol 2009;38:495-513.

11. de Noronha Santos Netto J, Machado Cerri J, Miranda AM, Pires FR. Benign fibro-osseous lesions: Clinicopathologic features from 143 cases diagnosed in an oral diagnosis setting. Oral Surg Oral Med Oral Pathol Oral Radiol 2013;115:e56-65.

12. Yaga US, Mengji AK, Kesary SPR, Gollamudi N. Central cemento-ossifying fibroma of posterior maxilla. J Indian Acad Oral Med Radiol 2015;27:282-5.

13. Tompodung LM, Sensusiati AD. Ossifying fibroma of the maxilla: A case report with literature review. Radiol Case Rep 2024;19:915-21.

14. Dujardin F, Binh MBN, Bouvier C, Gomez-Brouchet A, Larousserie F, Muret A de, *et al*. MDM2 and CDK4 immunohistochemistry is a valuable tool in the differential diagnosis of low-grade osteosarcomas and other primary fibro-osseous lesions of the bone. Mod Pathol 2011;24:624-37.

15. Tel A, Arboit L, De Martino M, Isola M, Sembronio S, Robiony M. Systematic review of the software used for virtual surgical planning in craniomaxillofacial surgery over the last decade. Int J Oral Maxillofac Surg 2023;52:775-86.

16. Beyer M, Brasse A, Abazi S, Beyer M, Vinayahalingam S, Seifert L, *et al*. An innovative AI-based dual segmentation application for head surgery. Int J Oral Maxillofac Surg 2026;55:489-95.

17. Gernandt S, Tomasella O, Scolozzi P, Fenelon M. Contribution of 3D printing for the surgical management of jaws cysts and

benign tumors: A systematic review of the literature. J Stomatol Oral Maxillofac Surg 2023;124:101433.

18. Bhatt MA, Kemmu A, Choudhary A, Baghel A, Parthasarathy B, Aishwarrya P. Use of virtual surgical planning in oral surgery: A systematic review. Cureus 2025;17:e81051.

19. Masanet S, Jutand MA, Margue G, Hoarau H, Bernhard JC. Using 3D-printing technology for patient education: A review of the literature. 3D Print Med 2025;11:49.

Üç Boyutlu Sanal Model Kullanılarak Yönetilen Maksiller Ossifiye Fibrom: Olgu Sunumu

ÖZET

Giriş: Maksillofasiyal bölgenin benign ancak lokal agresif karakter sergileyebilen bir neoplazmı olan ossifiye fibrom, normal kemik dokusunun yerini mineralize materyal içeren selüler fibröz dokunun aldığı, sıklıkla tesadüfi olarak saptanan fibro-osseöz bir lezyondur. Tedavi seçenekleri enükleasyon ve küretaj gibi konservatif yaklaşımlardan, rezeksiyonlara kadar değişebilmektedir.

Vaka raporu: Bu olgu sunumunda, 48 yaşında kadın hastada sağ maksilla posterior bölgede rastlantısal olarak saptanan ossifiye fibromun üç boyutlu sanal planlama desteğiyle cerrahi yönetimi sunulmaktadır. Sanal planlama rehberliğinde lezyon enükle edilmiş ve periferal osteotomi uygulanmıştır. Bir yıllık klinik ve radyolojik takipte nüks izlenmemiştir.

Sonuç: Üç boyutlu sanal modelleme, cerraha uzamsal farkındalık sağlayarak güvenli ve hassas cerrahiye katkı sağlayabilecek bir araç olmakta; ayrıca aydınlatılmış onam sürecini ve hasta-hekim iletişimini de güçlendirebilecek potansiyel taşımaktadır.

Anahtar Kelimeler: Bilgisayar yardımlı cerrahi; Görüntü işleme, bilgisayar yardımlı; Görüntüleme, üç-boyutlu; Konu olarak hasta eğitimi

ANKARA DİŞHEKİMLERİ ODASI

Ziya Gökalp Cad. No:37/14 Kat:7 Kızılay-Çankaya/Ankara
Tel: (0.312) 435 90 16 ● Faks:(0.312) 435 80 28
E-posta:info@ado.org.tr